Improving the seismic performance of structures with Direction and Displacement Dependent Viscous dampers

Nikoo Khanmohammadi Hazaveh

A thesis presented for the degree of

Doctor of philosophy

in

Structural Engineering

at the

University of Canterbury

Christchurch, New Zealand.

September 2017

Abstract

Modern structures demand greater protection from natural hazards, such as strong winds and severe earthquakes. Structures have traditionally been designed to sustain significant sacrificial damage to absorb and dissipate the input energy, while preserving life safety. However, this approach causes significant direct and indirect economic cost, which leads to long term societal costs.

Instead of damaging the main structural elements to absorb energy, supplemental energy absorbing dissipation devices can be incorporated to protect structures, creating low damage structures. In particular, devices capable of respectably dissipating energy without requiring inspection, repair or replacement are highly desirable in this role. Fluid viscous dampers are one well-known, highly repeatable damping device with numerous experimental and analytical investigations. However, while viscous dampers can reduce displacement demand, they can increase the overall base shear demand for nonlinear structures or with high levels of added damping, as they provide resistive forces in all four quadrants of the force-displacement hysteresis loop.

This thesis presents analytical and experimental studies on improving seismic structural performance using novel Displacement and Direction Dependent (D3) viscous devices. These proposed devices offer the adaptability of semi-active devices in an entirely passive device design, and thus include the high reliability

and low complexity of passive devices. A number of structural applications such as linear, nonlinear, and rocking systems, utilising D3 devices are described and analysed.

A distinguishing feature of this research is the novel design of a large-scale D3 device developed and experimentally validated. This design dramatically extends the capabilities of viscous devices by readily manipulating the device response to structural demands. In particular, the unique ability to use these devices to reshape or sculpt structural hysteretic behaviour in a fully passive device offers significant new opportunities in low damage structures with dissipation devices, which were previously only possible using much more costly, complex, and less robust, active or semi-active devices.

Time history analysis of linear structures and rocking systems with bi-linear elastic hysteresis, shows response reductions in both displacement and base-shear demand are only available with the 2-4 control method and devices, which dissipate energy only for motions towards equilibrium. These results indicate the robustness of simple 2-4 viscous dampers could be used to better mitigate structural response damage and potential foundation damage. These results extend prior results with semi-active, stiffness based devices to passive, velocity based dissipation devices.

To enable guidelines for adding a 2-4 device into the design procedure, damping reduction factors (RF_{ξ}) are developed, as they play an important role in design and

thus provide a means of linking these novel devices to standard design procedures. Three methods are presented to obtain damping reduction factors and equivalent viscous damping of a structure with a 2-4 semi-active viscous damper. In the first method, the relationship between RF_{ξ} and the damping of a structure with the 2-4 viscous devices can be obtained by calculating the area enclosed by the force-deformation diagram. The second and third methods are a modified version of the Eurocode8 (EC8) formula for damping reduction factors and smoothed results from time-history analysis, respectively. Finally, a simple method is proposed to incorporate the design or retrofit of structures using 2-4 viscous D3 dampers and standard design approaches.

Given the potential and link to standard design procedures, the D3 device design concept is presented and experimental tests undertaken on a prototype device. Sinusoidal displacement inputs provide a range of velocity inputs and device forces used to characterize the damping behaviour of the prototype and illustrate the ability to provide controllable viscous damping in any single or multiple quadrant(s) of the force-displacement response. Performance is characterized in term of device design dimensions and parameters. The overall results provide a proof-of-concept for a new class of relatively low cost passive device that enable customized hysteretic behaviour for any given structural application.

The overall outcomes of the thesis are experimentally validated in combination via the seismic performance of a 1/2 scale, two storey steel frame building with passive 2-4 D3 dampers subjected to uni-directional shake table testing.

Performance in mitigating structural response and foundation demand are assessed by evaluating base shear, maximum drift and acceleration. The test results show very good agreement with the nonlinear time history analysis and a numerical structural model.

Overall, this research presents a methodology for designing, testing and applying this new generation of viscous damping devices in enhancing seismic structural performance. The results show the ability to obtain simultaneous reductions in displacement, base-shear and acceleration demand for nonlinear and linear structures using passive 2–4 D3 viscous fluid dampers. This device is entirely passive and provides a unique retrofit option that would not require strengthening of columns and foundations.

Acknowledgements

I would like to begin this thesis by acknowledging all the people that helped make it possible. Without their continuing support and contribution this research would not have been completed.

I wish to thank and acknowledge my supervisors, Prof. Stefano Pampanin, Distinguished Prof. Geoff Chase and Associate Prof. Geoff Rodgers for the patient guidance, encouragement and advice they have provided throughout this research. I have been extremely lucky to have supervisors who cared so much about my work and accepted nothing less than excellence from me. And a special thanks to Prof. Geoff Chase whose office door was always open whenever I ran into a trouble or had a question about my research.

Besides my advisors, I would like to express my deepest gratitude to my colleague, best friend, love and husband Ali A. Rad for his unwavering love, support and understanding especially during the challenging times of conducting experimental tests at UOA.

My acknowledgment is also extended to the technicians and staff of the Department of Civil and Mechanical Engineering at the University of Canterbury and the Department of Civil Engineering at the University of Auckland who

helped me during this project. In particular, I would like to acknowledge Dr. Quincy Ma from UoA who helped us carry out shake table tests in UoA, Kevin Stobbs from UC, and Shane Smith and Mark Byrami from UoA for their support during experimental testing. I wish to thank Elizabeth Ackermann for her support and help with administrative tasks during my PhD study.

Finally, but foremost, I would like to extend my thanks to my family: my parents, Fariba Davari and Hossein Hazaveh, and my brother, Ehsan, who were always there for me and provided unwavering life-long love and understanding throughout what were sometimes tough times.

Contents

List of Publications

The following papers have been published based on the work reported in this thesis.

Journal Papers

- **Hazaveh, N. K.**, G. W. Rodgers, J. G. Chase, and S. Pampanin. (2017). Experimental Test and Validation of a Direction and Displacement Dependent (D3) Viscous Damper. Journal of Engineering Mechanics (ASCE), DOI: 10.1061/(ASCE)EM.1943-7889.0001354.
- **Hazaveh, N. K.**, G. W. Rodgers, J. G. Chase, and S. Pampanin. (2017). Passive Direction Displacement Dependent Damping (D3) Device. Bulletin of the New Zealand Society for Earthquake Engineering, BNZSEE1710.
- **Hazaveh, N. K.**, G. W. Rodgers, J. G. Chase, and S. Pampanin. (2017). Seismic behavior of a self-centering system with 2-4 viscous damper, Journal of Earthquake Engineering, in press.
- **Hazaveh, N. K.**, G. W. Rodgers, J. G. Chase, and S. Pampanin. (2017). Reshaping structural hysteresis response with viscous damping. Bulletin of Earthquake Engineering, 15(4), pp. 1789–1806.
- **Hazaveh N. K.**, Rodgers G., Pampanin S., & Chase, J. G. (2016). Damping reduction factors and code-based design equation for structures using new viscous dampers. Earthquake Engineering & Structural Dynamics, 45(15), 2533-2550.
- **Hazaveh, N. K.**, Pampanin, S., Rodgers, G. W., & Chase, J. G. (2015). Smart semi-active MR damper to control the structural response. Bulletin of the New Zealand Society for Earthquake Engineering, 48(4).

Conference Papers

- **Hazaveh, N. K.,** Ali A. Rad, Geoffrey W. Rodgers, J. Geoffrey Chase, Stefano Pampanin and Quincy Ma, (2018) "Numerical and experimental validation of Passive Direction Displacement Dependent Damping (D3) Device" 11th United States National Conference on Earthquake Engineering (11NCEE), Los Angeles, California.

- **Hazaveh, N. K.,** Ali A. Rad, Geoffrey W. Rodgers, J. Geoffrey Chase, Stefano Pampanin and Quincy Ma, (2018) "Shake Table Testing of Low Damage Steel Building: Comparative Testing with 2-4 Displacement Dependent (D3) Damper and a Typical Viscous damper" the 8th International Conference on Behavior of Steel Structures in Seismic Areas (STESSA), Christchurch New Zealand
- **Hazaveh, N. K.**, G. W. Rodgers, J. G. Chase, and S. Pampanin, Q.T. Ma. (2107) Shake table test a structure retrofitted using 2-4 Direction Displacement Dependent (D3) viscous dampers. , New Zealand Society for Earthquake Engineering (NZSEE), Wellington, New Zealand.
- **Hazaveh, N. K.**, G. W. Rodgers, J. G. Chase, and S. Pampanin, (2017) Spectral Analysis of Customized 2-4 Viscous Damping for Mitigating Seismic Response. 16th World Conference on Earthquake, 16WCEE, Santiago, Chile.
- **Hazaveh, N. K.**, S. Pampanin, G. Chase, & G. Rodgers. (2016) Design and experimental test of a Direction Dependent Dissipation (D3) device with off-diagonal (2-4) damping behaviour, NZSEE, Christchurch, New Zealand.
- **Hazaveh, N. K.**, S. Pampanin, G. Chase, & G. Rodgers. (2015) Semi-active viscous damper for Seismic response control", the 14th World Conference on Seismic Isolation, Energy Dissipation and Active Vibration Control of Structures (14WCSI) in San Diego, USA.
- **Hazaveh, N. K.,** S. Pampanin, G. Chase, & G. Rodgers, (2015) "Control of Structural Response with a New Semi-active Viscous Damping Device" the 8th International Conference on Behaviour of Steel Structures in Seismic Areas (STESSA) in Shanghai China.
- **Hazaveh, N. K.,** S. Pampanin, G. Chase, & G. Rodgers, (2015) Mitigating Structural Response using Semi-active Viscous Dampers to Reshape Structural Hysteresis. NZSEE , Rotorua, New Zealand.
- **Hazaveh, N. K.**, S. Pampanin, G. Chase, & G. Rodgers.(2014) Semi-active Direct Control of Smart Base Isolation System with Magnetorhological Damper", the 2nd European Conference on Earthquake Engineering and Seismology (2EECS) Istanbul, Turkey.
- **Hazaveh, N. K.**, S. Pampanin, G. Chase, & G. Rodgers (2014) Novel Semi-active Viscous Damping Device for Reshaping Structural Response" the 6th World Conference on Structural Control and Monitoring (6WCSCM) in Barcelona.
- **Hazaveh, N. K.,** S. Pampanin, G. Chase, & G. Rodgers, (2014) Semi-active Control of structure with MR Damper Using Wavelet-Based LQR, NZSEE , Auckland, New Zealand.

List of Figures

List of Tables

Chapter 1: Introduction

1.1. Background

Modern buildings are designed to sustain significant sacrificial damage in response to large earthquake ground motions, as a means to absorb the input energy while preserving life safety. Thus, current seismic design philosophy implies acceptance of extensive and often irreparable damage. This choice implies the acceptability or inevitability of associated repair/rebuild and added economic costs due to down time, and lost premises and business. It can thus take a society up to 10-20 years recover economically from a large earthquake (Ardalan et al. 2011; Chang 2000; Chang 2010; Horwich 2000; Kuwabara et al. 2008).

Figure 1-1. Buildings partially collapsed by the 1999 earthquake in Taiwan.

To improve performance, supplemental control devices can be added to absorb a portion of the seismic response and protect structures from damage. Structural control mechanisms can be divided into three broad categories: active, semi-active and passive. Each choice offers advantages with trade-offs in performance, cost and complexity.

Passive devices can dissipate significant energy, such as viscous dampers (Kobori 1990; Lin and Chopra 2003; Symans and Constantinou 1995; Taylor and Washiyama 2004a; Taylor and Washiyama 2004b; Tsopelas and Constantinou 1994a, Silwal et al. 2015), as seen in base isolation or direct use. In some specific applications, it is possible to add traditional viscous damping without increasing base-shear. However, this choice increases base shear and foundation demand for non-linear structures or with high level of added damping, reducing the ability to use them broadly in retrofit without significant added cost (Filiatrault et al. 2001; Lin and Chopra 2002; Miyamoto and Singh 2002; Symans et al. 2008; Vargas and Bruneau 2007). There are some issues associated with yielding replaceable fuses and other similar devices (Dolce et al. 2000; Iqbal et al. 2010; Marriott et al. 2008; Marriott et al. 2009; Palazzo et al. 2015; Pampanin 2012). Hence, on the basis of a traditional performance-based seismic design and retrofit philosophy, designers are challenged with a difficult trade-off, when using passive devices, between cost and acceptable damage (or targeted performance), while offering minimal added complexity.

More than 40 years ago, Yao (1972) suggested active control as an alternative method to conventional methods of passive damping devices to improve the dynamic structural response. The goal was to break these trade-offs and directly alter the structural dynamics by offering minimal added complexity. The advantage is the ability to alter device behaviour and damping inputs in response to changes in structural dynamics, increasing robustness compared to passive solutions. However, actively producing large seismic mitigation forces requires too much energy to be practical. In addition, these control algorithms and devices are complex and may not be robust over the long term (Francis 1987; Kogut and Leugering 2012) and across a range of possible input ground motion. Hence, active control offers opportunity but with significant cost and added complexity.

Thus, devices which semi-actively manage response forces offer a strictly dissipative solution and potentially offer an optimized active-passive compromise. Semi-active devices manage response forces without requiring large power sources and energy. Device response forces are manipulated by changes in the physical space or material properties of the device that create actively controlled dissipation forces. There are many semi-active devices developed including MR dampers (Hazaveh et al. 2015; Spencer Jr et al. 1997; Yang et al. 2002) and resettable devices (Mulligan et al. 2009; Rodgers et al. 2006; Rodgers et al. 2009), as two main, common types. Therefore, semi-active devices cannot in principle destabilize the structure because they do not add energy to the system, but simply absorb or store vibratory energy (Chase et al. 2006). In addition, using smart

device control they can provide more robust, low-damage solutions to mitigate damage in a manner that is robust to the seismic input motion (Chase et al. 2006).

In particular, specific semi-active devices offer the unique ability to sculpt device hysteretic behaviour (Amini et al. 2013; Barroso et al. 2003; Chase et al. 2006; Dolce et al. 2008; Hazaveh et al. 2015; Jansen and Dyke 2000; Mulligan et al. 2010; Spencer Jr et al. 1997; Symans and Constantinou 1995; Yang et al. 2002; Yoshida and Dyke 2004, Occhiuzzi and Serino 2003, Bitaraf & Hurlebaus 2013, Bitaraf et al. 2012, Bitaraf et al. 2010, Ozbulut and Hurlebaus 2011, Ozbulut et al. 2011, Ozbulut and Hurlebaus 2012, Kim et al. 2009, Kim et al. 2011, Cha et al. 2013). Broadly, these specific devices provide larger damping forces in specific quadrants by design. Hybrid systems with a combination of springs and dissipation passively offer this behaviour in quadrant 1 and 3, as shown in Figure 1-2a (Tsopelas and Constantinou 1994b). More typical of previous solutions, Figure 1-2.b shows a variable damping viscous device, as described in NCEER-95-0011 report (Symans and Constantinou 1995), where this device does not allow for individual control of specific quadrants of the hysteresis loop but rather just adjusts the level of damping. To date, only a limited selection of semi-active devices allows damping to be provided in only single or selected quadrants. However, they do so at the cost of significant added complexity.

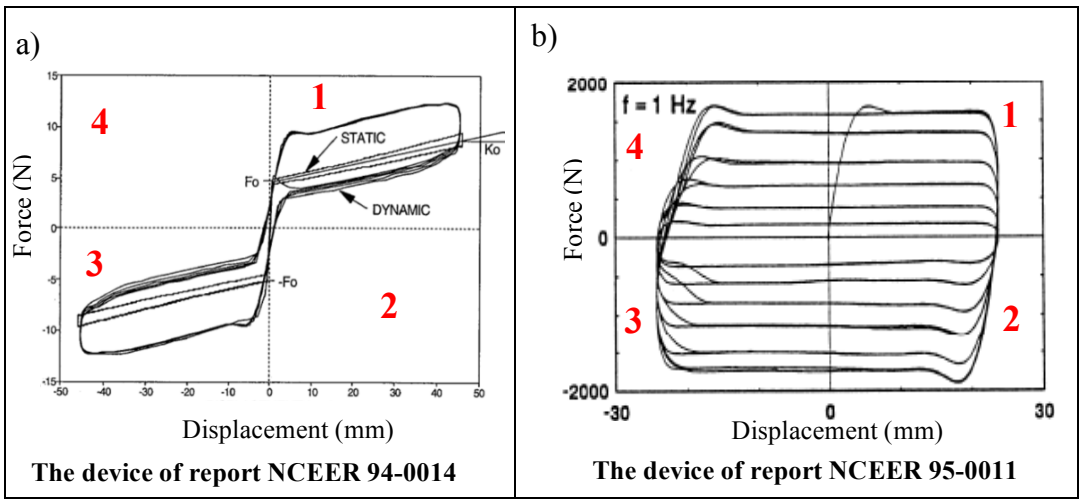

Figure 1-2. The device of report NCEER 94-0014 and NCEER 95-0011

Thus, the ability to sculpt the hysteretic response of a device, and thus of the whole structure, is only obtained by direct control of the device motion in each direction (Chase et al. 2006; Mulligan 2007; Rodgers et al. 2007), as shown in Figure 1-2. Finally, many prior semi-active devices have been air or fluid based systems based on the principles of variable stiffness (Chase et al. 2006; Mulligan et al. 2009; Rodgers et al. 2007). As noted they are complex and do not necessarily produce the very large control forces often required for controlling structures. Eliminating the semi-active aspect would significantly improve robustness and reduce cost via reduced complexity. Equally, larger forces of viscous devices might offer better force capacity for some specific application without increasing device costs.

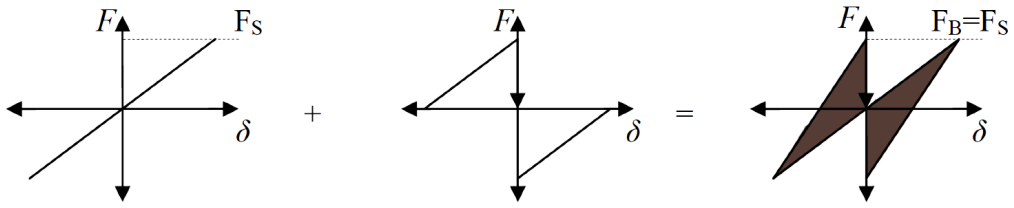

Figure 1-3.Change in hysteretic response of a linear structure with the addition of a resettable device. (Mulligan 2007)

1.2. Specific Need

Based on this summary introduction there is a need to capture the best aspects of existing devices and systems to create more reliable, lower cost approaches to mitigating seismic damage and dissipating seismic response energy without increasing base shear or structural accelerations. Such solutions would reduce or eliminate the trade-off of acceptable damage and life safety with its associated high economic cost. Hence, the goal of this thesis is to evaluate, determine, and capture the best elements of active, semi-active and passive energy dissipation devices.

1.3. Objective and Scope

This thesis seeks to address this need by answering the following questions:

1. What shape of semi-active viscous damper hysteresis loop is most effective in optimizing seismic structural responses?
2. How would such a device be designed into a structure in application?

3. In particular, what is the effect of the proposed device in emerging low-damage rocking systems?
4. How could this hysteretic shape be produced with a passive system with a hybrid or single device?
5. Can such a device or system be successfully designed and validated experimentally, both alone and within a test structure?

1.4. Thesis Outline

Chapter 1: This chapter has presented the overall motivation and main scope of this research. Seismic building performance can be increased using dissipation systems like viscous dampers. However, these improvements are offset by the added cost if the total base shear and acceleration increase. Hence, there is a significant need to find more reliable, lower-cost, and less complex systems and devices to improve structural response that can simultaneously reduce displacement, acceleration and total base shear. The overall goal of this research is to create devices and design procedures for their use that significantly change the trade-off between seismic damage, life safety, and economic impact; which an appealing solution are suitable for more economic new designs, as well as retrofit cases.

Chapter 2: In this chapter, the semi-active viscous damper is introduced. This chapter uses a spectral analysis of semi-active viscous dampers to compare the impact of three methods of re-shaping structural hysteretic dynamics that resist: 1)

motion in all 4 quadrants (1-4); 2) motion only away from equilibrium (1-3); and 3) motion only towards equilibrium (2-4). Performance is assessed by evaluating reduction factors (RFs) from an uncontrolled structure for maximum displacement (S_d) total base-shear (V_b), and maximum acceleration (S_a), which assess performance in mitigating response damage, the risk of foundation damage due to adding devices, and contents damage, respectively. In particular, this chapter seeks to answer Question 1.

Chapter 3: Presents guidelines for adding a 2-4 device into structural design procedures. Damping reduction factors (RF_ξ) are developed, as they play an important role in these procedures, and thus provide a means of linking devices to design procedures. Three methods are presented to obtain damping reduction factors and equivalent viscous damping of a structure with a 2-4 semi-active viscous damper. Finally, a simple method is proposed to incorporate the design or retrofit of structures with simple, robust and reliable 2-4 semi-active viscous dampers using standard design approaches. This chapter seeks to answer Question 2 and is generalizable to any such 2-4 damping device, creating an unique link between research and the profession.

Chapter 4: This chapter demonstrates the efficacy of a 2-4 viscous device in self-centering rocking structures with a bi-linear elastic response and is compared with typical standard viscous dampers and 1-3 viscous devices. In addition, the design approach in Chapter 4 is modified to propose a simple method to incorporate 2-4 viscous dampers into the structural design of self-centering systems, as they are a

reliably emerging classes of low-damage structures. This chapter seeks to answer Question 3.

Chapter 5: While semi-active devices offer the opportunity to customize the device response, and thus overall structural hysteretic response, they are actively controlled and thus entail a significant addition of complexity and potentially cost for the added performance. This chapter introduces the concept, design and experimental validation of an entirely passive Direction and Displacement Dependent (D3) viscous damping device. D3 devices can provide viscous damping in any individual or multiple quadrants of the force-displacement response. Previously only achievable using semi-active devices, this research presents an entirely passive, and thus more robust and lower cost, device. This chapter seeks to answer Question 4.

Chapter 6: Presents the design and construction of a shake table test to validate the effect of the proposed D3 device in an experimental test specimen. The seismic performance of a 1/2 scale, two storey steel frame building with the passive 2-4 D3 dampers and subjected to uni-directional shake table testing are evaluated. This chapter seeks to answer Question 5.

Chapters 7: Presents the overall conclusions to the research, and discusses possible extensions and future work.

1.5. References

Amini F, Hazaveh NK, Rad AA (2013) Wavelet PSO-Based LQR Algorithm for Optimal Structural Control Using Active Tuned Mass Dampers Computer-Aided Civil and Infrastructure Engineering 28:542-557

Ardalan A, Mazaheri M, Vanrooyen M, Mowafi H, Nedjat S, Naieni KH, Russel M (2011) Post-disaster quality of life among older survivors five years after the Bam earthquake: implications for recovery policy Ageing & Society 31:179-196

Barroso LR, Chase JG, Hunt S (2003) Resettable smart dampers for multi-level seismic hazard mitigation of steel moment frames Journal of Structural Control 10:41-58

Bitaraf M, Hurlebaus S (2010) Application of semi-active control strategies for seismic protection of buildings with MR dampers, Engineering Structures 32 (10), 3040-3047.)

Bitaraf M, Hurlebaus S, Barroso LR (2012) Active and semi- active adaptive control for undamaged and damaged building structures under seismic load, Computer- Aided Civil and Infrastructure Engineering, 27 (1), 48-64.

Bitaraf M, Hurlebaus S (2013) Semi-active adaptive control of seismically excited 20-story nonlinear building, Engineering Structures 56, 2107-2118.

Cha YJ, Kim Y, Raich AM, Agrawal AK (2013) Multi-objective optimization for actuator and sensor layouts of actively controlled 3D buildings, Journal of Vibration and Control 19(6), 942-960

Chang SE (2000) Disasters and transport systems: loss, recovery and competition at the Port of Kobe after the 1995 earthquake Journal of transport geography 8:53-65

Chang SE (2010) Urban disaster recovery: a measurement framework and its application to the 1995 Kobe earthquake Disasters 34:303-327

Chase JG et al. (2006) Re-shaping hysteretic behaviour using semi-active resettable device dampers Engineering Structures 28:1418-1429

Dolce M, Cardone D, Marnetto R (2000) Implementation and testing of passive control devices based on shape memory alloys Earthquake Engineering & Structural Dynamics 29:945-968

Dolce M et al. Jet-pacs project: joint experimental testing on passive and semiactive control systems. In: Proc. 14th World Conference on Earthquake Engineering, 2008.

Francis BA (1987) A course in H [infinity] control theory. Berlin; New York: Springer-Verlag.

Hazaveh NK, Chase JG, Rodgers GW, Pampanin S (2015) Smart Semi-Active Mr Damper To Control The Structural Response Bulletin of the New Zealand Society for Earthquake Engineering 48:235-244

Horwich G (2000) Economic lessons of the Kobe earthquake Economic development and cultural change 48:521-542

Iqbal A, Pampanin S, Palermo A, Buchanan AH Seismic Performance of Full-scale Posttensioned Timber Beam-column Joints. In: 11th World Conference on Timber Engineering, Riva del Garda, Trentino, Italy, 2010.

Jansen LM, Dyke SJ (2000) Semiactive control strategies for MR dampers: comparative study Journal of Engineering Mechanics 126:795-803

Kim Y, Langari R, Hurlebaus S (2009) Semiactive nonlinear control of a building with a magnetortheological damper sytem, Mechanical Systems and Signal Processing 23(2), 300-315

Kim Y, Langari R, Hurlebaus S (2011) MIMO fuxxy identification of building-MR damper systems, Journal of intelligent & fuzzy systems, 22 (4), 185-205

Kobori T State-of-the-art of seismic response control research in Japan. In: Proc. of the US National Workshop on Structural Control Research, 1990. pp 1-12

Kogut PI, Leugering G (2012) Optimal L1-control in coefficients for Dirichlet elliptic problems: H-optimal solutions Zeitschrift für Analysis und ihre Anwendungen 31:31-53

Kuwabara H et al. (2008) Factors impacting on psychological distress and recovery after the 2004 Niigata–Chuetsu earthquake, Japan: Community-based study Psychiatry and Clinical Neurosciences 62:503-507

Lin W-H, Chopra AK (2003) Earthquake response of elastic single-degree-of-freedom systems with nonlinear viscoelastic dampers Journal of engineering mechanics 129:597-606

Marriott D, Pampanin S, Bull D, Palermo A (2008) Dynamic testing of precast, post-tensioned rocking wall systems with alternative dissipating solutions

Marriott D, Pampanin S, Palermo A (2009) Quasi-static and pseudo-dynamic testing of unbonded post-tensioned rocking bridge piers with external replaceable dissipaters Earthquake engineering & structural dynamics 38:331-354

Mulligan K, Chase J, Mander J, Rodgers G, Elliott R, Franco-Anaya R, Carr A (2009) Experimental validation of semi-active resetable actuators in a ⅕th scale test structure Earthquake Engineering & Structural Dynamics 38:517-536

Mulligan KJ (2007) Experimental and analytical studies of semi-active and passive structural control of buildings

Mulligan KJ, Chase JG, Mander JB, Rodgers GW, Elliott RB (2010) Nonlinear models and validation for resetable device design and enhanced force capacity Structural Control and Health Monitoring 17:301-316

Occhiuzzi A, Serino G (2003), "A Semi-active Oleodynamic Damper for Earthquake Control. Part 2: Evaluation of Performance through Shaking Table Tests", Bulletin of Earthquake Engineering, Volume 1, Issue 2, pp 241–273.

Ozbulut OE, Hurlebaus S (2011) Optimal design of superelastic-friction base isolation for seismic protection of highway bridges against near-field earthquakes, Earthquake Engineering & Structural Dynamics 40 (3), 273-291.

Ozbulut OE, Bitaraf M, Hurlebaus S (2011) Adaptive control of base-isolated structures against near-field earthquake using variable friction dampers, Engineering Structures 33(12), 3143-3154.

Ozbulut OE, Hurlebaus S (2012) Application of an SMA-based hybrid control device to 20-story nonlinear benchmark building

Palazzo B, Castaldo P, Marino I (2015) The dissipative column: a new hysteretic damper Buildings 5:163-178

Pampanin S (2012) Reality-check and renewed challenges in earthquake engineering: Implementing low-damage structural systems-from theory to practice

Rodgers G, Mander J, Chase J, Mulligan K, Deam B, Carr A (2006) Re-shaping hysteretic behaviour using resetable devices to customise structural response and forces

Rodgers GW, Chase JG, Mulligan KJ, Mander JB, Elliott RB (2009) CUSTOMISING SEMI-ACTIVE RESETABLE DEVICE BEHAVIOUR FOR ABATING SEISMIC STRUCTURAL Bulletin of the New Zealand Society for Earthquake Engineering 42

Rodgers GW, Mander JB, Geoffrey Chase J, Mulligan KJ, Deam BL, Carr A (2007) Re-shaping hysteretic behaviour—spectral analysis and design equations for semi-active structures Earthquake engineering & structural dynamics 36:77-100

Spencer Jr B, Dyke S, Sain M, Carlson J (1997) Phenomenological model for magnetorheological dampers Journal of engineering mechanics

Silwal B, Michael RJ, Ozbulut OE (2015) A superelastic viscous damper for enhanced seismic performance of steel moment frames, Engineering Structures 105, 152-164

Symans MD, Constantinou MC (1995) Development and experimental study of semi-active fluid damping devices for seismic protection of structures

Taylor D, Washiyama Y Fluid Viscous Dampers in Mega Brace Elements for the 57- Floor Torre Mayor Building at Mexico City. In: Proceedings of the JSSI 10th Anniversary Symposium, Tokyo Institute of Technology, , Tokyo, Japan, 2004a.

Taylor D, Washiyama Y Taylor Fluid Viscous Dampers. In: Proc. SEC '04 International Symposium on Network and Center Based Research for Smart Structures Technology and Earthquake Engineering, , Osaka University,Osaka, Japan., 2004b.

Tsopelas P, Constantinou MC (1994a) NCEER-Taisei Corporation Research Program on Sliding Seismic Isolation Systems for Bridges: Experimental and Analytical Study of a System Consisting of Sliding Bearings and Fluid Restoring Force/Damping Devices. National Center for Earthquake Engineering Research,

Tsopelas P, Constantinou MC (1994b) NCEER-Taisei Corporation Research Program on Sliding Seismic Isolation Systems for Bridges: Experimental and Analytical Study of a System Consisting of Sliding Bearings and Fluid Restoring Force/Damping Devices. National Center for Earthquake Engineering Research, State University of New York at Buffalo, Department of Civil Engineering, Buffalo, New York 14260

Yang G, Spencer Jr B, Carlson J, Sain M (2002) Large-scale MR fluid dampers: modeling and dynamic performance considerations Engineering structures 24:309-323

Yao JT (1972) Concept of structural control Journal of the Structural Division 98:1567-1574

Yoshida O, Dyke SJ (2004) Seismic control of a nonlinear benchmark building using smart dampers Journal of engineering mechanics 130:386-392

Chapter 2: Reshaping Structural Hysteresis Response with Semi-active Viscous Damping[1]

Semi-active control devices offer significant promise for their ability to add supplemental damping and reduce seismic structural responses in an easily controllable manner, and can be used to modify or reshape overall structural hysteretic response. This chapter uses a spectral analysis of semi-active viscous dampers to compare the impact of three methods of re-shaping structural hysteretic dynamics that resist: 1) motion in all 4 quadrants (1-4): 2) motion away from equilibrium (1-3); and 3) motion towards equilibrium (2-4). Performance is assessed by evaluating reduction factors (RFs) from an uncontrolled structure for maximum displacement (S_d) total base-shear (V_b), and maximum acceleration (S_a) which assess performance in mitigating response damage, a risk of foundation damage, and contents damage, respectively.

Several studies (Barroso et al. 2003; Chase et al. 2006; Feng et al. 1993; Jabbari and Bobrow 2002; Jansen and Dyke 2000; Mulligan et al. 2009; Mulligan et al. 2010; Rodgers et al. 2007; Yoshida and Dyke 2004) have demonstrated the effectiveness of semi-active dissipation for enhancing the seismic performance of structures. They demonstrate, often only on analytically, safety levels that are not easily achieved in conventional structures designed with current design criteria.

[1] Based on: Hazaveh, N., Rodgers, G., Chase, J. & Pampanin, S. [2017] "Reshaping structural hysteresis response with semi-active viscous damping," Bulletin of Earthquake Engineering, 15, 1789-1806.

Thus, the potential of many classes of semi-active devices and control methods, including variable stiffness and variable damping, to mitigate damage during seismic events is well documented (Amini et al. 2013; Barroso et al. 2003; Chase et al. 2006; Jansen and Dyke 2000; Mulligan et al. 2007; Mulligan et al. 2010; Yoshida and Dyke 2004).

Many prior semi-active devices have been air or fluid based systems based on the principles of variable stiffness (Chase et al. 2006; Mulligan et al. 2009; Mulligan et al. 2010; Rodgers et al. 2007). However, these devices are complex and could not produce the very large control forces or responsiveness often required for controlling realistic structures. A further, potentially more robust, means of achieving such semi-active device forces is to use a controllable, electromechanical, variable-orifice valve to alter the resistance to flow of a conventional hydraulic fluid damper.

Feng and Shinozuka (1993) were the first to consider this concept. However, the extra plumbing and less responsive, low resolution orifices made this device essentially very similar to the resettable device of Jabbari and Bobrow (2002), and produced primarily on/off or high/low control without the ability to realize much of the potential benefit. Similar on/off results can be achieved with a range of calibrated pressure release valves.

This chapter evaluates the potential of a simple variable orifice viscous damping devices and examines three types of device control laws to sculpt hysteretic

behaviour. Because fluid-based velocity dissipaters are well-known, robust and can offer significant resistive forces, they may present significant advantages compared to complex stiffness based devices previously developed by others. In particular, it is intended to quantify the potential reductions in risk of damage at design level to aid design and determine the potential benefits. Equally, the addition of viscous damping changes dynamic response much differently than variable stiffness (Chase et al. 2006; Rodgers et al. 2007) or force-based devices (Dolce et al. 2008; Jansen and Dyke 2000) which, is best assessed in terms of change in risk. As the proposed devices are velocity based and well-known in many applications, viscous dampers should be more robust in operation and have lower equivalent complexity to control the device and be able to generate higher response forces more easily.

2.1. Method

2.1.1. Device type

Semi-active viscous damping devices offer the opportunity to sculpt the resulting structural hysteresis loop to meet design needs (Chase et al. 2006; Hazaveh et al. 2016; Rodgers et al. 2007). The impact and efficiency of different control laws is investigated. Three methods of re-shaping structural hysteretic dynamics of the device, and thus of the whole structural system, are denoted as 1-4, 1-3, and 2-4, referring to the main quadrants of the structural response being controlled, as illustrated in Figure 2-1.

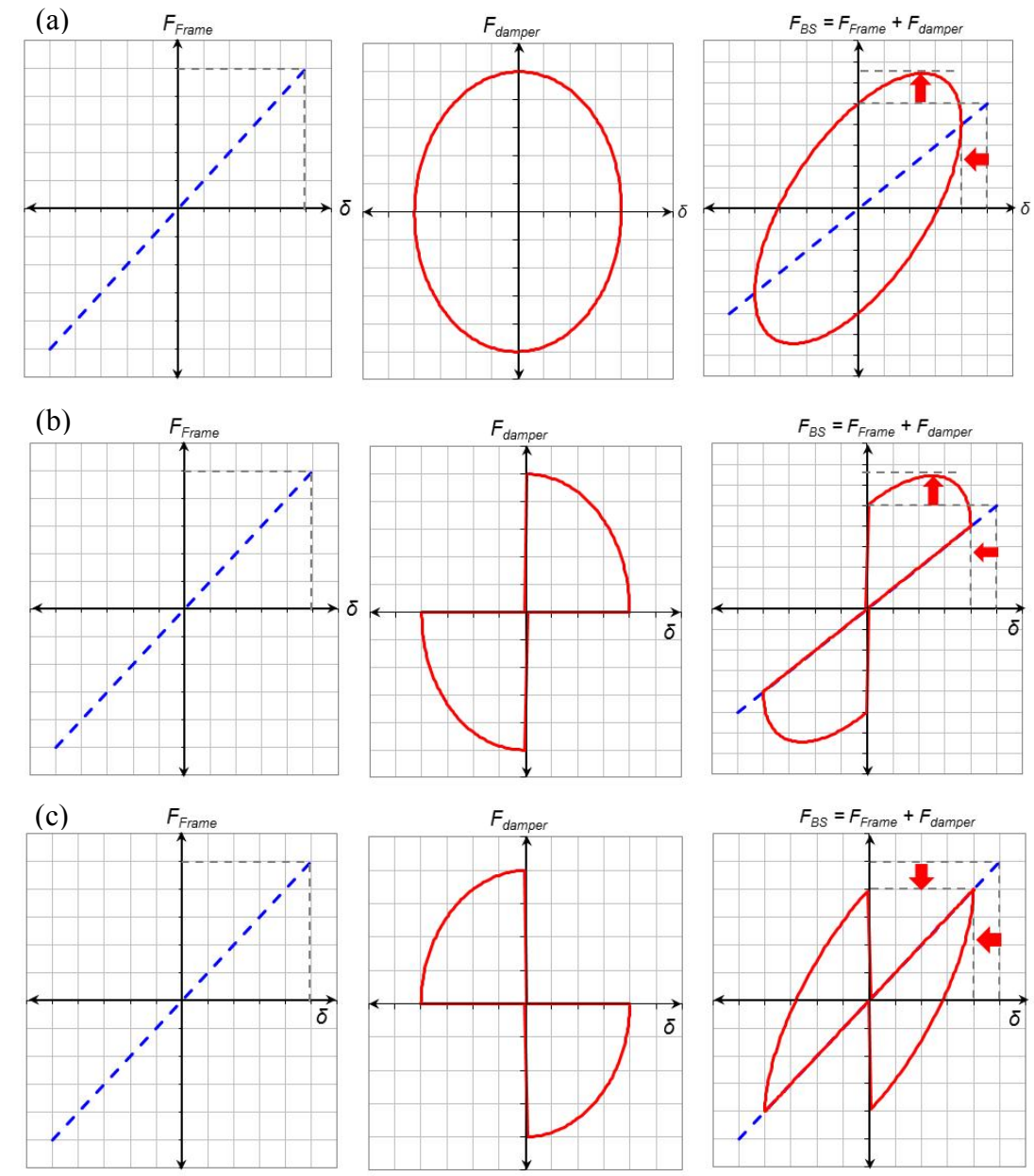

Figure 2-1. Schematic device hysteresis loop for a) 1-4 device, b) 1-3 device, and c) 2-4 device.

In Figure 2-1, the left column represents the baseline structure (the frame without devices), while the middle column represents the device response to a reduced

amplitude displacement input, assumed to be smaller given the presence of damping leads to a reduced peak displacement. The right column presents the schematic representation of the undamped structure and the damped structure, where the total base shear can be larger for the damped structure, despite the response reduction leading to reduced displacement response, and therefore less structural force. This figure is only intended to be a broad schematic representation of the combination of forces, and is not intended to represent or quantify specific displacement reductions.

Three control laws are used to control the opening and closing of orifices in the semi-active device to achieve these three different device hysteresis loops. In this proposed device, the orifices of the devices are opened or closed depending on velocity and displacement in each time step to produce damping in the desirable quadrant. It thus relies on measurement and feedback of device input motion. When the orifices are closed there is a minimal total opening for the fluid to flow through and thus significant damping force is produced by the device. When the orifices are open the total orifice area is large enough to allow essentially free motion with minimum dissipation. There are thus three control laws:

- 1-4 control law: the orifices of the device have to be closed in all quadrants (1, 2, 3, and 4), and is thus equivalent to standard, passive linear viscous damper (Figure 2-1a).

- 1-3 control law: the orifices of the device have to be closed in quadrants 1 and 3, thus resisting motion away from zero towards peak displacement, but not back toward zero (Figure 2-1b).
- 2-4 control law: the orifices of the device have to be closed in quadrants 2 and 4, thus resisting motion from peak displacement back towards zero, but not when it moves away from zero towards that peak (Figure 2-1c).

The force-velocity relationship of the 1-4 (standard viscous damper), 1-3 and 2-4 control law enabled devices are thus defined:

1-4 (viscous) device $$F_d = C \times \dot{x} \quad (2\text{-}1)$$

1-3 device $$\begin{cases} if\ \ sgn(x) \neq sgn(\dot{x}) & F_d \approx 0 \\ if\ \ sgn(x) = sgn(\dot{x}) & F_d = C \times \dot{x} \end{cases} \quad (2\text{-}2)$$

2-4 device $$\begin{cases} if\ \ sgn(x) \neq sgn(\dot{x}) & F_d = C \times \dot{x} \\ if\ \ sgn(x) = sgn(\dot{x}) & F_d \approx 0 \end{cases} \quad (2\text{-}3)$$

where F_d denotes the damper force, C represents the damping coefficient, $\dot{x}$ stands for the relative velocity between the ends of the damper, x is displacement, and *sgn()* is the sign function returning + or -. In a structural application, there are several sensors that could be used to record displacement and velocity in each time step. Dependent on the direction of displacement and velocity, the orifices of the

device are closed or opened. For example, in a 2-4 semi-active device when velocity and displacement are of different sign the orifices are closed and there is a resisting force. In the second quadrant of the force-displacement device hysteresis loop, as shown in Figure 2-1. Conversely, when the velocity and displacement are of the same sign, the orifices are open and there is a low resistive force.

A linear structure equipped with a 1-4 device and subject to a sinusoidal input motion has the hysteresis loop definitions schematically shown in Figure 2-1.a. where the circular force-deflection response of the 1-4 device is added to the linear force deflection response of the structure. The 1-4 device is a typical viscous damper can dissipate significant energy. However, the resulting base-shear force is increased. The overall system base shear is also increased when implementing a 1-3 devices, as in Figure 2-1b. In contrast, a 2-4 device can reduce the overall base-shear demand, by providing damping forces and dissipating energy only in quadrants 2 and 4, thus out-of-phase with the structural system response, as shown in Figure 2-1c.

All three types of semi-active viscous damping devices and control laws enable the opportunity to re-shape and modify the overall structural hysteretic behaviour, while also providing supplemental damping to reduce the structural response. They are thus dependent on structural response velocity compared to prior resettable devices (Chase et al. 2006; Jabbari and Bobrow 2002) that depend on displacement. Finally, note that there is a trade-off between these reductions and any device reaction load that increases base shear. Figure 2-2 shows a step-by-step

example of the control mechanism and response for a 2-4 viscous device under sinusoidal loading.

It should be noted that if the right combination of device design details and pre-load was obtained, whether created semi-actively or passively, then these systems would be equally applicable to the work presented here. Such passive devices might be accomplished by independently permitting different fluid flow in each direction of motion and for each half of the device. More specifically, this study is generalizable to any device or system (passive or semi-active) that can provide the 2-4 damping behaviour noted in Figure 2-1.c, which is the primary focus of this chapter, as this approach to added dissipation offers the opportunity to reduce response and base shear (Chase et al. 2006; Rodgers et al. 2007; Mulligan et al. 2009).

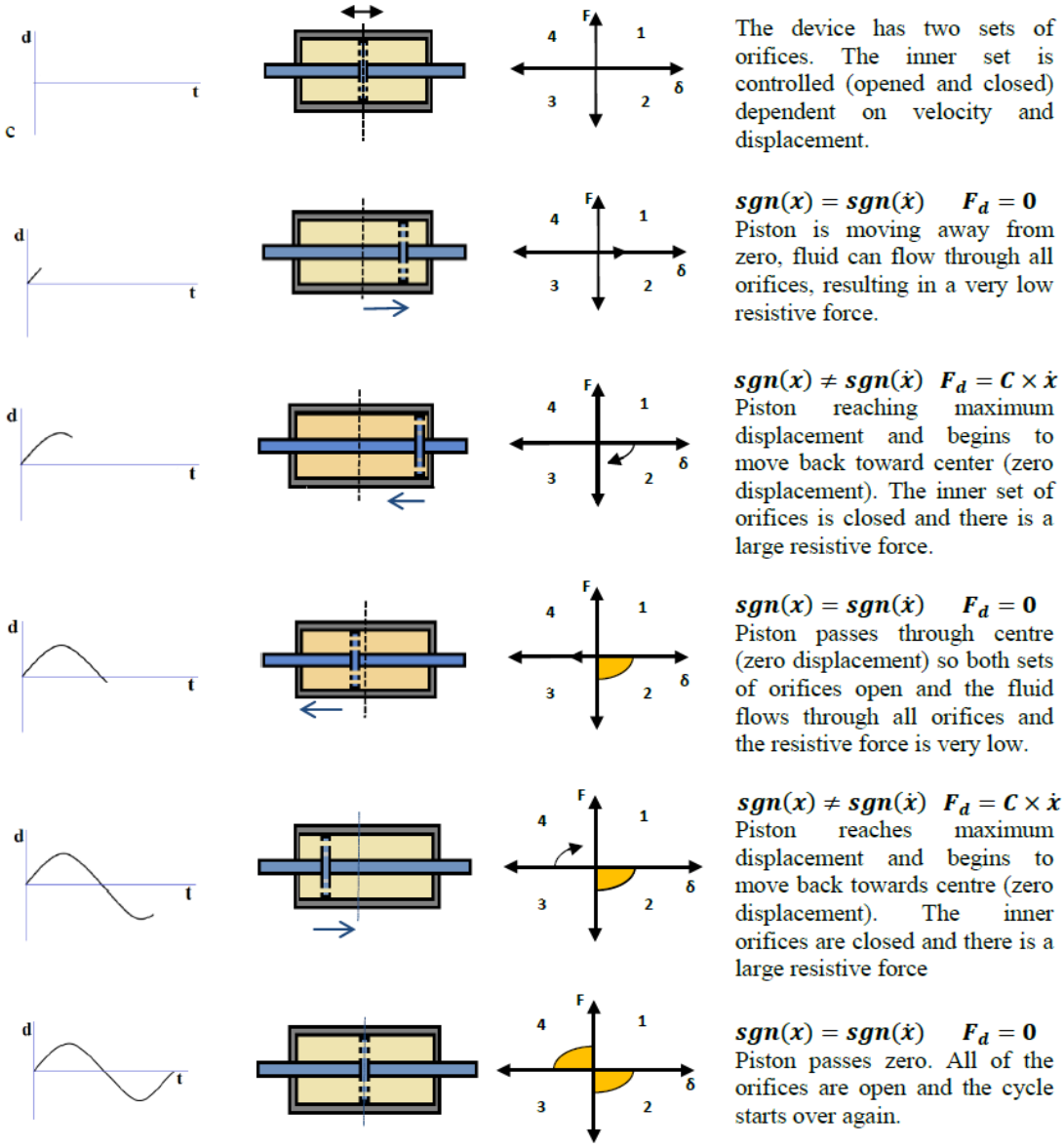

Figure 2-2. Step-by-step representation of valve and device control for a 2-4 control law/device under a sinusoidal input motion to achieve the desired hysteresis loop.

Significant prior research exists in the area of damping device design and a combination of selected aspects of these existing works could be used to obtain the 2-4 response behaviour studied here. This chapter is primarily concerned with

quantifying the potential gains and ramifications of the shape of the damping response provided and what quadrants of the hysteresis loop it occurs within, rather than the specific device design details required to produce this behaviour. However, the optimal design detail of such a device is very important and is the focus of later chapters.

2.1.2. Analysis

This chapter investigates the relative effectiveness of the three semi-active control laws on the seismic response of a simple SDOF structural system fitted with a semi-active variable orifice viscous damper (Figure 2-3). The use of a SDOF structure to generate a wide range of damping factors are limitations, where more specificity to a given structure or damping factor could yield greater insight. However, it is important to note that the main goal of this chapter is to present a range of factors to provide a generalizable result.

Equally, the use of SDOF design spectra structures and analyses, which would be expected to remain largely linear with such added low-to-no damage damping systems, are used because of their widespread use in structural design, particularly for initial structural design and scoping where such added damping systems might be considered to assess further design effort (Chopra 1995; Priestley et al. 2007). Hence, the damping factors presented are parameterized over a wide range. Thus, the use of the SDOF modelling approach provides an early means of linking to

design codes from these results, but may not be a full end result for any specific structural case.

The model structure used in this analysis includes inherent structural equivalent viscous damping of 5%, which is typical for many structures. The semi-active viscous damping devices are assumed add 10%, 15%, 20% and 30% additional damping to the structure when activated, and ~0% when not activated, to enable a parametric analysis across a range of device capabilities. The 15% value is readily achievable, but large enough to have a notable effect, while the others can provide context for this analysis, and provide insight into the value of an optimal added level of damping.

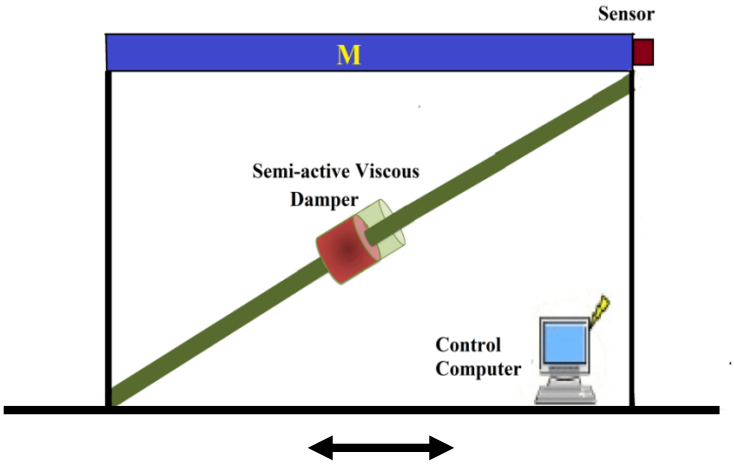

Figure 2-3. Schematic of a SDOF structural system fitted with the semi-active damper

The analyses utilizes an earthquake suite from the SAC (Structural Engineers Association of California (SEAOC), Applied Technology Council (ATC), and Consortium of Universities for Research in Earthquake Engineering (CUREE))

project (Sommerville et al. 1997). The suite, referred to as medium suite and representing design level events, consists of ground motions with probabilities of exceedance of 10% in 50 years in the Los Angeles region with the soil type of C (Table 2-1). Response statistics can then be generated from the results of this probabilistically scaled suite, which has an expected return period of 475 years. Figure 2-4 shows the response spectra of each ground motion from the medium suite of the SAC project and the median spectra of those results.

Table 2-1. Details of selected Los Angeles ground motions with (probability of exceedance of 10% in 50 years).

SAC Name	Record	Earthquake Magnitude	Distance (km)	Scale Factor	Duration (s)	PGA (cm/s^2)
LA01	Imperial Valley,1940, El Centro	6.9	10	2.01	39.38	452.03
LA02	Imperial Valley,1940, El Centro	6.9	10	2.01	39.38	662.88
LA03	Imperial Valley,1979, Array #05	6.5	4.1	1.01	39.38	386.04
LA04	Imperial Valley,1979, Array #05	6.5	4.1	1.01	39.08	478.65
LA05	Imperial Valley,1979, Array #06	6.5	1.2	0.84	39.08	295.69
LA06	Imperial Valley,1979, Array #06	6.5	1.2	0.84	39.08	230.08
LA07	Landers,1992, Barstow	7.3	36	3.2	79.98	412.98
LA08	Landers,1992, Barstow	7.3	36	3.2	79.98	417.49
LA09	Landers,1992, Yermo	7.3	25	2.17	79.98	509.7
LA10	Landers,1992, Yermo	7.3	25	2.17	79.98	353.35
LA11	Loma Prieta, 1989, Gilroy	7	12	1.79	39.08	652.49
LA12	Loma Prieta, 1989, Gilroy	7	12	1.79	39.08	950.93
LA13	Northridge, 1994, Newhall	6.7	6.7	1.03	59.98	664.93
LA14	Northridge, 1994, Newhall	6.7	6.7	1.03	59.98	664.93
LA15	Northridge, 1994, Rinaldi RS	6.7	7.5	0.79	14.94	523.3
LA16	Northridge, 1994, Rinaldi RS	6.7	7.5	0.79	14.94	568.58
LA17	Northridge, 1994, Sylmar	6.7	6.4	0.99	59.98	558.43
LA18	Northridge, 1994, Sylmar	6.7	6.4	0.99	59.98	801.44
LA19	North Palm Springs, 1986	6	6.7	2.97	59.98	999.43
LA20	Northridge, 1994, Sylmar	6	6.7	2.97	59.98	967.61

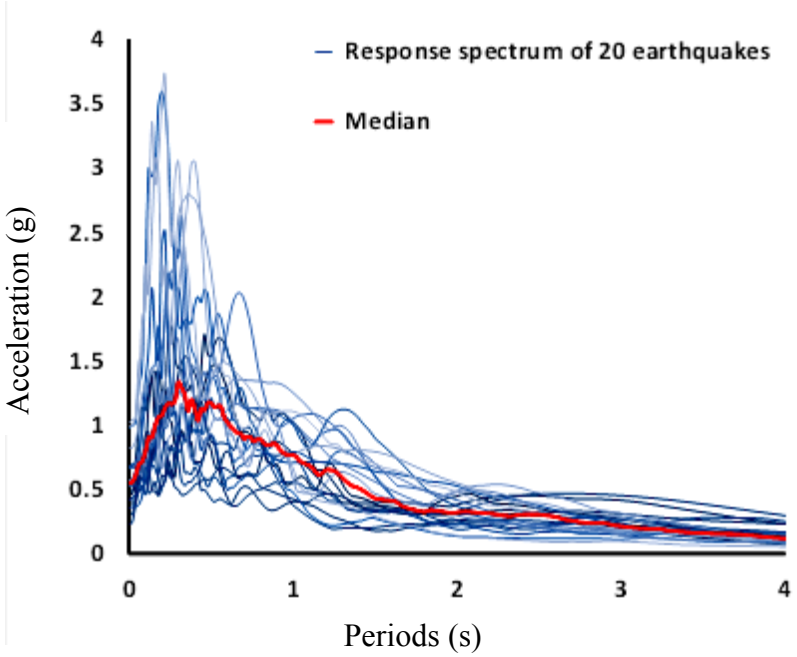

Figure 2-4. Individual response spectra of the 20 ground motions from the medium suite of SAC project and the median response spectrum resulting from them, with 5% inherent structural viscous damping.

Response spectra are produced for this suite of ground motions per a standard approach (Chopra 1995). The structural displacement (S_d) and total base shear (V_b) of 49 structures with periods of 0.2 s to 5.0 s, in 0.1 s increments, are presented in the response spectra. The period is changed by modifying the stiffness, keeping a constant mass of 1,000kg. The total base shear is an indication of the required foundation strength, as well as of shear and internal actions subjected to structural elements are subjected, and is defined as the sum of structural forces and inherent damping for a linear structure, and the resisting forces arising from the added semi-active viscous damping device.

Reductions achieved by the addition of semi-active viscous damping devices are represented as reduction factors (RFs), normalized to the uncontrolled case (without device) results. These multiplicative factors enable easy comparison of the different control laws relative to the structural design case risk. Hence, the results can be applied to any sized structure because they are only dependent on the control law type, standard period, and damping of the device. RFs less than 1.0 indicate reduction in the response metric, whilst RFs greater than 1.0 indicate an increase in response. Since a probabilistically scaled suite of ground motions, the resulting RFs represent changes in risk at the design level.

The 5^{th}, 25^{th}, 50^{th} (median), 75^{th}, and 95^{th} percentiles (Limpert et al. 2001) over all 20 response spectra capture the variation in response over the suite of design level ground motions. Therefore, these of the RFs and the overall distribution they desirable define changes in the relative risks of exceedance at these levels. The median (50^{th} percentile) is the middle (expected) result. The 95^{th} percentile shows the largest RF likely to occur for ground motions with this likelihood of occurrence, excluding extreme outlier events. These statistics provide the framework for a probabilistic or risk-based performance based design approach indicating the likely range of benefit (RF < 1.0) or degradation (RF >1.0). This approach thus eliminates the likelihood of erroneous conclusions being drawn about the viability of a control law or a design assumption, due to atypical performance for a single or few earthquakes, and should be robust to variabilities across ground motions.

2.2. Results

Figure 2-5 compares the different percentile RFs for S_d and V_b for all three control laws with 15% additional damping provided by the device. The results indicate the 90% range of total base-shear force RFs with the 1-4 device and control law is 0.55-0.90, 0.57-1.00 and 0.57-1.35 for periods of 0.5, 2.5 and 4.5 seconds, respectively, which broadly represent stiff, seismic, and wind governed periods. In addition, the 95^{th} and 75^{th} percentile RFs for V_b for the 1-4 device and control law exceeds 1.0 after T=2.5 and 3.8 seconds, respectively. In contrast, as might be expected, the 1-4 law offers greater reduction for S_d than the 1-3 and 2-4 control laws as it provides resistive force during all part of all response cycles, and thus absorbs more energy. The 1-4 control law provides S_d RFs= 0.50-0.80 for T=0.5, 2.5, and 4.5 seconds, respectively.

Like the 1-4 control law, the 1-3 control law has RF <1.0 for S_d for most periods and the total base shear greater than 1.0 for longer period structures, as shown in Figure 2-5. However, for the 1-3 devices and control law, the 95^{th} and 75^{th} percentile RF exceeds 1.0 for periods longer than T=1.6 and 3.4 seconds, respectively. The 50^{th} percentile V_b exceeds 1.0 for periods over 4.5 seconds.

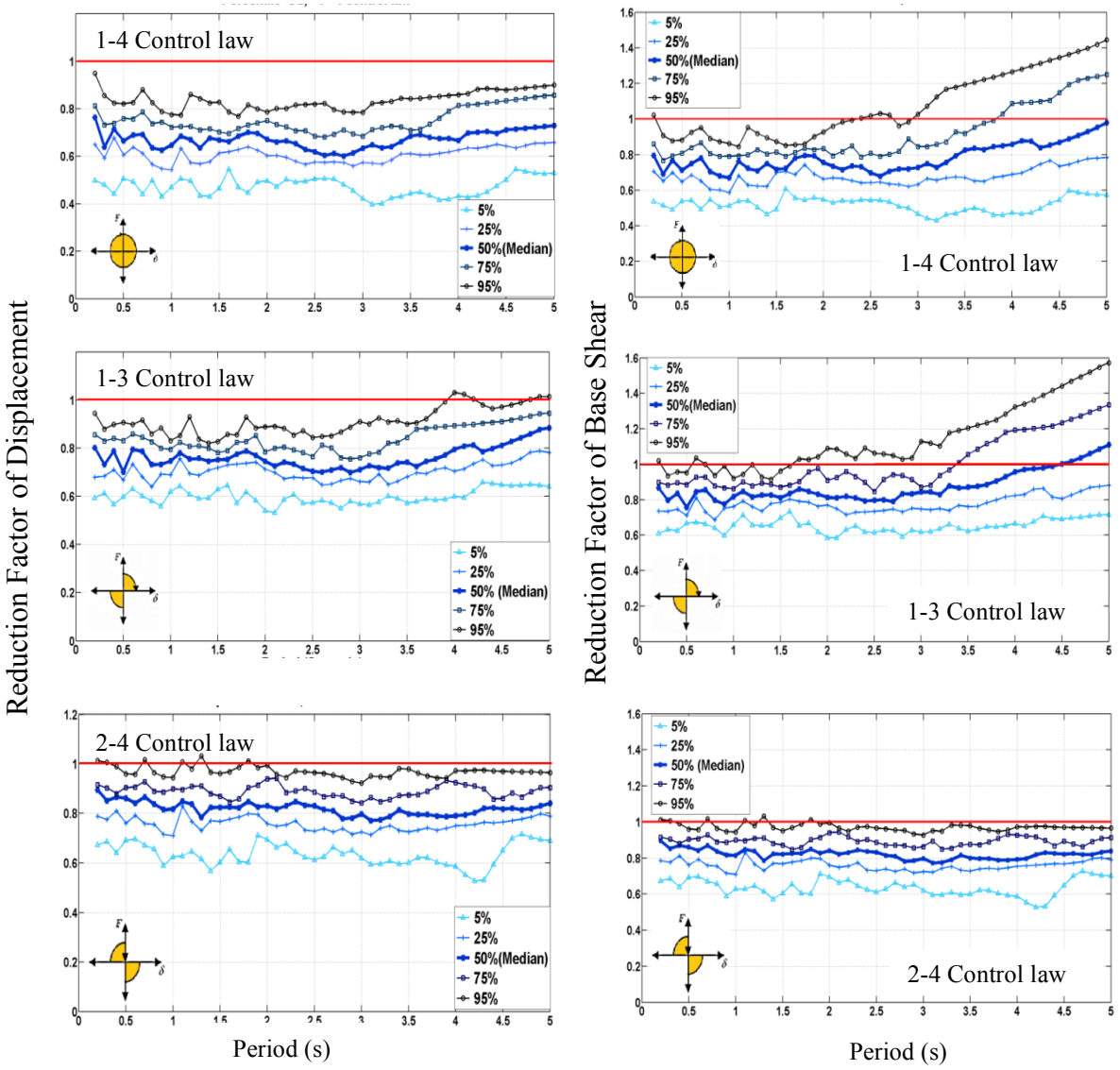

Figure 2-5. The different percentiles of displacement (S_d) and total base-shear (V_b) response reduction factor (RF) spectra for the 1-4, 1-3 and 2-4 control laws with 15% additional damping.

For the 2-4 device, similar to the 1-3 and 1-4 control laws, a S_d RF < 1.0 is valid for all periods from 0.2 to 5.0 seconds. However, the RFs for V_b are less than 1.0 for the 2-4 device and control law for all periods. Thus, this 2-4 devices and control law simultaneously reduces both S_d and V_b, as hypothesized in Figure 2-1.

Overall, Figure 2-5 shows similar results for S_d for each device control law. However, the 1-3 and 1-4 devices and control laws have significant likelihood of increasing the base shear forces (V_b). There is more than a 50% likelihood of an increase at some periods. More importantly, the RFs exceed 1.0 by a significant amount, including 20, 30 and 50% increases in V_b that may be for too excessive to manage in term of increased foundation demands, whether in a new design or, especially, in a retrofit scenario. In contrast, the RF of base shear, V_b, for the 2-4 control law devices is consistently less than 1.0 for all periods. The 2-4 device thus creates no increased risk of foundation damage mitigating construction and/or retrofit time frames and costs. Figure 2-6 shows the median RF for S_d and V_b for each control law for comparison.

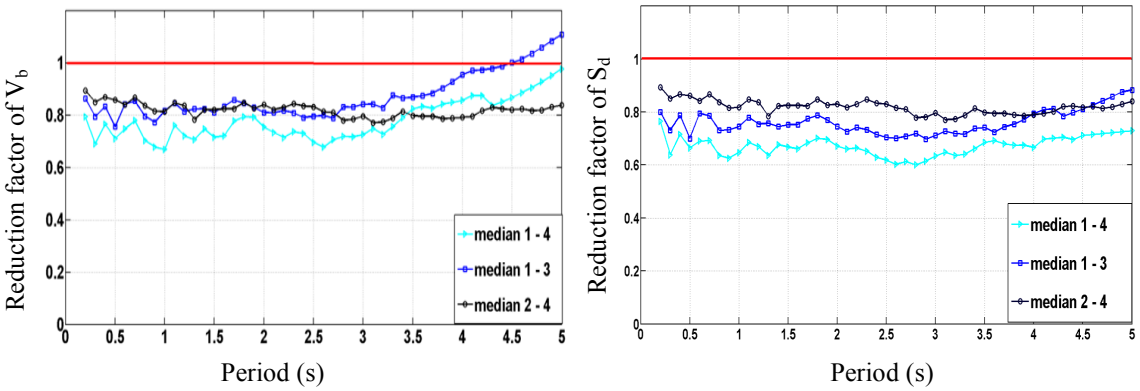

Figure 2-6. Medians of total base-shear (V_b) and displacement (S_d) response reduction factor (RF) spectra for the 1-4, 1-3, and 2-4 control laws.

Table 2-2. Maximum, Minimum and range of Reduction Factors, RF, of S_d and V_b for three Control Laws.

Control Laws	*Maximum RF of S_d*	*Minimum RF of S_d*	*Max-Min (RF of S_d)*	*Maximum RF of V_b*	*Minimum RF of V_b*	*Max-Min (RF of V_b)*
1-4	0.95	0.40	**0.55**	1.44	0.43	**1.01**
1-3	1.03	0.53	**0.50**	1.57	0.59	**0.99**
2-4	1.03	0.53	**0.50**	1.03	0.53	**0.50**

More specially, the extreme 5th and 95th percentile values RFs for base shear for the 1-4 and 1-3 control laws are significantly wider than the 2-4 control law, as delineated in Table 2-2. This latter result implies the 2-4 control law is more consistent and robust in the controlling response reductions across this diverse suite of events, implying greater robustness and consistency in seismic response with these devices.

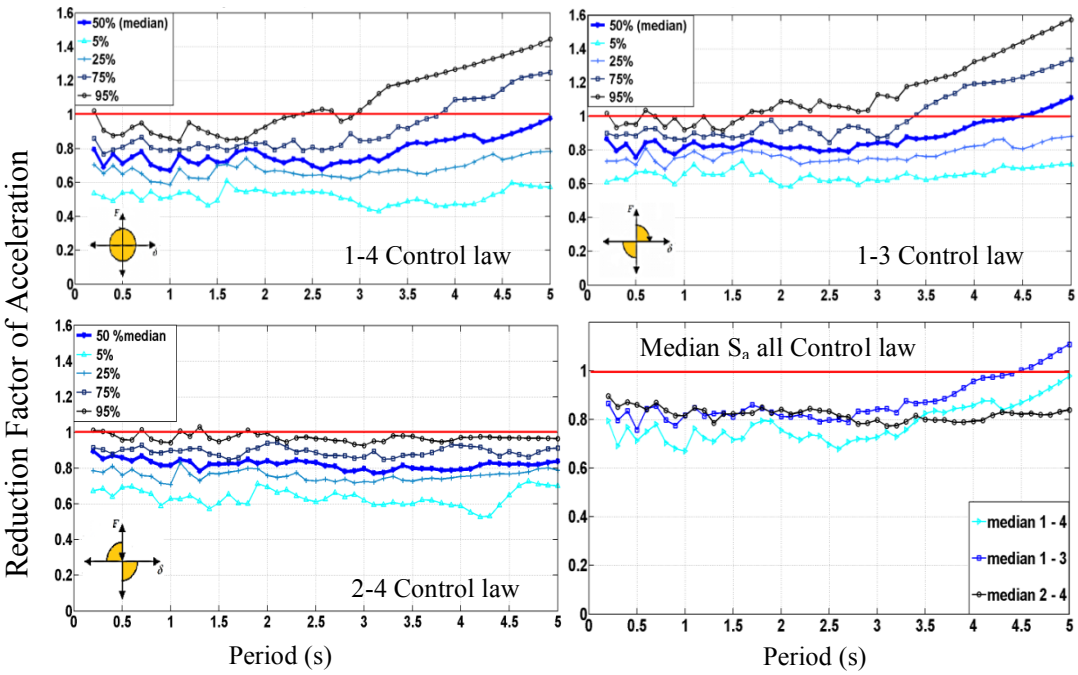

Figure 2-7. The difference percentiles and Median of acceleration (S_a) response reduction factor (RF) spectra for the 1-4, 1-3 and 2-4 control laws with 15% additional damping.

The different percentiles and median response spectra for the acceleration (S_a) RF response spectra for the 1-4, 1-3 and 2-4 device and control laws are shown in Figure 2-7. The SDOF mass multiply by the total acceleration is equal to the total base shear. Therefore, like the reduction factors for V_b, the 95th and 75th percentile RFs for S_a for the 1-3 and 1-4 control devices and laws are greater than 1.0, indicating an increased acceleration response. Similarly, and in contrast, the 2-4 device and control law have RFs for S_a at or below 1.0 for essentially all periods.

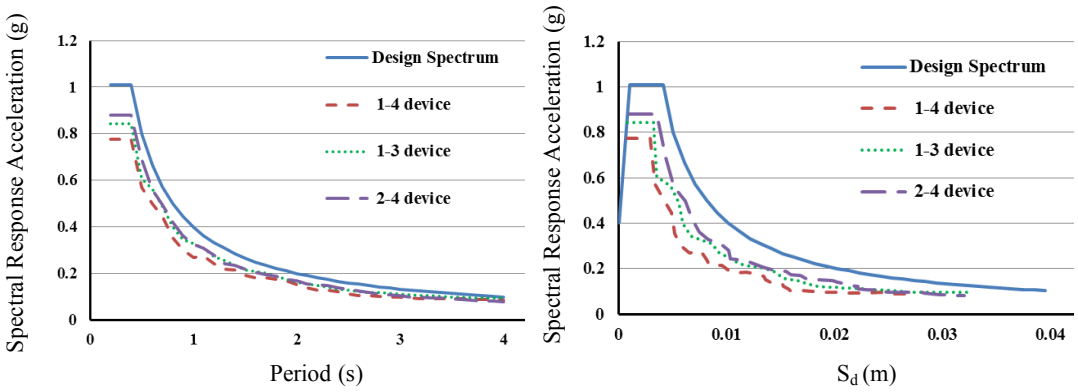

Figure 2-8. Design Spectra for structure without and with 1-4,1-3 and 2-4 damper devices (ξ=15%)

The acceleration-period and acceleration-displacement response spectra for soil type B for the structure, with and without semi-active dampers, are presented in Figure 2-8 for each case (ASCE7-10). The results show reductions in response of structures that reduces the potential damage to occupants and contents. This result summarizes and places the results of Figure 2-5 in design context.

Overall, these results indicate that it will be designer's choice, in discussion with the client, to select an acceptable level of risk. The median, 50th percentile risk

case indicates good levels of S_d, V_b and S_a reduction for all three control laws at all periods. However, that choice excludes 50% of likely events, where the damping system performs less well in some cases and may show increasing response in others. Hence, the choice would depend on the designer and any relevant codes/guidelines specifying a maximum acceptable risk of exceedance.

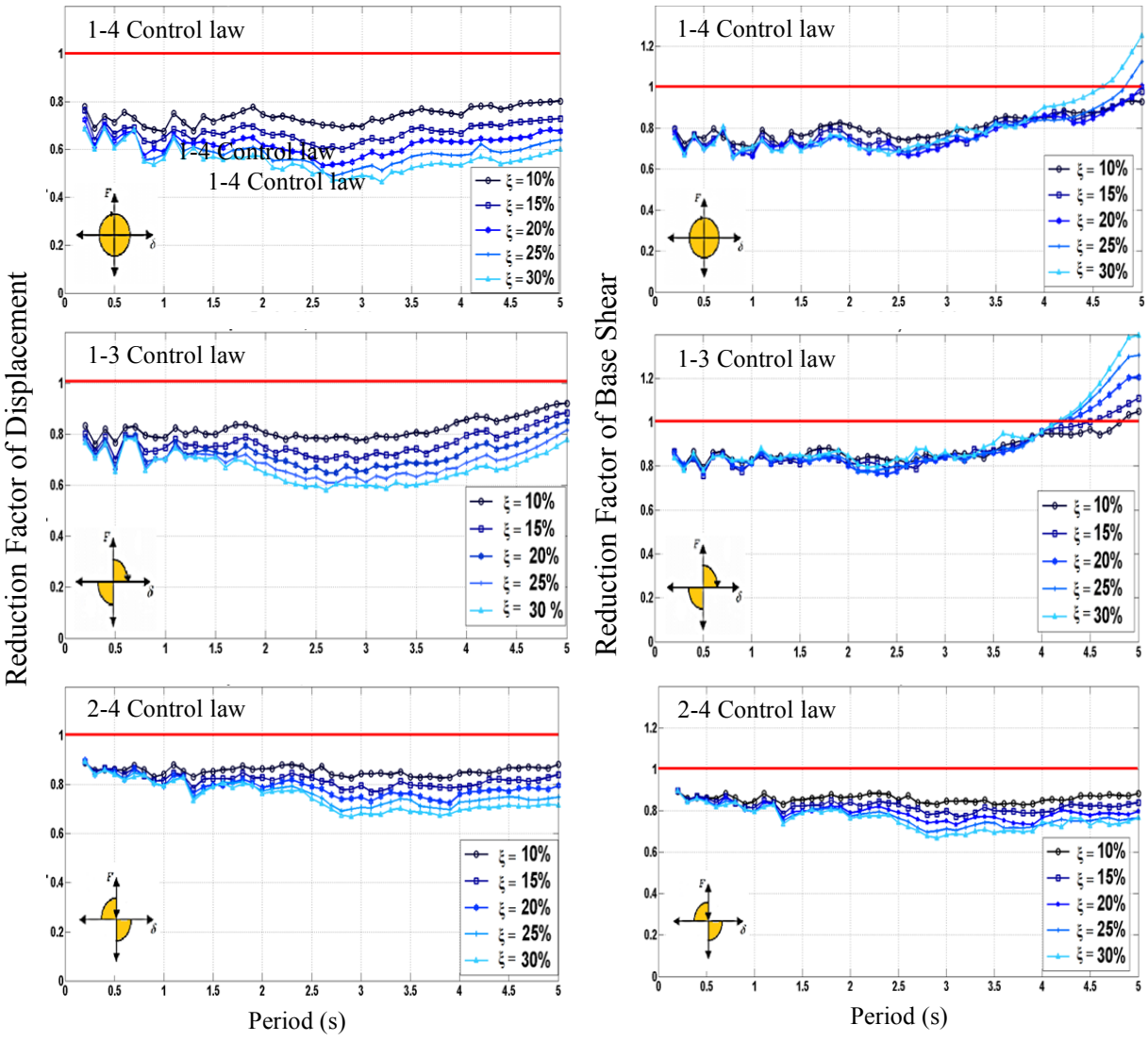

Figure 2-9. The median reduction factor of structural displacement and total base shear for the three control laws, with values of 10, 15, 20, 25, and 30% additional damping.

Figure 2-9 shows the median RF for S_d and V_b considering the range of 10, 15, 20, 25, and 30% added damping (ratio) from the device for all three control where the 15% results match presented in Figure 2-5. As expected, the maximum structural displacement decreases with increasing device damping. As before, the 1-4 control law offers the greatest reduction in displacement as it has the biggest area enclosed within the hysteretic loop, but at a cost in base shear increases at higher periods. Similarly, as in Figure 2-5, higher percentiles (not shown) provide greater base shear increases.

Figure 2-9 also shows base-shear reduction factors are approximately constant (range of 0.05-0.10 or 5-10% risk) at this median level within the natural period range T=0.2-4.0 seconds. However, the base shear RF for periods T= 4.0-5.0 seconds using the 1-4 and 1-3 devices exceeds 1.0 and increases significantly with adding damping. In contrast, the 2-4 control law has more stable behaviour, and constant ranges of displacement and base shear RF for all periods. Moreover, the S_d and base shear RF are all less than 1.0 for all periods for this 2-4 case, again matching the results in Figure 2-5.

As expected, the standard viscous damper (Equation 2-1 to 2-3) provides larger reductions in displacement than the other control laws. However, adding damping increases base shear for high period structures when using the 1-4 device, while the 2-4 device has constant ranges of RF of V_b (Figure 2-9), which are less than 1.0. Thus, the 2-4 approach offers significantly improved trade-off between these factors.

Table 2-3 presents the maximum, minimum and relative percentage range of the RF for the maximum displacement and base shear of the three semi-active device control laws with 10% to 30% additional damping, which is an added, unique outcome. It is evident the structural responses are strongly related to the level of added damping change when the 1-3 and 1-4 device are used. However, the 2-4 device is not very sensitive to changes in the level of added device damping. The structural systems with the 2-4 control law devices have reliable and robust responses during the earthquakes, even across a range of different damper sizes, indicating a relative insensitivity to the specific device design. Therefore, should the damper performance vary slightly from the intended design performance; the structural response will not be as largely affected. Such reduced sensitivity offers some robustness to a range of device and implementation errors and variability.

Table 2-3. Maximum, Minimum and increasing percentile of RF of S_d and V_b for three Control Laws with 10% to 30% additional damping.

Control Laws	*Maximum RF of S_d*	*Minimum RF of S_d*	$\frac{(Max-Min)*100}{Min\ (RF\ of\ S_d)}$	*Maximum RF of V_b*	*Minimum RF of V_b*	$\frac{(Max-Min)*100}{Min\ (R_F\ of\ V_b)}$
1-4	0.80	0.46	**73%**	1.25	0.66	**90%**
1-3	0.92	0.67	**38%**	1.40	0.78	**79%**
2-4	0.89	0.67	**33%**	0.89	0.67	**33%**

2.3. Limitation and other Issues

When considering a semi-active device controlled by valves, it is also important to consider the impact of valve actuation speed and delays from computation on the overall device performance. These factors would influence the results determined in this study, where an ideal device control law with no delays was considered. The work on stiffness-based resettable devices by Rodgers et al. (2007) and Mulligan et al. (2009) experimentally measured these delays and quantified their impact on performance. In particular, from this work, a general rule of thumb was that valve speed and thus delay in response should be 20-100x faster than the structural period being considered (Corman et al. 2012a; Corman et al. 2012b), to minimize any deviation from the ideal performance and mitigate any issues that may be introduced by computation and actuation delays.

This criteria thus implies that valve speeds of 0.02-0.1 seconds (10-50 Hz) are required for a structure with period, T = 2.0 s. These rates are readily commercially available. More specifically, when simulated with 20-100 ms valve delays matching these criteria, and a period of T = 2.0 s, the results are essentially identical those reported here, and following similar valve delay criteria at other periods yield the same results. Thus, this limitation should not significantly affect the results presented here, as long as the design and valve selection ensures that these criteria are met.

When designing or selecting a viscous damper for a given structure, as estimate of the structural velocities is required to determine the required size and capacity of the device, and to detail any connections. The structural velocity can be approximated from the design displacement and structural period, using the methods presented in (Pekcan et al. 1999). This structural velocity may then require a geometric transformation to convert the structural velocity to device velocity in some applications, such as when the viscous damper is in an inclined bracing element.

2.4. Summary

This chapter presents a novel semi-active viscous damping device control method to re-shape structural hysteretic behaviour with three semi-active control laws. Maximum displacement (S_d) and total base-shear (V_b) reduction factor (RF) spectra are created to determine the impact and efficiency of different control laws on seismic structural performance over a range of ground motions with equal probability of occurrence. The following conclusions can be drawn:

- Displacement spectral (S_d) reduction factors showed considerable reductions for all devices and control laws.

- The largest reductions were recorded for the 1-4 device as it has the biggest area enclosed by the device hysteresis loop and consequently the higher energy absorption and dissipation.
- The 1-3 and 1-4 control laws have median, 50^{th} percentile RF > 1.0 for V_b for high period structures and higher percentiles responses extended RF>1.0 for more periods. However, for all periods the RF of base shear for the 2-4 control law is below 1.0, significantly offering this traditional trade-off.
- The 2-4 approach also offered the greatest robustness and thus minimum variability across the 90 percentile range in risk, over all events.
- The 2-4 control approach thus offers minimal risk of increased foundation demand along with reduced displacement and acceleration demands.

Overall, the 2-4 control law appears to be an appealing solution for reducing seismic response, with minimal to no risk of structural or foundation damage, implying it is suitable for more economic new design, as well as retrofit. The analysis and results presented are generally able to any similar viscous damping devices, no matter how they are implemented.

2.5. Reference

Amini F, Hazaveh NK, Rad AA (2013) Wavelet PSO-Based LQR Algorithm for Optimal Structural Control Using Active Tuned Mass Dampers Computer-Aided Civil and Infrastructure Engineering 28:542-557

ASCE7-10 (2013) Minimum Design Loads for Buildings and Other Structures. American Society of Civil Engineers,

Barroso LR, Chase JG, Hunt S (2003) Resettable smart dampers for multi-level seismic hazard mitigation of steel moment frames Journal of Structural Control 10:41-58

Chase JG et al. (2006) Re-shaping hysteretic behaviour using semi-active resettable device dampers Engineering Structures 28:1418-1429
Chopra AK (1995) Dynamics of structures vol 3. Prentice Hall New Jersey,
Corman S, Chase JG, MacRae GA, Rodgers GW (2012a) Development and spectral analysis of an advanced diamond shaped resetable device control law Engineering Structures 40:1-8
Corman S, MacRae GA, Rodgers GW, Chase JG (2012b) Nonlinear design and sizing of semi-active resetable dampers for seismic performance Engineering Structures 39:139-147
Dolce M et al. Jet-pacs project: joint experimental testing on passive and semiactive control systems. In: Proc. 14th World Conference on Earthquake Engineering, 2008.
Feng MQ, Shinozuka M, Fujii S (1993) Friction-controllable sliding isolation system Journal of engineering mechanics 119:1845-1864
Hazaveh NK, Rodgers GW, Pampanin S, Chase JG (2016) Damping reduction factors and code-based design equation for structures using semi-active viscous dampers Earthquake Engineering & Structural Dynamics doi:10.1002/eqe.2782
Jabbari F, Bobrow JE (2002) Vibration suppression with resettable device Journal of Engineering Mechanics 128:916-924
Jansen LM, Dyke SJ (2000) Semiactive control strategies for MR dampers: comparative study Journal of Engineering Mechanics 126:795-803
Limpert E, Stahel WA, Abbt M (2001) Log-normal Distributions across the Sciences: Keys and Clues On the charms of statistics, and how mechanical models resembling gambling machines offer a link to a handy way to characterize log-normal distributions, which can provide deeper insight into variability and probability—normal or log-normal: That is the question BioScience 51:341-352
Mulligan K, Chase J, Mander J, Elliot R Semi-active resetable actuators incorporating a high pressure air source. In: Proceeding of the New Zealand Society for Earthquake Engineering Conference, 2007.
Mulligan K, Chase J, Mander J, Rodgers G, Elliott R, Franco-Anaya R, Carr A (2009) Experimental validation of semi-active resetable actuators in a ⅕th scale test structure Earthquake Engineering & Structural Dynamics 38:517-536
Mulligan KJ, Chase JG, Mander JB, Rodgers GW, Elliott RB (2010) Nonlinear models and validation for resetable device design and enhanced force capacity Structural Control and Health Monitoring 17:301-316
Pekcan G, Mander JB, Chen SS (1999) Fundamental considerations for the design of non-linear viscous dampers Earthquake engineering & structural dynamics 28:1405-1425
Priestley M, Calvi G, Kowalsky M Direct displacement-based seismic design of structures. In: 5th New Zealand Society for Earthquake Engineering Conference, 2007.
Rodgers GW, Mander JB, Geoffrey Chase J, Mulligan KJ, Deam BL, Carr A (2007) Re-shaping hysteretic behaviour—spectral analysis and design equations for semi-active structures Earthquake engineering & structural dynamics 36:77-100
Sommerville P, Smith N, Punyamurthula S, Sun J (1997) Development of ground motion time histories for phase II of the FEMA/SAC Steel Project, SAC Background Document Report SAC. BD-97/04,
Yoshida O, Dyke SJ (2004) Seismic control of a nonlinear benchmark building using smart dampers Journal of engineering mechanics 130:386-392

Chapter 3: Damping reduction factors and code-based design equation for structures using semi-active viscous dampers[1]

Chapter 2 evaluated the concept of semi-active viscous dampers and examined three types of semi-active device control laws (1-4, 1-3 and 2-4) to sculpt hysteretic behaviour. This semi-active device offers damping in selected quadrants and the difference between the 1-4, 2-4 and 1-3 devices is the application of a set amount of viscous damping in these different quadrants. The damping value of the semi-active viscous damper is set based upon a set level of damping for standard viscous damper and remains constant for all control laws. Therefore, the total enclosed area within the hysteresis loop is approximately cut in half when comparing a 2-4 or 1-3 device to a standard viscous damper (1-4).

Chapter 2 showed this semi-active 2-4 viscous damping approach to be an appealing solution for reducing seismic response, with minimal risk of structural or foundation damage. In particular, the use of large-scale passive viscous fluid dampers in industrial applications has proven their reliability and robustness to high demands and adverse operating conditions (Martinez-Rodrigo and Romero 2003; Rama Raju et al. 2014; Taylor and Washiyama 2004). The semi-active functionality does not change the damping of the device, but reshapes the

[1] Based on: Hazaveh, N., Rodgers, G. W., Pampanin, S. & Chase, J. G. [2016] "Damping reduction factors and code-based design equation for structures using semi-active viscous dampers," Earthquake Engineering & Structural Dynamics, 45, 2533-2550.

hysteresis loop by closing and opening the orifices. Therefore, the only difference between typical passive devices and semi-active viscous dampers is the ability to actively modify the orifice state, and thus dynamically change the damping behaviour within a response cycle. However, uptake is inhibited. In particular, suitable design procedures are lacking for widespread application of semi-active viscous dampers in structures.

The spectrum definition of forced based design (FBD) and Displacement Based Design (DBD) procedures is for structures with 5% inherent damping. However, in reality, structural and non-structural systems may have damping ratios other than 5% of critical damping. The concept of equivalent viscous damping and damping reduction factors for the seismic design and analysis of the structure has been used to find the spectral values for a range of likely damping ratios. For example, the η factor in EC8 (Bisch et al. 2012) or the R_ξ factor in displacement based design procedures (Blandon and Priestley 2005; Lin et al. 2003; Pampanin et al. 2010; Priestley et al. 2007a; Priestley and Grant 2005). Figure 3-1 shows the effect of equivalent viscous damping and damping reduction factor in Force-Based Design (FBD) and Displacement Based Design (DBD) procedures.

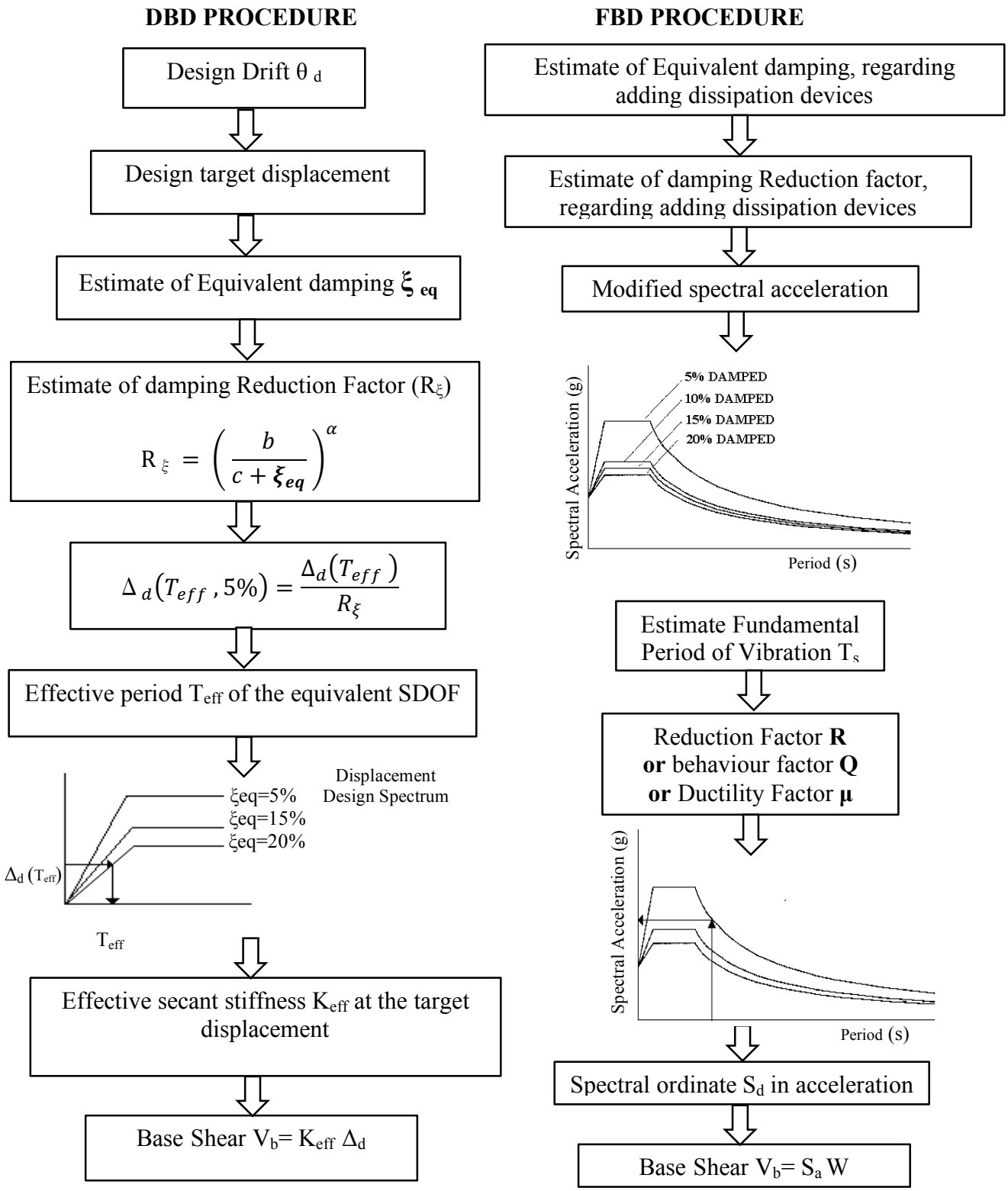

Figure 3-1. Schematic flow chart of Displacement Based Design (DBD) and Force-Based Design (FBD) procedure, modified after (Pampanin et al. 2010).

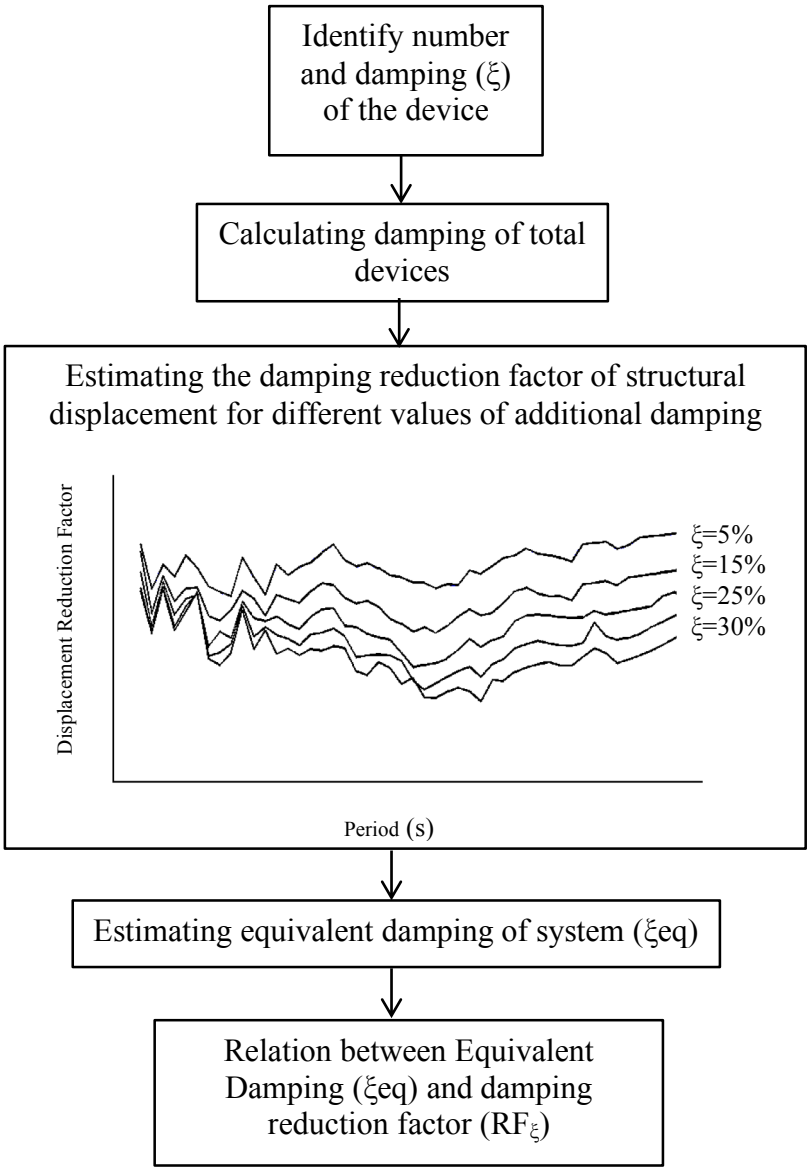

Figure 3-2. The relation between damping of semi-active viscous devices, equivalent damping and damping reduction factor (RF_{ξ}).

A main objective of this chapter is thus to quantify the effect of the semi-active viscous devices on structure performance, in term of equivalent viscous damping, to enable their use and integration into standard design procedures. The expected reduction in displacement (structural damage) and base shear (structure and

foundation damage and cost) using semi-active viscous dampers with different levels of supplemental damping are analysed and reported. The results are used to derive design-oriented relationships between the damping of a structure with devices and the corresponding damping reduction factor (Figure 3-2) either in terms of displacement or accelerations/forces. Successful outcomes would indicate the benefit of developing and characterizing specific, low-cost device designs for implementation by providing an easy, well-accepted means for design and uptake.

3.1. Modelling and evaluation approach

This chapter investigates the relative effectiveness of these three semi-active variable orifice viscous damping devices on the seismic response of a linear single degree of freedom (SDOF) structural system to provide estimates of the equivalent damping values for comparison and use with existing design codes. The semi-active viscous damping devices can add 5% to 45% additional damping to the structure when activated, and ~0% when not active. It thus builds upon the results of Chapter 2.

As in Chapter 2, the analyses presented utilize an earthquake suite from the SAC project (Sommerville et al. 1997) (The Structural Engineers Association of California (SEAOC), the Applied Technology Council (ATC), and Consortium of Universities for Research in Earthquake Engineering (CUREE) (SEAOC-ATC-

CUREE)) project, scaled for equal probability of occurrence. The suite, referred to as medium suite and representing design level events, consists of ground motions with probabilities of exceedance of 10% in 50 years in the Los Angeles region, as shown previously in Figure 2-4 and Table 2-1.

Response spectra are produced for this suite of ground motions using a standard approach (Chopra 1995). Structural displacement (S_d) and total base shear (V_b) demand are evaluated for a range of periods T = 0.2 – 5.0 s with increments of ΔT= 0.1 second (49 structures). The model structure used in this analysis includes inherent structural equivalent viscous damping of 5%. The period is changed by modifying the stiffness, keeping a constant mass of 1000 kg. Reductions in S_d and V_b achieved by the addition of semi-active viscous damping devices are represented by damping reduction factors (RF_ξ), normalized to the uncontrolled (without device), case results.

Finally, the relationships between damping of the device and damping reduction factors of the structural responses are evaluated using three methods: 1) area-based method; 2) Eurocode (EC8) approach; and 3) smoothing the analytical results. In the area-based method, the relationship between the RF_ξ and damping of semi-active structure can be obtained by calculating the energy absorbed as the area enclosed within the force-deformation diagram (Blandon and Priestley 2005; Lin et al. 2003; Pampanin et al. 2010; Priestley et al. 2007a; Priestley and Grant 2005). On the basis of assumptions that the system is under harmonic excitation, hysteretic damping, ξ_{hyst}, which represents the dissipation from the nonlinear

hysteretic behaviour of viscous and semi-active viscous damping devices can be defined in DBD procedures as (Blandon and Priestley 2005; Lin et al. 2003; Pampanin et al. 2010; Priestley et al. 2007a; Priestley and Grant 2005):

$$\xi_{hyst} = \frac{1}{4\pi} \cdot \frac{E_D}{E_S} = \frac{1}{2\pi} \cdot \frac{A_h}{F_D\, U_D} \tag{3-1}$$

where E_D and E_S are the dissipated and stored energies, respectively, and A_h is the value of the dissipated energy, F_D is the maximum force and U_D is the maximum deformation.

In the second method the modified damping reduction factor of EC8 which was suggested by Priestley et al. (2007b) is used. It is computed:

$$RF_{\xi EC8} = \eta = \left(\frac{0.1}{0.05+\xi_T} \right)^{0.5} \tag{3-2}$$

$$\xi_T = \xi_{el} + \xi$$

where ξ_T is total damping ratio of the structure that equals the damping ratio of the device (ξ) plus the constant 5% damping ratio of linear structure (ξ_{el}).

A simplified, equation derived by smoothing the results is also used in the third method. All of these three methods use the damping reduction factor to relate the semi-active viscous device to structural demand. Finally, this study proposes a

robust and simple design and analysis process to evaluate the effect of adding the 2-4 device to SDOF structures.

3.2. Results and discussion

Figure 3-3 shows the median damping reduction factor (RF_{ξ}) of 49 structures (T=0.2-5.0 s) in terms of structural displacement ($RF_{\xi\text{-}Sd}$) and total base shear ($RF_{\xi\text{-}Vb}$) with different sizes of semi-active damping devices to produced 5% to 45% supplemental damping (ξ). As expected, the maximum structural displacement decreases with increasing device damping. The viscous damper or 1-4 control law offers the greatest reduction of displacement as it has the biggest area enclosed with the device hysteretic loop. These results match those of Figure 2-9 in Chapter 2, the foundation of this analysis.

Figure 3-3 also shows that the $RF_{\xi\text{-}Vb}$ for periods T= 3.6-5.0 seconds using the viscous damper (or 1-4 control law) and 1-3 devices exceeds 1.0 and increases significantly when adding damping. In contrast, the 2-4 device provides damping in the second and fourth quadrants, and provides more stable behaviour, and constant ranges of $RF_{\xi\text{-}Sd}$ and $RF_{\xi\text{-}vb}$ for all periods. Moreover, in the 2-4 case, the $RF_{\xi\text{-}Sd}$ and $RF_{\xi\text{-}vb}$ are all less than 1.0 for all periods for this 2-4 case. The 2-4 approach thus offers the greatest robustness and, thus, minimum variability in median level risk, over all events. However, the choice between these devices

would depend on the designer and any relevant codes/guidelines specifying a maximum acceptable risk of exceedance.

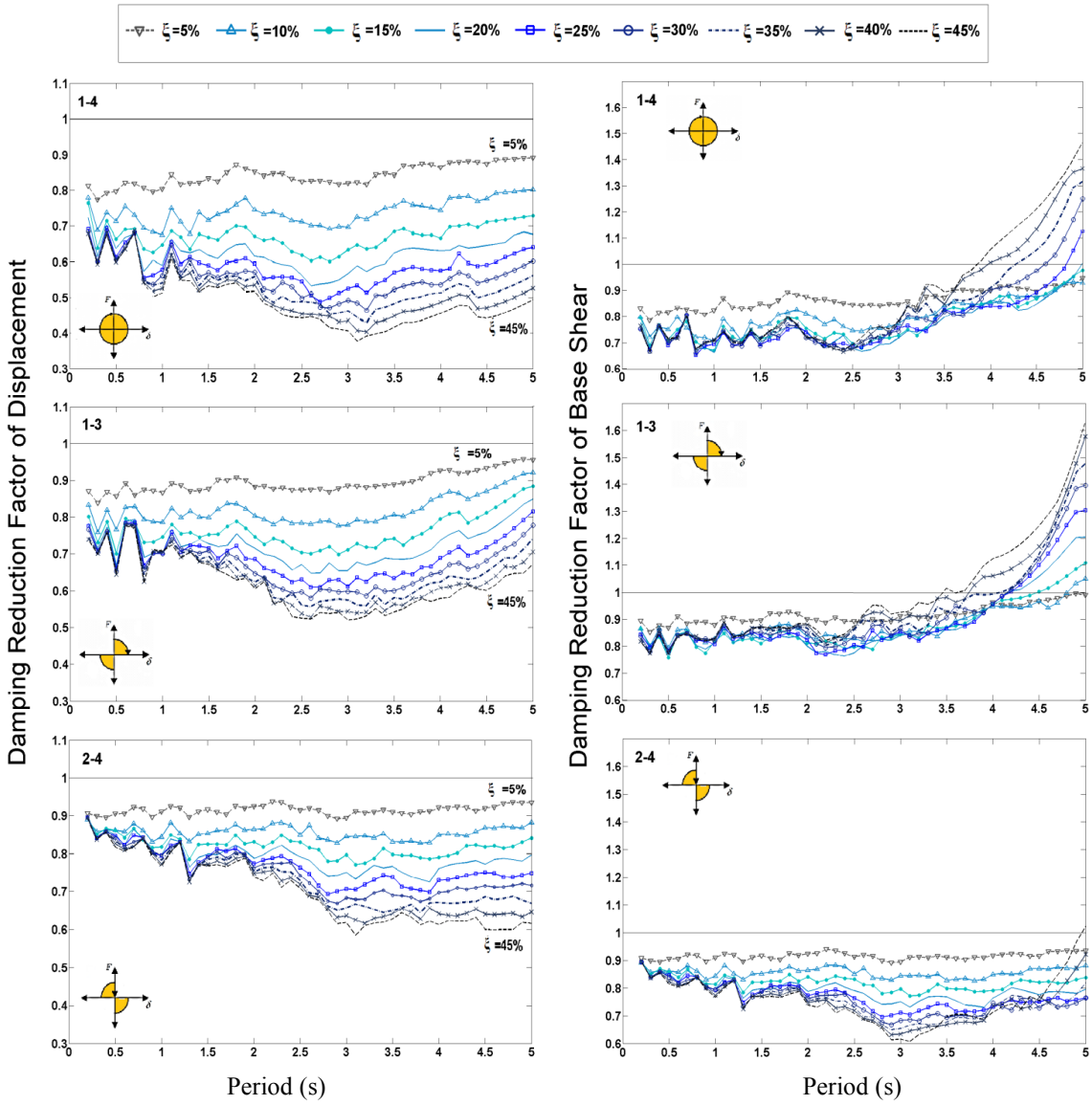

Figure 3-3. The median damping reduction factor of structural displacement and total base shear for the three control laws, with values of 5% to 45% additional damping.

3.3. Relationships between damping reduction factor and device damping

Damping reduction factors, such as η factor in EC8 (Bisch et al. 2012) or the R_ξ factor in the DBD Procedure (Blandon and Priestley 2005; Lin et al. 2003; Pampanin et al. 2010; Priestley et al. 2007a; Priestley and Grant 2005)) are typically suggested in any force-based or displacement based design procedures to reduce the elastic design acceleration and displacement spectrum, respectively. In this chapter, the relation between RF_ξ and damping of the device (ξ) are discussed in term of three methods: 1) area based; 2) Eurocode; and 3) smoothing equation result. These results are compared and the results obtained from the time-history analysis.

3.3.1. Area based method

The equivalent viscous damping is normally obtained by calculating the device damping and combining it with the structural response (Blandon and Priestley 2005; Lin et al. 2003; Pampanin et al. 2010; Priestley et al. 2007a; Priestley and Grant 2005). The equivalent hysteretic damping ratio may be derived based on the dissipated energy. Here, the equivalent damping of the structure considering the (5% inherent) energy dissipation of the structure and of the added device is discussed.

Figure 3-4 illustrates graphically the concepts of hysteretic damping, ξ_{hyst}, which was presented in Equation 3-1 for three devices. E_D is the large amount of energy dissipated per cycle, corresponding to the area enclosed with the hysteresis loop. The area of the loop of the linear viscous damper can be calculated by integration (Pampanin et al. 2010; Priestley et al. 2007a):

$$E_D = A_h = \pi F_D U_D \tag{3-3}$$

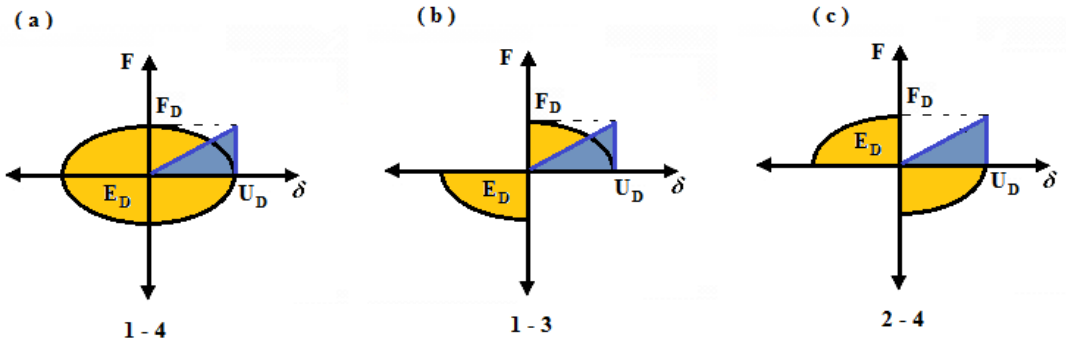

Figure 3-4. Estimation of Equivalent damping ratio for a) Viscous (1-4) device, b) 1-3 device, and c) 2-4 device.

The A_h value for the 1-3 and 2-4 semi-active viscous damper with the same damping constant, C, are half of the area of the viscous damper, as seen graphically in Figure 3-4. Therefore, the value of $\xi_{hyst\text{-}device}$ for the viscous damper (1-4 control law), and the 1-3 or 2-4 semi-active viscous devices can be defined:

$$\begin{cases} \xi_{hyst-device} = \frac{1}{2\pi}.\frac{\pi F_D U_D}{F_D U_D} = 50\% & for\ a\ 1-4\ device\ \ (or\ viscous\ damper) \\ \xi_{hyst-device} = \frac{1}{4\pi}.\frac{\pi F_D U_D}{F_D U_D} = 25\% & for\ a\ \ 1-3\ and\ 2-4 \end{cases} \tag{3- 4}$$

The equivalent damping of the structure is equal to (Pampanin et al. 2010; Priestley et al. 2007a):

$$\xi_{eq} = Z_1(\xi_{el} + \xi_{hyst-Structure}) + Z_2(\xi_{hyst-device}) \quad (3\text{-}5)$$

where ξ_{el} represents the inherent elastic damping and $\xi_{hyst\text{-}structure}$ the hysteretic dissipation of the frame of structure. The term $\xi_{hyst\text{-}device}$ is hysteretic damping of the device, while Z_1 and Z_2 are the contribution of the structure and devices to damping of the system, respectively. In this case, Z_1 and Z_2 can be written, using Figure 2-1 and Figure 3-4, as:

$$Z_1 = \frac{F_S}{F_D+F_S} \;;\; Z_2 = \frac{F_D}{F_D+F_S} \quad (3\text{–}6)$$

where F_S and F_D are the maximum force of the linear structure and device, respectively.

In this analysis, the initial damping (ξ_{el}) of the linear SDOF in the elastic range is considered as 5% and $\xi_{hyst\text{-}structure}$ =0% for a linear structure. Figure 3-5 shows the contribution of the viscous damper (1-4 control law), and the 1-3 and 2-4 device ($Z_2 = \frac{F_D}{F_D+F_S}$) to the overall damping of the structure.

Figure 3-6 shows total force-displacement of the structure with T=1.0 s under the LA01 ground motion that used a 2-4 device, which adds 15% more damping to the system. The equivalent damping based on the enclosed area method (Equation 3-1) is equal to 0.086. The resulting values of Z_1 and Z_2 are 0.8386 and 0.1614,

respectively. Therefore, the equivalent damping based on Equation 3-5 is equal to 0.083, which is about the same as the equivalent damping value of 0.086 based on the area based method.

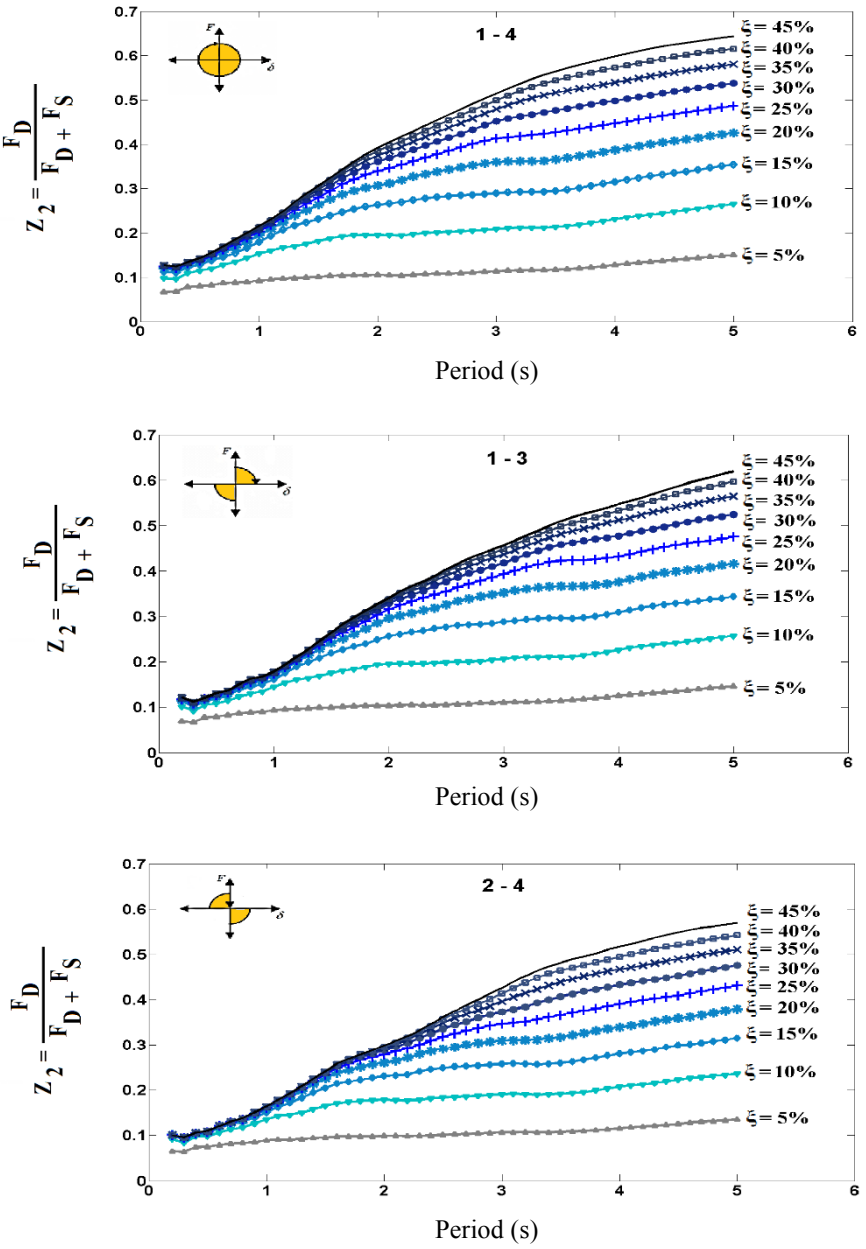

Figure 3-5. The contribution of the 1-4, 1-3 and 2-4 device (z_2) with damping from 5% to 45% added to structures with inherent damping of 5%.

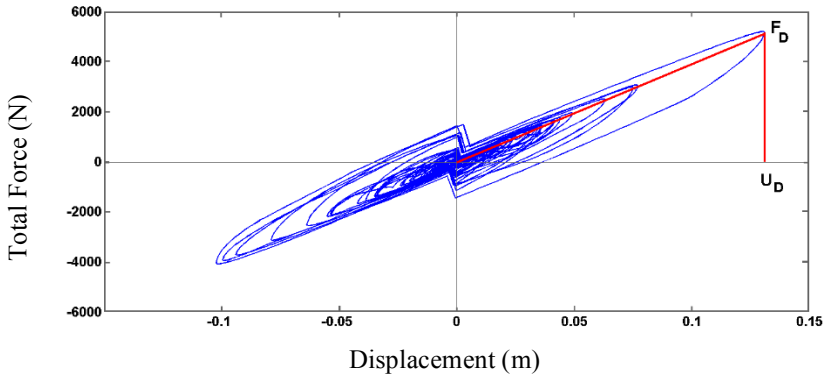

Figure 3-6 Force-displacement of the 2-4 device that adds 15% damping to the structure with T=1.0 s under LA01 ground motion.

Figure 3-7 shows the equivalent damping of the whole structure implementing the supplemental viscous damping of Equation 3-5 over the period range of 0.2-5.0 s under the 20 earthquakes of the SAC project. An empirical expression proposed to fit the results in Figure 3-7 for the 2-4 device is defined:

$$\xi_{eq} = aT^2 + bT + c \qquad (3\text{-}7)$$

$$a = 0.0383\xi^2 - 0.0231\xi + 0.001$$

$$b = -0.2537\xi^2 + 0.1968\xi - 0.0066$$

$$c = -0.0283\xi + 0.068$$

where T is the period of the structures and ξ is damping of the device.

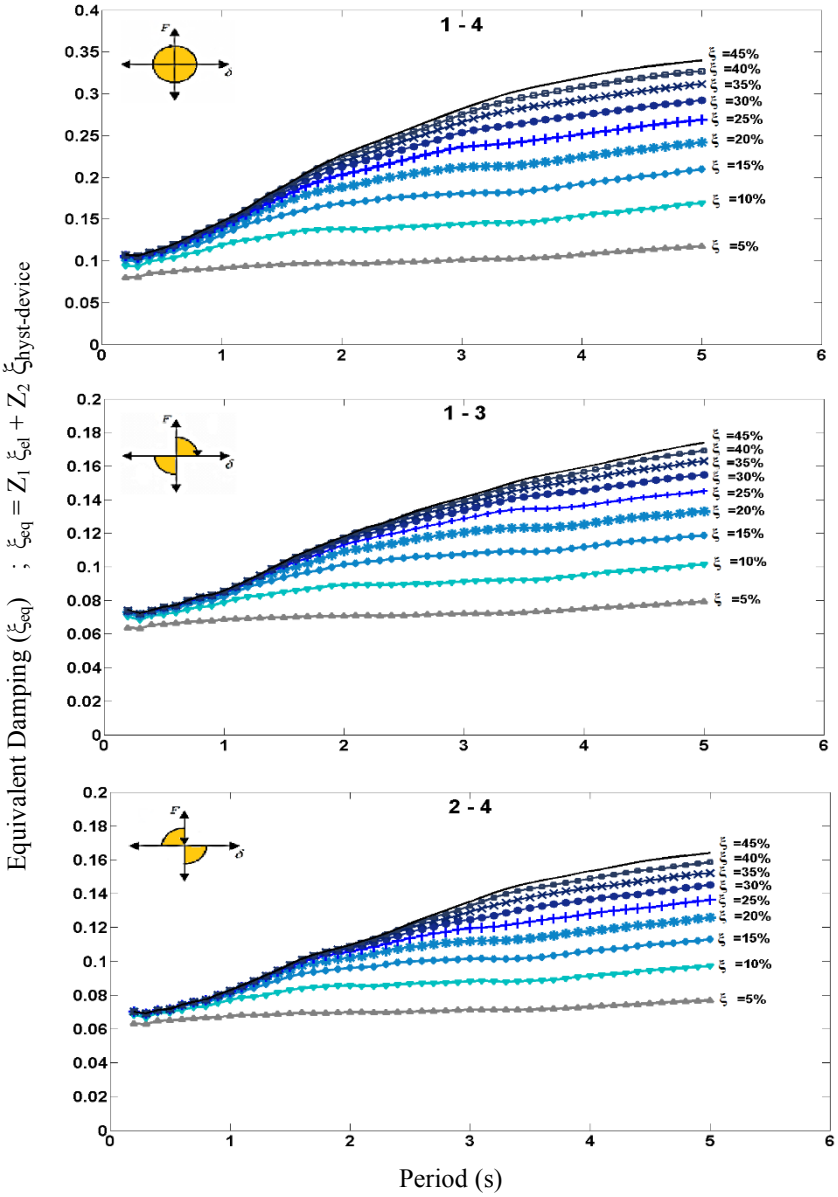

Figure 3-7. The equivalent damping of structures with the 1-4, 1-3 and 2-4 device that added 5%-45% damping (ξ).

Table 3-1 shows the maximum and minimum of equivalent damping ($\xi_{eq}=Z_1.\xi_{el}+Z_2.\ \xi_{hyst\text{-}device}$) for a structure utilizing a viscous damper (1-4 control law) and, separately, a 2-4 device and also expresses the reductions from the 2-4

device as a percentage of those achieved with the 1-4 device. Although the dissipative device hysteretic area of the 2-4 device is half that of the viscous damper (1-4 control law) device, the results show the equivalent damping of the 2-4 device is about 52%-80% of the viscous damper (the 1-4 device). This result is due to the non-linear relationship between these quantities.

Table 3-1. The maximum and minimum and difference of equivalent damping of structures (T=0.2- 5.0 s) with the 1-4 and 2-4 device.

ξ device	1-4 device (Viscous)		2-4 device		Percent of viscous damper(1-4) achieved by 2-4	
	Max ξ_{eq}	Min ξ_{eq}	Max ξ_{eq}	Min ξ_{eq}	([4]/[2])%	([5]/[3])%
[1]	[2]	[3]	[4]	[5]	[6]	[7]
5	11.76	7.98	7.92	6.33	67%	79%
10	16.93	9.30	10.14	6.84	60%	74%
15	20.95	9.97	11.87	7.01	57%	70%
20	24.16	10.23	13.31	7.12	55%	70%
25	26.88	10.40	14.50	7.16	54%	69%
30	29.20	10.48	15.48	7.19	53%	69%
35	31.13	10.53	16.29	7.21	52%	68%
40	32.67	10.57	16.93	7.22	52%	68%
45	33.96	10.61	17.39	7.23	51%	68%

Figure 3-8 shows the equivalent damping of structures with periods of 0.2-5.0s with 2-4 devices and 5%-45% added device damping ratio (ξ) and their RF_{ξ}. The results show that increasing the damping constant of the 2-4 device can significantly change the damping reduction factor, with structures with periods greater than 0.6s exhibiting more than 10% change in the RF_{ξ}. For example the RF_{ξ} of the structure with a period of 5.0 s implementing the 5% and 45% 2-4 semi-active viscous damper are 0.93 and 0.61, respectively (34% relative difference). However, increasing the damping of the device does not significantly

change the RF_{ξ} of low period structures, where structural periods are less than 0.6s.

In addition, if the semi-active 2-4 viscous device adds more than 10% damping to the structure, the RF_{ξ} values are more dependent on the structural period. For example, adding a 2-4 device with just 5% adding damping (ξ=5%) for all of the periods gives about a RF_{ξ} =0.9. However, RF_{ξ} values decrease more for higher periods than for lower ones when the 2-4 device adds the maximum 45% damping considered in this analysis to the structure. As before, this result indicates that devices with more than 10% damping reduces the response of structures with higher periods more so than for those with lower periods.

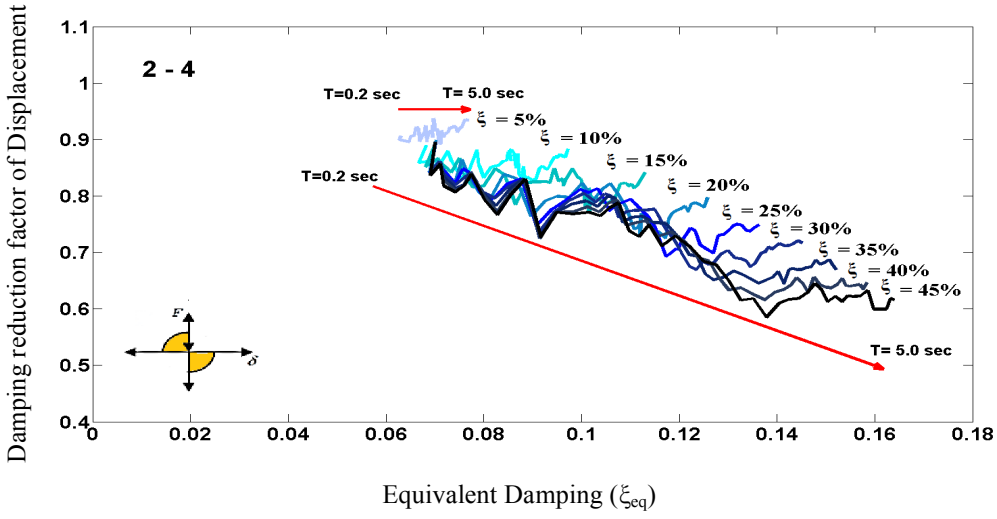

Figure 3-8. The damping reduction factor of displacement ($RF_{\xi\text{-}Sd}$) for the equivalent damping of 2-4 devices with different damping from T=0.2-5.0 s.

An expression proposed to fit the results in Figure 3-8 is defined:

$$RF_{area} = a\xi_{eq}^2 + b\xi_{eq} + c \qquad (3-8)$$

$$a = 3.37\xi^{-1.241}$$

$$b = -71.78\xi^2 + 59.46\xi - 16.87$$

$$c = -0.6836\xi + 1.4023$$

Therefore, as shown in Figure 3-2, the equivalent viscous damping, ξ_{eq}, could be used to calculate the RF_{ξ} of the structure and vice versa, enabling its use in standard, well-known design codes and procedures.

Table 3-2 shows the maximum and minimum damping reduction factor of S_d for the viscous damper (1-4 control law), per Chapter 2, and also expresses the reductions from the 2-4 device as a percentage of those achieved with the viscous device (1-4 control law). The smaller damping reduction factors indicate a large reduction in response due to the added damping. The results indicate that, although the 2-4 device has half of the area of the 1-4 device, the minimum RF_{ξ} of viscous damper (1-4 control law) is only 0.66-0.87 times that of the 2-4 device.

Table 3-2. The maximum, minimum and difference of the RF_{ξ} of structure with the 1-4 and 2-4 device.

ξ device	1-4 device		2-4 device		Percent of 1-4 viscous damper achieved by 2-4	
	Max $RF_{\xi area}$	Min $RF_{\xi area}$	Max $RF_{\xi area}$	Min $RF_{\xi area}$		
					([4]/[2]) %	([5]/[3])%
[1]	[2]	[3]	[4]	[5]	[6]	[7]
5	0.89	0.77	0.94	0.89	95%	87%
10	0.80	0.68	0.89	0.83	90%	82%
15	0.76	0.60	0.89	0.77	85%	78%
20	0.72	0.53	0.90	0.72	80%	73%
25	0.69	0.49	0.90	0.69	78%	70%
30	0.69	0.46	0.89	0.67	77%	69%
35	0.69	0.43	0.90	0.64	77%	67%
40	0.69	0.40	0.90	0.62	95%	87%
45	0.68	0.38	0.90	0.58	90%	82%

3.3.2. Eurocode

In this study, the modification damping factor, RF_{ξ} of the 2012 EC8 (Equation 3-2) is used, as suggested by Priestley et al. (Lin et al. 2003; Priestley et al. 2007a). The average reduction factors of 49 structures from periods from 0.2 s to 5.0 s with different damping ratios of added viscous damping are compared to the expression of Equation 3-2 in Figure 3-9. This averaging across all periods is undertaken for comparison to EC8, as this code does not incorporate structural period into its reduction factors. The results show Equation 3-2 estimates RF_{ξ} very reasonably.

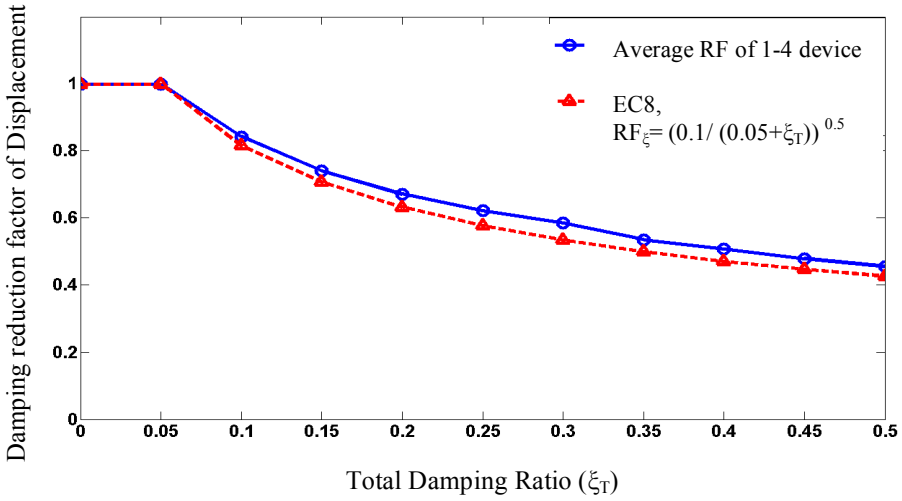

Figure 3-9. Damping Modifiers to elastic spectral displacements compared to EC8.

Equation 3-2 is used for adding a viscous damper (1-4 device) to the structure. However, Equation 3-2 can be used to find the relationship between adding the semi-active viscous damper to the structure and the corresponding damping

reduction factor. Therefore, the effective damping of the 2-4 device being added to the structure can be estimated using Equation 3-2 as follows:

$$\xi_T = \frac{0.1}{RF^2} - 0.05 \tag{3-9}$$

$$\xi_T = \xi_l + \xi_{eff} \tag{3-10}$$

$$\xi_{eff} = \frac{0.1}{RF^2} - 0.1 \tag{3-11}$$

If the analytical results of the RF_ξ values obtained in the previous section in Figure 3-3 are used in Equation 3-11, it becomes:

$$\xi_{eff} = 0.2028\,\xi + 0.0159 \tag{3 –12}$$

and

$$\xi = 4.93\,\xi_{eff} - 0.078 \tag{3-13}$$

Thus, ξ_{eff} can be estimated considering the nominal damping capacity, ξ, of the devices used, which can then be used to calculate the value of RF_ξ, and vice versa.

3.3.3. Smoothing of time-history results

Figure 3-10 presents linear, smoothed curves approximations of the damping reduction factor of spectral displacement (S_d) and base shear (V_b) as derived in Figure 3-3, when the total damping of the structure increases by increasing the added damping capacity of the 2-4 device. Simplified analytical expressions of

such displacement damping reduction factors, $RF_{\xi\text{-}Sd}$, can be derived for both the analysis and design of SDOF systems incorporating semi-active viscous dampers with the 2-4 control law, yielding:

$$\begin{cases} RF_{Smoothing} = (0.048\,(\xi_{el}+\xi)^{-0.5} - 0.15) * T + 0.9 & T \le 2.7\,s \\ RF_{Smoothing} = \left(\frac{0.07}{0.02+(\xi_{el}+\xi)}\right)^{0.22} & 2.7 < T \le 5\,s \end{cases} \quad (3\text{-}14)$$

Therefore, for a target level of displacement damping reduction factor, RF_{ξ}, the required damping of the device can be obtained by inverting the above expression, yielding:

$$\begin{cases} \xi = \left(\frac{0.048T}{RF_{Smoothing}-0.9+0.15T}\right)^2 - 0.05 & T \le 2.7\,s \\ \xi = \left(0.07 - 0.02\,\sqrt[0.22]{RF_{Smoothing}}\right) RF_{Smoothing}^{\,-4.54} & 2.7 < T \le 5\,s \end{cases} \quad (3\text{-}15)$$

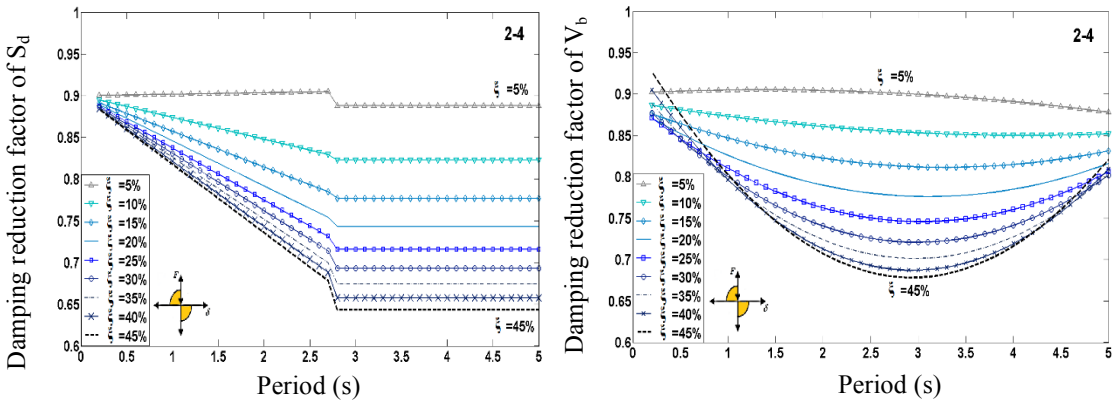

Figure 3-10. Smoothed damping Reduction Factor of S_d and V_b when the 2-4 device is incorporated into elastic SDOF structures with period from 0.2 s to 5.0 s.

Moreover, an expression of V_b proposed in Figure 3-10 for RF_ξ of V_b is defined:

$$RF_{\xi-Vb} = aT^2 + bT + c \tag{3-16}$$

$$a = 0.088\xi - 0.0065$$

$$b = -0.5\xi + 0.031$$

$$c = 1.08 * \xi^2 - 0.38\xi + 0.9$$

3.3.4. Comparison of the three methods

The three considered expressions for finding RF_ξ when a semi-active device with a 2-4 hysteresis loop is added to a structure are compared, and the full time-history simulation results. These results are presented in Figure 3-11 for 15%, 25%, 35% and 45% added damping. The outcomes indicate all three proposed methods provide good estimates of the results obtained from the full simulation, where directly calculated results are those from time history analysis.

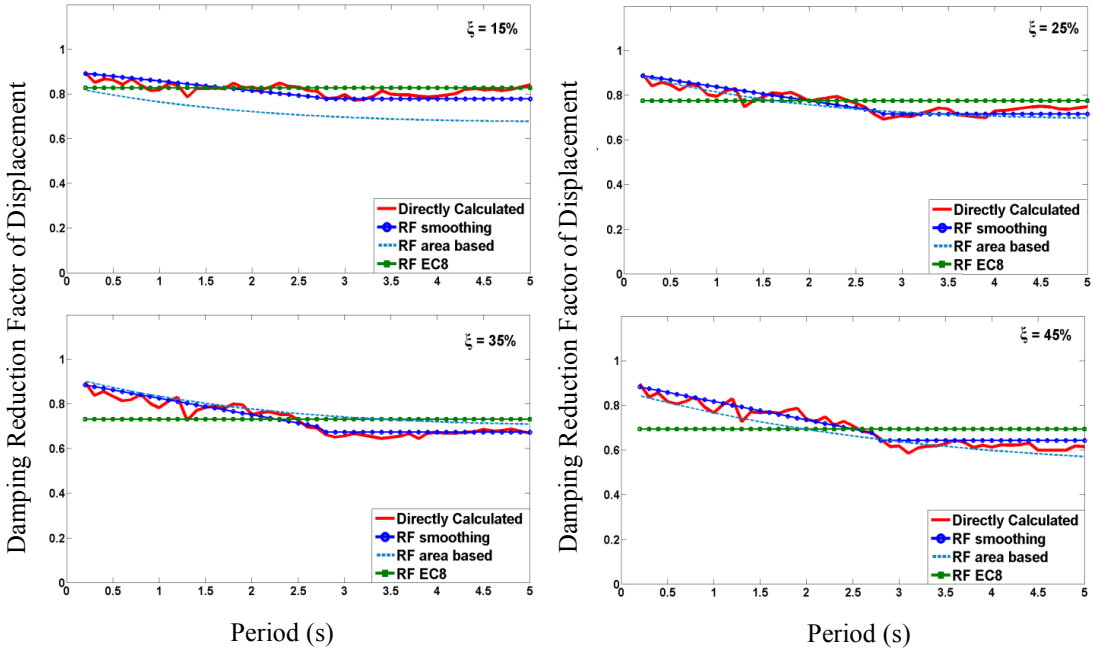

Figure 3-11. Comparing three formulas for calculating RF_ξ of structures with periods from 0.2-5.0 sonds and the RF_ξ directly calculated from the time-history analyses.

For example, the RF_ξ of a structure with period of 2.5 seconds with 35% added damping from a 2-4 device is 0.75 , 0.73 and 0.71 using the area based method (Equation 3-9), EC8 method (Equation 3-2) and smoothing method (Equation 3-14), respectively. The actual damping reduction factor from simulation, directly calculated from the time history, is 0.72. This value is well estimated by all three methods.

3.4. Design and analysis procedure

Figure 3-12 shows the flowchart for calculating the value of RF_ξ for a structure when a number, N, of 2-4 semi-active viscous dampers are added to the system. For example, five 2-4 semi-active dampers, each with 5% added damping, are

installed to a structure with a period of 2.0 s. Therefore, the total damping of the devices is 25%. The ξ_{eff} is 6.66% (Equation 3-12) and RF_{ξ} is 0.75, 0.77 and 0.77 using area based method (Equation 3-8), Eurocode method (Equation 3-2) and smoothing method (Equation 3-14), respectively. The procedure is summarized in Figure 3-12. In addition, the RF_{ξ} for V_b is 0.76 (Equation 3-16).

Damping reduction factor determination for 2-4 viscous damper

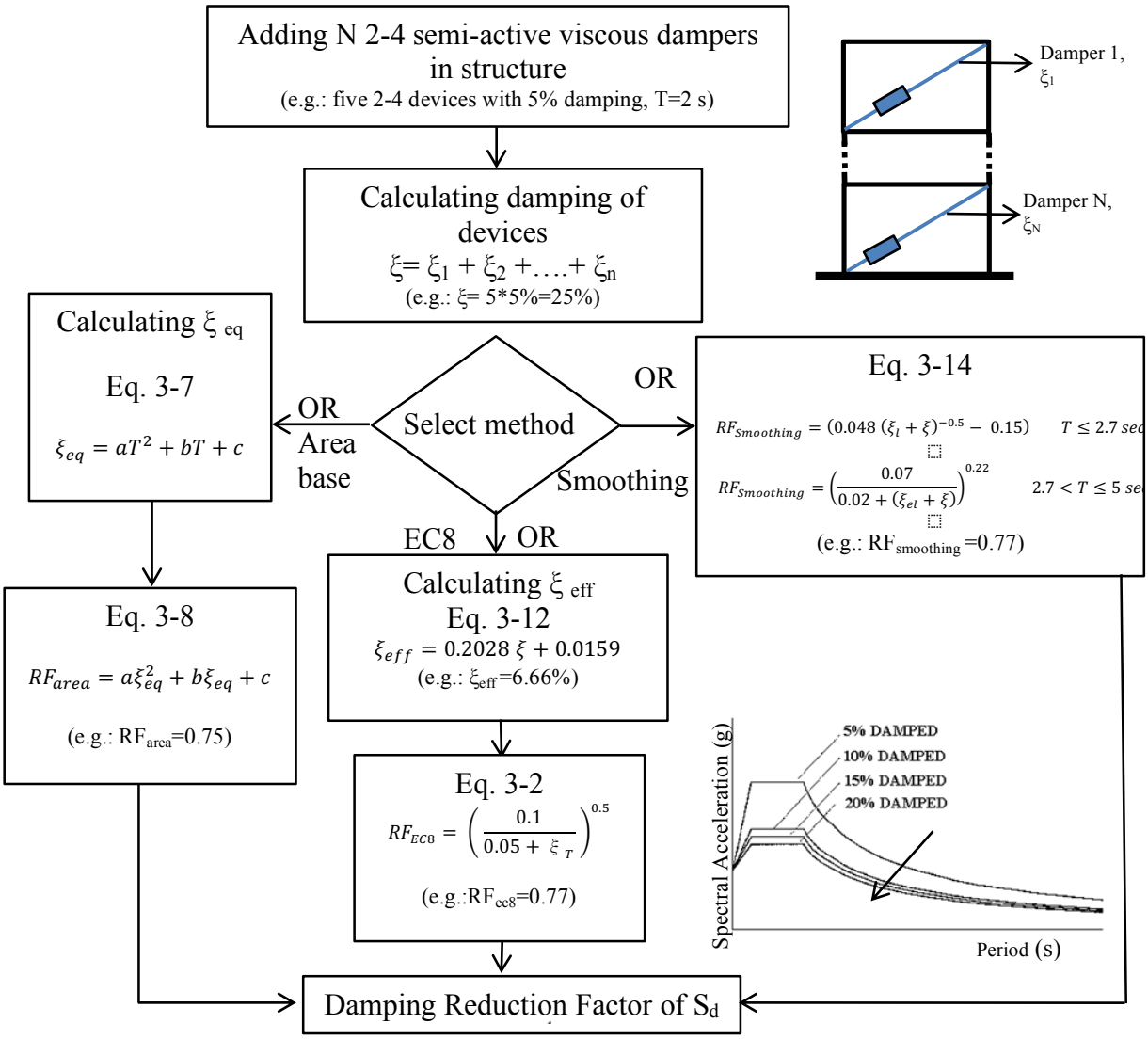

Figure 3-12. The flowchart for calculating the RF_{ξ} when the N 2-4 semi-active viscous dampers are added to the system.

Required 2-4 viscous damping devices to achieve a desirable RF_{ξ}

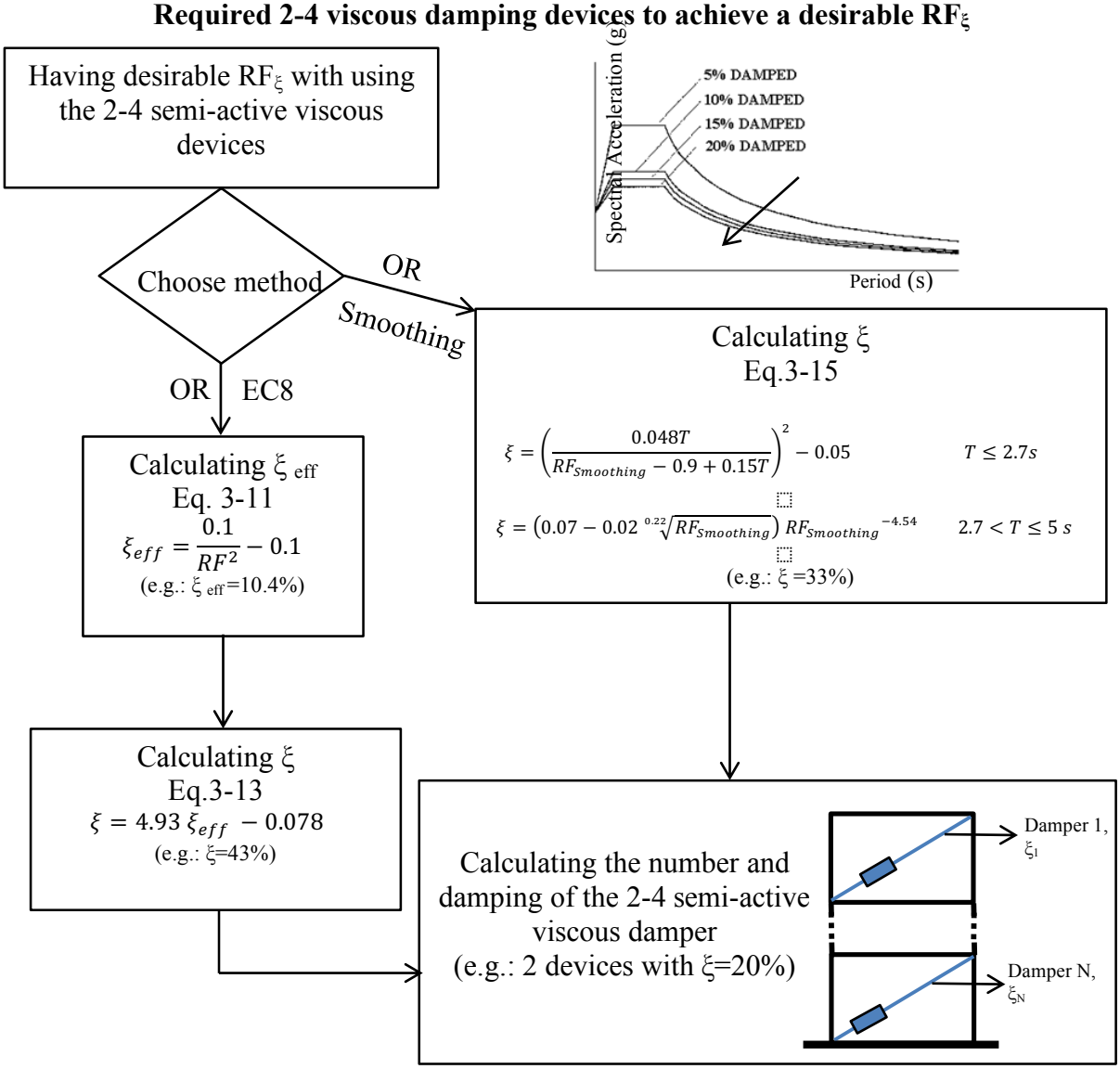

Figure 3-13. Flowchart to find out the required dampers to have a desirable damping Reduction Factor.

Figure 3-13 shows the flowchart for calculating the required size and number of 2-4 semi-active viscous dampers to achieve the desired damping reduction factor (RF_{ξ}). For instance, assume a 0.70 displacement damping reduction factor of 0.70 for a structure with T=3.0 seconds is desired. The effective damping of the device using the EC8 method is 10.4% by Equation 3-11. Therefore, a device or devices

with 33% and 43% damping are needed, using smoothed curve (Equation 3-15) and EC8 method (Equation 3-13), respectively. For an ~ 40% device damping ratio, about average of 33% and 43% damping, two devices with 20% added damping or four devices with 10% added damping could be used. In addition, the RF_{ξ} of the total base shear of this structure with these 2-4 devices adding 40% more damping is about 0.68 (Equation 3-16).

3.5. Summary

This chapter presented the performance, design and analysis of linear SDOF systems with added semi-active viscous dampers that reshape structural response. Damping reduction factor (RF_{ξ}) spectra in terms of maximum displacement (S_d) and total base-shear (V_b) have been derived to determine the impact and efficiency of different semi-active viscous dampers on seismic structural performance, over a range of ground motions with equal probability of occurrence. The results of this first part of the chapter, as per Chapter 2, have shown that only the 2-4 device, providing damping in the second and fourth quadrants, allows reduced structural displacement with no increase in base shear, and thus overturning moment and risk of foundation damage. This outcome implies that the 2-4 semi-active viscous damper potentially offers the greatest

robustness, and thus minimum variability in risk, over all type of design level events.

The second and more important part of the analysis presented derived the relationship between damping of the 2-4 semi-active viscous device (ξ) and structural damping reduction factor, RF_{ξ}. Although the area of the 2-4 device is half that of a typical viscous damper device (1-4 device), the results show that the equivalent damping and RF_{ξ} of the 2-4 device is about 52%-80% and 60%-90% of the standard viscous damper (or the 1-4 device), respectively. Finally, a simple method to determine the effect of the 2-4 device when added to new or existing (SDOF-equivalent) structural systems has been provided to enable easy uptake in existing design procedure.

3.6. Reference:

Bisch P et al. (2012) Eurocode 8: Seismic Design of Buildings Worked Examples Luxembourg: Publications Office of the European Union

Blandon CA, Priestley M (2005) Equivalent viscous damping equations for direct displacement based design Journal of earthquake Engineering 9:257-278

Chopra AK (1995) Dynamics of structures vol 3. Prentice Hall New Jersey,

Lin Y, Tsai M, Hwang J, Chang K (2003) Direct displacement-based design for building with passive energy dissipation systems Engineering structures 25:25-37

Martinez-Rodrigo M, Romero M (2003) An optimum retrofit strategy for moment resisting frames with nonlinear viscous dampers for seismic applications Engineering Structures 25:913-925

Pampanin S, Marriott D, Palermo A (2010) PRESSS design handbook. NZCS,

Priestley M, Calvi G, Kowalsky M Direct displacement-based seismic design of structures. In: 2007 NZSEE Conference, 2007a.

Priestley M, Calvi G, Kowalsky M Direct displacement-based seismic design of structures. In: 5th New Zealand Society for Earthquake Engineering Conference, 2007b.

Priestley M, Grant D (2005) Viscous damping in seismic design and analysis Journal of Earthquake Engineering 9:229-255

Rama Raju K, Ansu M, Iyer NR (2014) A methodology of design for seismic performance enhancement of buildings using viscous fluid dampers Structural Control and Health Monitoring 21:342-355 doi:10.1002/stc.1568

Sommerville P, Smith N, Punyamurthula S, Sun J (1997) Development of ground motion time histories for phase II of the FEMA/SAC Steel Project, SAC Background Document Report SAC. BD-97/04,

Taylor D, Washiyama Y Fluid Viscous Dampers in Mega Brace Elements for the 57- Floor Torre Mayor Building at Mexico City. In: Proceedings of the JSSI 10th Anniversary Symposium, Tokyo Institute of Technology, , Tokyo, Japan, 2004.

Chapter 4: Seismic behaviour of a self-centering system with 2-4 viscous damper[1]

Self-centering dissipating systems combine supplemental damping with re-centering elements to achieve low damage performance in large seismic events. An ideal supplemental damping device would offer reductions in displacement, total base shear and acceleration, three quantities that typically trade off. Prior chapters have shown a 2-4 viscous damper provides an effective dissipation solution in this context. This chapter demonstrates the efficacy of a 2-4 viscous device in self-centering rocking structures with a bi-linear elastic response compared with typical viscous dampers and 1-3 viscous devices.

In the last decade, rocking mechanisms and self-centering have become well known as a structurally efficient and robust technology for seismic-resistant buildings (Kam et al. 2010; Marriott et al. 2008; Marriott et al. 2009; Priestley 1991; Sarti et al. 2015). Therefore, to achieve adequate energy dissipation capacity under seismic excitations, various alternative energy dissipation elements, hysteretic, viscous or visco-elasto-plastic, need to be added in series and/or in parallel to self-centering systems (Kam et al. 2010; Mander et al. 2009; Marriott et al. 2008; Marriott et al. 2009; Rodgers et al. 2010).

[1] Based on: Hazaveh, N. K., G. W. Rodgers, J. G. Chase, and S. Pampanin. (2017). Seismic behaviour of a self-centering system with 2-4 viscous damper, Journal of Earthquake Engineering, in press.

Among supplemental dissipation devices, viscous dampers have been widely used in rocking wall and post-tensioned rocking bridge piers to improve the seismic behaviour of these self-centering system, as shown in Figure 4-1 (Kam et al. 2010; Marriott et al. 2008; Marriott et al. 2009). Viscous dampers dissipate significant energy, but their reaction loads can increase foundation and overall base shear demands, reducing the ability to use them broadly in retrofit without significant added cost (Filiatrault et al. 2001; Hazaveh et al. 2016b; Kam et al. 2008; Kam et al. 2010; Lin and Chopra 2002; Miyamoto and Singh 2002; Vargas and Bruneau 2007). Thus, on the basis of a traditional performance-based seismic design and retrofit philosophy, designers are challenged by the difficult trade-off between costs and acceptable damage, or targeted performance.

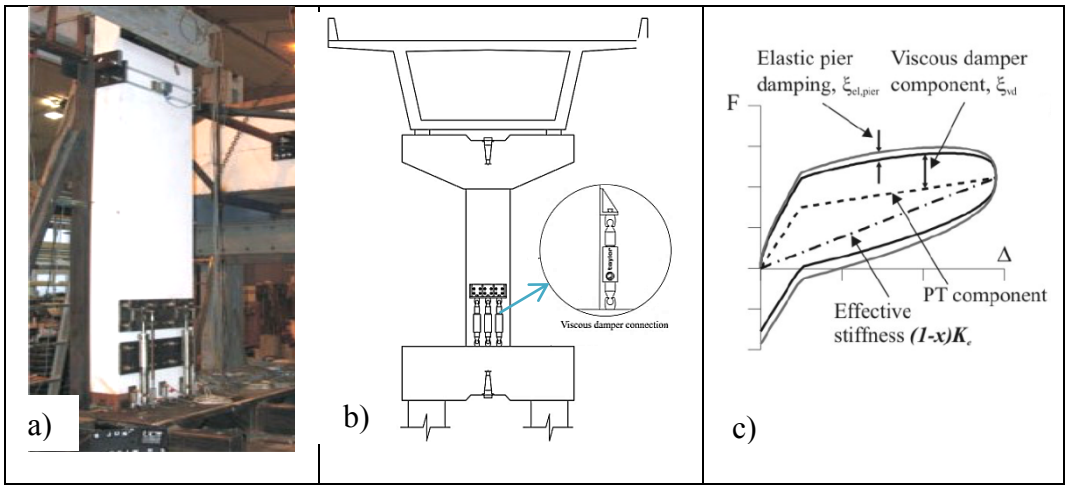

Figure 4-1 (a) experimental test of rocking wall with viscous damper (Marriott et al. 2008), (b) using viscous damper in pier of bridge (Marriott et al. 2008), (c) Decomposition of the transverse response of a post-tensioned bridge system with supplementary viscous (Marriott et al. 2008).

To address these issues, Hazaveh et al. (2015; 2016a; 2016b) introduced and examined two types of semi-active viscous damper concepts, as discussed in

Chapters 2-3. Based on semi-active resettable stiffness devices (Mulligan et al. 2009; Rodgers et al. 2007), a 1-3 viscous damper provides resisting forces only in the first and third quadrants of the force-displacement plot. Similarly, a 2-4 viscous damper provides damping in the second and fourth quadrants. Spectral analysis in Chapter 2 shows typical viscous dampers increase the base shear of long period linear structures, typically greater than 2.7 s (Hazaveh et al. 2016b). However, adding a 2-4 viscous damper decreases base shear and displacement for all periods (Hazaveh et al. 2015; Hazaveh et al. 2016b; Mulligan et al. 2009; Rodgers et al. 2007). However, the effect of this 2-4 viscous damper was only investigated on linear elastic structures (Hazaveh et al. 2015; Hazaveh et al. 2016b). Therefore, there is a need to investigate the seismic behaviour of self-centering system with these devices to validate this potential and growing area before application, including the need for design method to enable uptake.

Hazaveh et al. (Hazaveh et al. 2016b) also suggested a method to calculate the damping reduction factor of linear structures with a 2-4 viscous damper, as discussed in Chapter 3. However, the resulting design procedure only considered linear elastic structures, and thus does not necessarily generalize to other structural systems, particularly those considering ductility. Therefore, to enable more widespread application of 2-4 viscous dampers in self-centering systems, suitable design procedures are also required.

This chapter addresses these needs by evaluating the effect of typical (1-4), 1-3 and 2-4 viscous damping devices in self-centering SDOF rocking systems at a

number of periods. The goal is to identify the range of potential reductions in displacement (structural demand), base shear (foundation demand) and acceleration (contents demand) with this type of device in comparison to a baseline case without supplemental damping. The analysis uses all 60 earthquake ground motions from the SAC LA low, medium and high suites (Somerville and Venture 1997). The results should also indicate the distribution of possible reductions for ground motions with different probabilities of occurrence. Finally, this study uses these results to prepare a robust and simple design and analysis process to evaluate the effect of adding the 2-4 device to rocking structural systems, as an extension to the one presented in Chapter 3.

4.1. Modelling and analysis methods

This chapter investigates the relative effectiveness of a traditional viscous damper, and the 1-3 and 2-4 viscous dampers on the seismic response of self-centering SDOF structural systems. Figure 4-2, illustrates the overall expected impact of three types of viscous dampers on the bilinear elastic structural response. The enclosed area is the energy dissipated per cycle due to supplemental damping. The self-centering rocking behaviour is modelled numerically with an idealized bi-linear elastic spring (Priestley and Tao 1993).

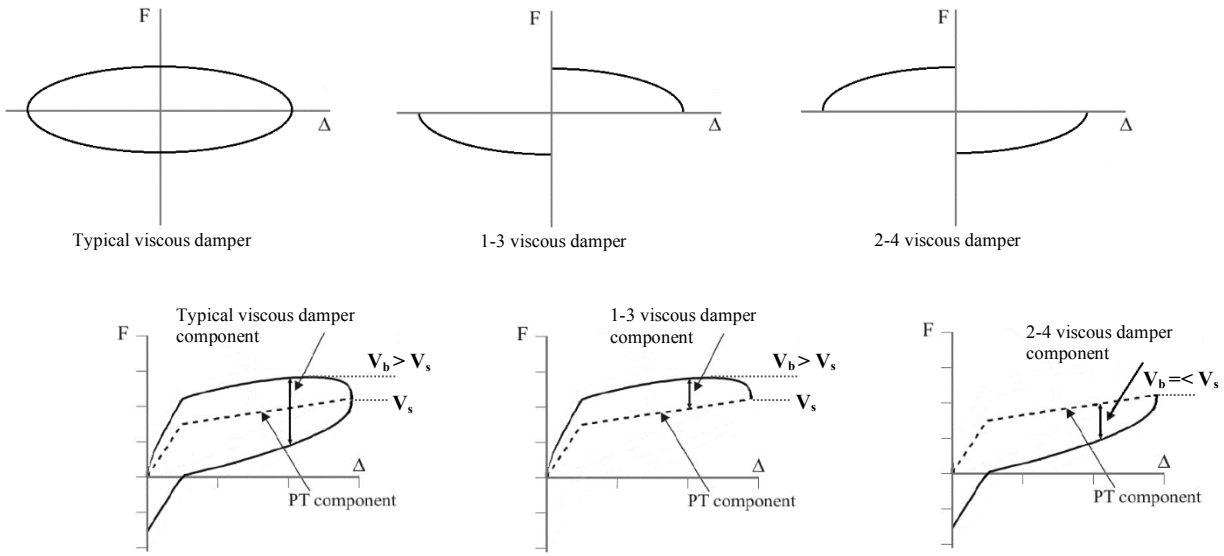

Figure 4-2. Schematic hysteresis for a typical, 1-3, and 2-4 viscous damper device, V_b = total base shear, V_S = base shear for undamped structure. $V_b > V_S$ indicates an increase due to the additional damping.

The concept of force reduction factor (R) and ductility (μ), which are fundamental tools in current seismic design are shown in Figure 4-3. For the equal displacement approximation, considered in this research, the displacement ductility factor is equal to the force-reduction factor (Priestley et al. 2007):

$$\mu = \frac{\Delta_{max}}{\Delta_y} = R = \frac{F_{el}}{F_R} \tag{4-1}$$

where F_{el} is the maximum force developed at peak displacement, Δ_{max}, for a linear structure (labelled 1 in Figure 4-3) and F_R is maximum force with force-reduction factor of R at yielding displacement Δ_y (labelled 2 and 4 in Figure 4-3).

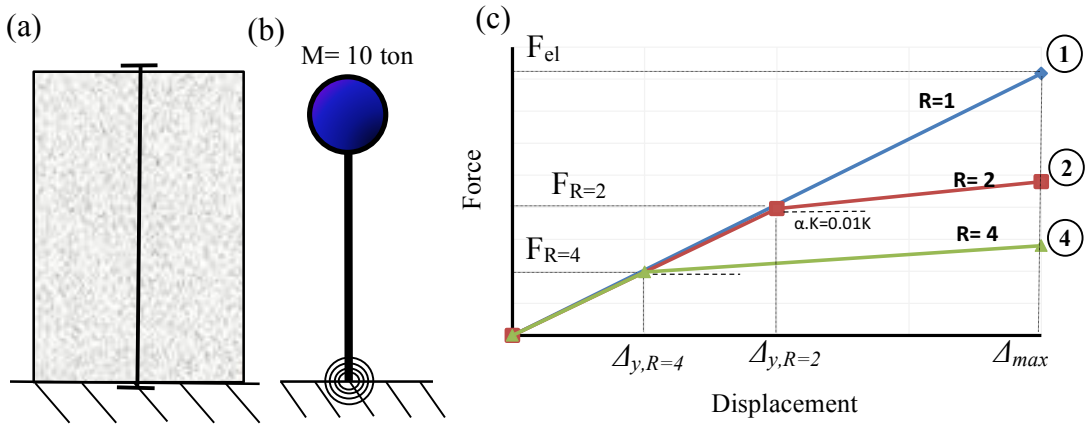

Figure 4-3. Prototype self-cantering wall; (b) simple SDOF representation; (c) The equal displacement approximation, the structure (1) is linear structure and the structure (2) and (4) have bilinear behaviour with ductility of 2 and 4, respectively.

In this chapter, structures are designed as an ordinary building in Wellington on site class C (NZS1170 2004) with force reduction factors (R) of 2.0 and 4.0 for periods from 0.5 to 4.5 s to capture the most important part of the design spectrum. Figure 4-4 shows the basic design data for all 13 test cases covering this range of periods. The initial linear elastic stiffness is computed from the target period using a constant mass of 10,000 kg. Elastic displacement is calculated from dividing the design displacement by the desired R value. The SDOF systems are taken to represent a prototype self-centering wall (Figure 4-3.a-b), designed to a drift of 2% and the post-rocking stiffness is defined as 1% of the initial elastic stiffness. The range of case-study structures using the same values of R and M in design creates a collection of 34 cases (17 periods times 2 different R-factors) to act like a traditional spectral analysis approach.

Period, T(s)	Design Displacement $S_d(T)$[mm]	Acceleration design coefficient $C_d(T)$ [g]
0.1	2.9	1.17
0.2	11.7	1.17
0.3	26.1	1.17
0.4	37.6	0.94
0.5	49.7	0.80
0.6	62.4	0.70
0.7	75.7	0.63
0.8	89.4	0.56
0.9	103.6	0.51
1	118.1	0.47
1.5	196.3	0.36
2	293.9	0.30
2.5	406.7	0.26
3	535.3	0.24
3.5	582.6	0.19
4	629.7	0.16
4.5	653.4	0.13

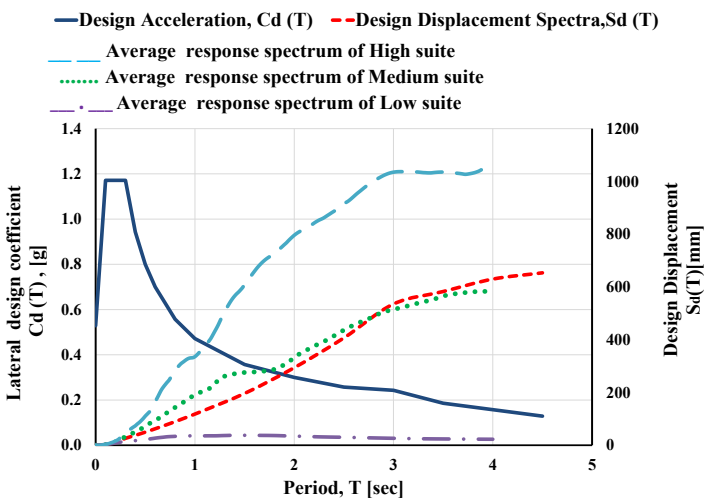

Figure 4-4. Elastic design displacement and acceleration spectra co-ordinates (5% damped), Z=0.4, soil C, Sp=1.0, D<2km (NZS1170 2004) and average displacement response spectrum of low, medium and high suit.

The model structures include inherent structural equivalent viscous damping of 5%. The damping constant, C, for each supplemental viscous damping device was determined based on a traditional viscous damper providing 15% equivalent viscous damping, as in the main analysis of Chapter 2. Thus, based on Figure 4-2, a 1-3 and 2-4 viscous damper encloses approximately half the area of a traditional viscous damper. As such, the 1-3 and 2-4 devices provide less equivalent viscous damping, as they provide resistive forces for a smaller portion of the response cycle. The same C value is then used for all supplemental viscous devices.

The analysis of each test structure utilizes all 60 earthquakes from the 3 earthquake suites of the SAC project (Somerville and Venture 1997). Each suite is comprised of 10 different time histories with two orthogonal directions for each

history. The 3 suites contain ground motions having probabilities of exceedance of 50%, 10% and 2% in 50 years in the Los Angeles region, denoted the low, medium and high suites, respectively. Each suite is comprised of 10 different time histories with two orthogonal directions for each history (Table 4-1). Figure 4-4 shows average displacement spectrums of all suites. Using suites of ground motions, rather than a single individual event, eliminates the likelihood of erroneous conclusions due to variability in ground motions compared to structural dynamics. It is also allows risks of exceedance to be determined for a range of specific probabilities of occurrence when comparing the impact of different devices or retrofits.

Table 4-1 Detail of selected Los Angeles ground motions with probability of exceedance of 50%, 10% and 2% in 50 (Somerville and Venture 1997).

SAC Name	Record	Earthquake Magnitude	Distance (km)	Scale Factor	Duration (s)	PGA (cm/s^2)
LA01	Imperial Valley,1940, El Centro	6.9	10	2.01	39.38	452.03
LA02	Imperial Valley,1940, El Centro	6.9	10	2.01	39.38	662.88
LA03	Imperial Valley,1979, Array #05	6.5	4.1	1.01	39.38	386.04
LA04	Imperial Valley,1979, Array #05	6.5	4.1	1.01	39.08	478.65
LA05	Imperial Valley,1979, Array #06	6.5	1.2	0.84	39.08	295.69
LA06	Imperial Valley,1979, Array #06	6.5	1.2	0.84	39.08	230.08
LA07	Landers,1992, Barstow	7.3	36	3.2	79.98	412.98
LA08	Landers,1992, Barstow	7.3	36	3.2	79.98	417.49
LA09	Landers,1992, Yermo	7.3	25	2.17	79.98	509.7
LA10	Landers,1992, Yermo	7.3	25	2.17	79.98	353.35
LA11	Loma Prieta, 1989, Gilroy	7	12	1.79	39.08	652.49
LA12	Loma Prieta, 1989, Gilroy	7	12	1.79	39.08	950.93
LA13	Northridge, 1994, Newhall	6.7	6.7	1.03	59.98	664.93
LA14	Northridge, 1994, Newhall	6.7	6.7	1.03	59.98	664.93
LA15	Northridge, 1994, Rinaldi RS	6.7	7.5	0.79	14.94	523.3
LA16	Northridge, 1994, Rinaldi RS	6.7	7.5	0.79	14.94	568.58
LA17	Northridge, 1994, Sylmar	6.7	6.4	0.99	59.98	558.43
LA18	Northridge, 1994, Sylmar	6.7	6.4	0.99	59.98	801.44
LA19	North Palm Springs, 1986	6	6.7	2.97	59.98	999.43
LA20	Northridge, 1994, Sylmar	6	6.7	2.97	59.98	967.61
LA21	1995 Kobe	6.9	3.4	1.15	59.98	1258

LA22	1995 Kobe	6.9	3.4	1.15	59.98	902.75
LA23	1989 Loma Prieta	7	3.5	0.82	24.99	409.95
LA24	1989 Loma Prieta	7	3.5	0.82	24.99	463.76
LA25	1994 Northridge	6.7	7.5	1.29	14.95	851.62
LA26	1994 Northridge	6.7	7.5	1.29	14.95	925.29
LA27	1994 Northridge	6.7	6.4	1.61	59.98	908.7
LA28	1994 Northridge	6.7	6.4	1.61	59.98	1304.1
LA29	1974 Tabas	7.4	1.2	1.08	49.98	793.45
LA30	1974 Tabas	7.4	1.2	1.08	49.98	972.58
LA31	Elysian Park (simulated)	7.1	17.5	1.43	29.99	1271.2
LA32	Elysian Park (simulated)	7.1	17.5	1.43	29.99	1163.5
LA33	Elysian Park (simulated)	7.1	10.7	0.97	29.99	767.26
LA34	Elysian Park (simulated)	7.1	10.7	0.97	29.99	667.59
LA35	Elysian Park (simulated)	7.1	11.2	1.1	29.99	973.16
LA36	Elysian Park (simulated)	7.1	11.2	1.1	29.99	1079.3
LA37	Palos Verdes (simulated)	7.1	1.5	0.9	59.98	697.84
LA38	Palos Verdes (simulated)	7.1	1.5	0.9	59.98	761.31
LA39	Palos Verdes (simulated)	7.1	1.5	0.88	59.98	490.58
LA40	Palos Verdes (simulated)	7.1	1.5	0.88	59.98	613.28
LA41	Coyote Lake, 1979	5.7	8.8	2.28	39.38	578.34
LA42	Coyote Lake, 1979	5.7	8.8	2.28	39.38	326.81
LA43	Imperial Valley, 1979	6.5	1.2	0.4	39.08	140.67
LA44	Imperial Valley, 1979	6.5	1.2	0.4	39.08	109.45
LA45	Kern, 1952	7.7	107	2.92	78.6	141.49
LA46	Kern, 1952	7.7	107	2.92	78.6	156.02
LA47	Landers, 1992	7.3	64	2.63	79.98	331.22
LA48	Landers, 1992	7.3	64	2.63	79.98	301.74
LA49	Morgan Hill, 1984	6.2	15	2.35	59.98	312.41
LA50	Morgan Hill, 1984	6.2	15	2.35	59.98	535.88
LA51	Parkfield, 1966, Cholame 5W	6.1	3.7	1.81	43.92	765.65
LA52	Parkfield, 1966, Cholame 5W	6.1	3.7	1.81	43.92	619.36
LA53	Parkfield, 1966, Cholame 8W	6.1	8	2.92	26.14	680.01
LA54	Parkfield, 1966, Cholame 8W	6.1	8	2.92	26.14	775.05
LA55	North Palm Springs, 1986	6	9.6	2.75	59.98	507.58
LA56	North Palm Springs, 1986	6	9.6	2.75	59.98	371.66
LA57	San Fernando, 1971	6.5	1	1.3	79.46	248.14
LA58	San Fernando, 1971	6.5	1	1.3	79.46	226.54
LA59	Whittier, 1987	6	17	3.62	39.98	753.7
LA60	Whittier, 1987	6	17	3.62	39.98	469.07

Reduction factors (RFs) for structural displacement (S_d), base shear (V_b) and acceleration (S_a) demand are evaluated as a ratio to the baseline (no-device) case at the same level of R and structural period, for each ground motion. They specifically evaluate the range of potential reductions in response and associated

risk of damage due to using these devices. These multiplicative RFs enable easy comparison of the different devices relative to the structural design case. Hence, the results can be applied to any sized structure, as they are only dependent on the device type, standard period, and damping of the device.

RFs less than 1.0 indicate a reduction in the response metric, while RFs greater than 1.0 indicate an increase in response. For each ground motion, RFs are determined, yielding 20 per suite. The median results are presented (50% risk), but any level could be chosen.

4.2. Results and discussion

Figure 4-5 shows the median structural displacement (RF_{Sd}) and base shear (RF_{vb}) reduction factors versus period for the 13 self-centering SDOF structures (T=0.1-4.5 s) with R = 2.0 and 4.0, as shown in Figure 4-4. RF_{Sd} is similar for R=2 and 4, but results differ significantly in all cases for RF_{vb}. As expected, the typical viscous damper (1-4 device) offers the greatest displacement reduction as it has the biggest area enclosed within the device hysteretic loop in Figure 4-2, but increases the overall base shear by the largest amount for almost all periods, in recompense.

For example, for a period of 3.0 s, $RF_{vb} \approx 3.0$ for the typical viscous device, indicating total base shear with the viscous damper is three times that of the

uncontrolled (no device) case. Thus, while adding a viscous damper in linear structures increases base shear only for high periods above 2.7 s (Hazaveh et al. 2016b), for bi-linear systems the base shear increases for almost all periods. Similarly, the 1-3 device has RF_{Sd} <1.0 and RF_{vb} >1.0 for most periods. However, the 1-3 viscous device reduces displacement less than the 1-4 typical viscous damper, as the area enclosed with the device hysteretic loop is approximately half the size, as shown in Figure 4-2. Only the low suite with R=2 offers reduced displacement with $RF_{vb} \approx 1.0$. All other cases trade off reduced displacement with increased base shear for typical viscous damping and a 1-3 device.

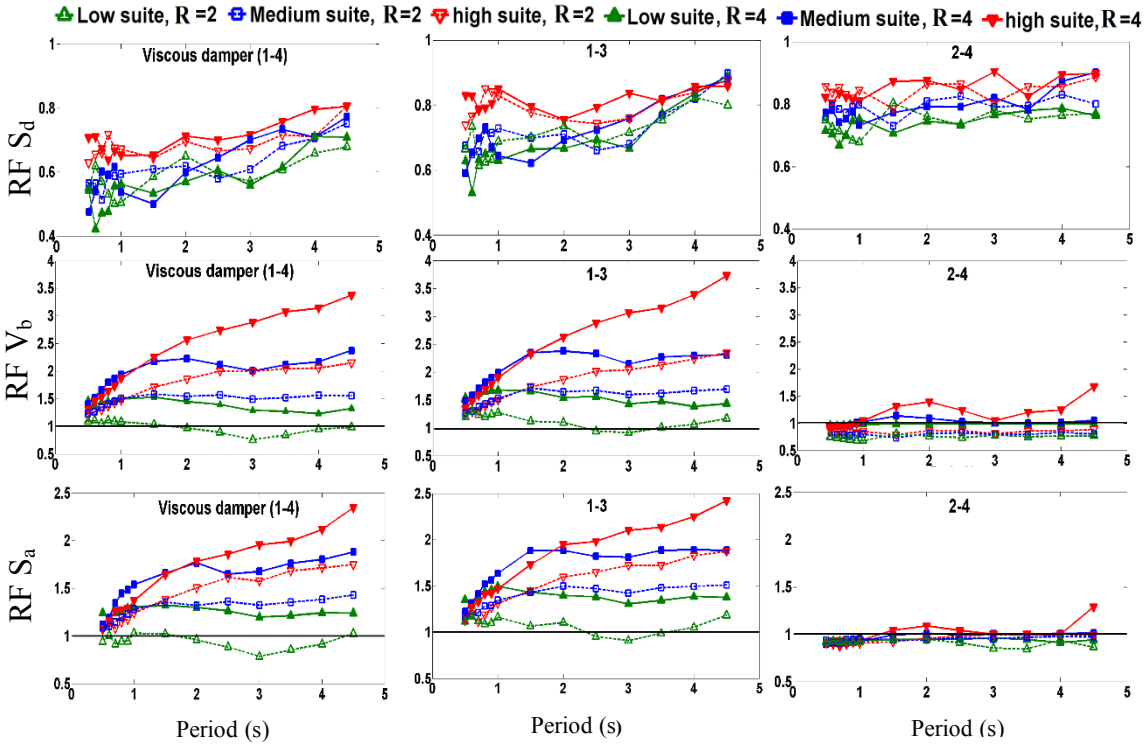

Figure 4-5. The median damping reduction factor of structural displacement, total base shear and acceleration of structures with periods 0.5s to 4.5 s and R of 2.0 and 4.0 with three type viscous devices, with values of 5% additional damping under low, medium and high suite ground motion.

In contrast, the 2-4 viscous device has RF_{Sd} <1.0 and RF_{vb} <1.0 in almost all cases. The exception is some select results with RF_{vb} >1.0, but by a much lesser amount than the 1-3 and typical viscous devices, and only for the high-velocity excitations in the high suite ground motions. In these specific few cases, the damper resisting force in quadrants 2 and 4 exceeds the standard structural restoring forces in quadrants 1 and 3, resulting in an increase in the total base shear. For example, the total base shear of the structure with the period of 2.0 s and R=4 under the LA38 earthquake with the 2-4 device increased for this reason, is illustrated in Figure 4-6. Hence, the 2-4 device offers reduced displacement and reduced base shear in all cases for all but the largest near field events with lowest probability of occurrence.

Overall, the 2-4 viscous device provides RF_{sd} and $RF_{vb} \leq 1.0$ at levels that are relatively constant across periods. The 2-4 viscous damper approach thus offers the minimum variability in median level risk and thus the greatest robustness across structural periods, to a level not available from the other two devices considered. More specifically, the 2-4 viscous damper offers minimal risk of increased foundation demand along with reduced displacement demands.

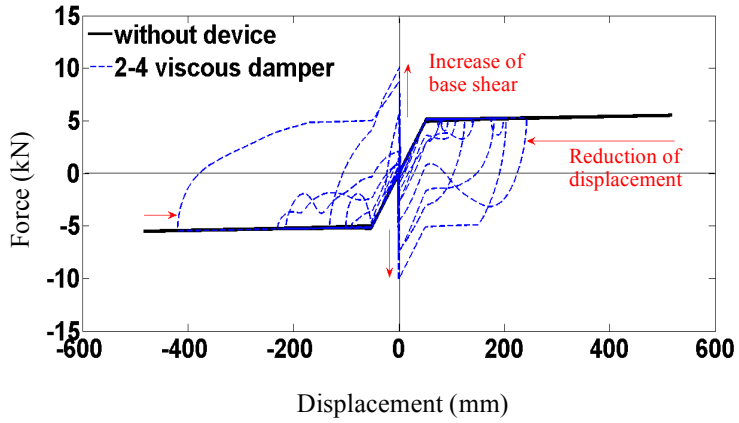

Figure 4-6. Force-displacement response of system with period of 2.0 s and ductility 4 under Palos Verdes earthquake (LA38 , high Suite).

In addition, all the results in Figure 4-5 show the total base shear of the structures with R=4.0 is greater than for R= 2.0 for all three types of viscous devices. This outcome can be explained by showing when any kind of viscous damper is added to the structure the RF_{vb} for R=4.0 is greater than R=2.0 based on a short derivation:

$$RF_{vb(R=2)} = \frac{F_{with\ device(R=2)}}{F_{without\ device(R=2)}} \tag{4-2}$$

with considering the small post tensioning ratio (1%) and the structural response is within the gap-opening regime (second section), the RF_{vb} can be approximated as:

$$RF_{vb(R=2)} = \frac{F_{with\ device(R=2)}}{F_{without\ device(R=2)}} \approx \frac{F_{without\ device\ (R=2)}+F_{device}}{F_{without\ device(R=2)}} \tag{4-3}$$

And from Figure 4-3 and the definition of force reduction factor, R:

$$F_{(R=4)} \approx \frac{1}{2} F_{(R=2)} \tag{4-4}$$

The reduction factor for base shear for R=4.0 can be computed similarly to that for R=2 in Equation 4-3:

$$RF_{vb(R=2)} = \frac{F_{with\ device(R=4)}}{F_{without\ device(R=4)}} \approx \frac{F_{without\ device\ (R=4)} + F_{device}}{F_{without\ device(R=4)}} \tag{4-5}$$

Equation 4-4 can be substituted into Equation 4-5 to find the relationship between the RF of base shear for R=2 and 4:

$$\left.\begin{aligned} RF_{vb(R=2)} &\approx \frac{F_{without\ device\ (R=2)} + F_{device}}{F_{without\ device\ (R=2)}} \\ RF_{vb(R=4)} &\approx \frac{F_{without\ device(R=2)} + 2F_{device}}{F_{without\ device(R=2)}} \end{aligned}\right\} RF_{vb(R=2)} < RF_{vb(R=4)} \tag{4-6}$$

The quantities used in Equations 4-2 to 4-6 and this outcome are illustrated graphically in Figure 4-7.

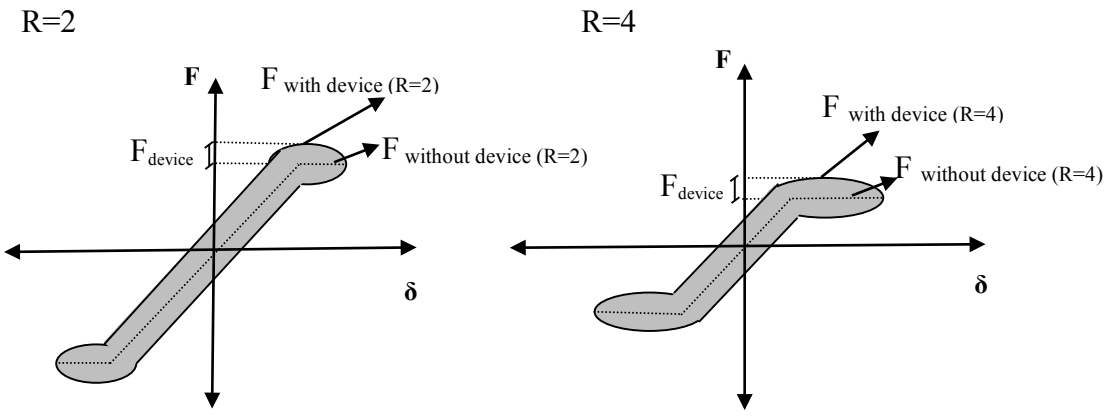

Figure 4-7. Force displacement of structures with R=2 and 4 and typical viscous damper

The median reduction factors for acceleration (RF_{Sa}) results are also shown in Figure 4-5. Like those for total base shear, RF_{Sa} >1.0 for the 1-3 and typical viscous devices for most periods, and increase with structural period. However, RF_{Sa} <1.0 in most cases for the 2-4 device, providing further evidence of the efficiency of this approach.

Figure 4-8 compares the different percentile RFs for S_d and V_b with R=2 and the design level medium suite. The results follow those in Figure 4-5 but provide an indication of the spread of results. The median results in Figure 4-8 matches the medium suite results with R=2 in Figure 4-5. Importantly, the $RF_{Vb} \leq 1.0$ for almost all 2-4 cases, but is RF_{Vb} >1.0 for the 1-3 and 1-4 devices for even the 5th percentile. Thus, these devices virtually always increase base shear for structures of this type with period over 1.0 s. Overall, these results indicate that it will be designer's choice in discussion with the client to select an acceptable level of risk balancing reduced displacement and any increased foundation demand.

Figure 4-9 shows the 5^{th} to 95^{th} percentile of RF_{Sa} results for the medium suite of ground motions. The results follow those in Figure 4-8. Only the 2-4 device offer $RF_{Sa} \leq 1.0$ over all periods, indicating no increase in risk of damage to contents.

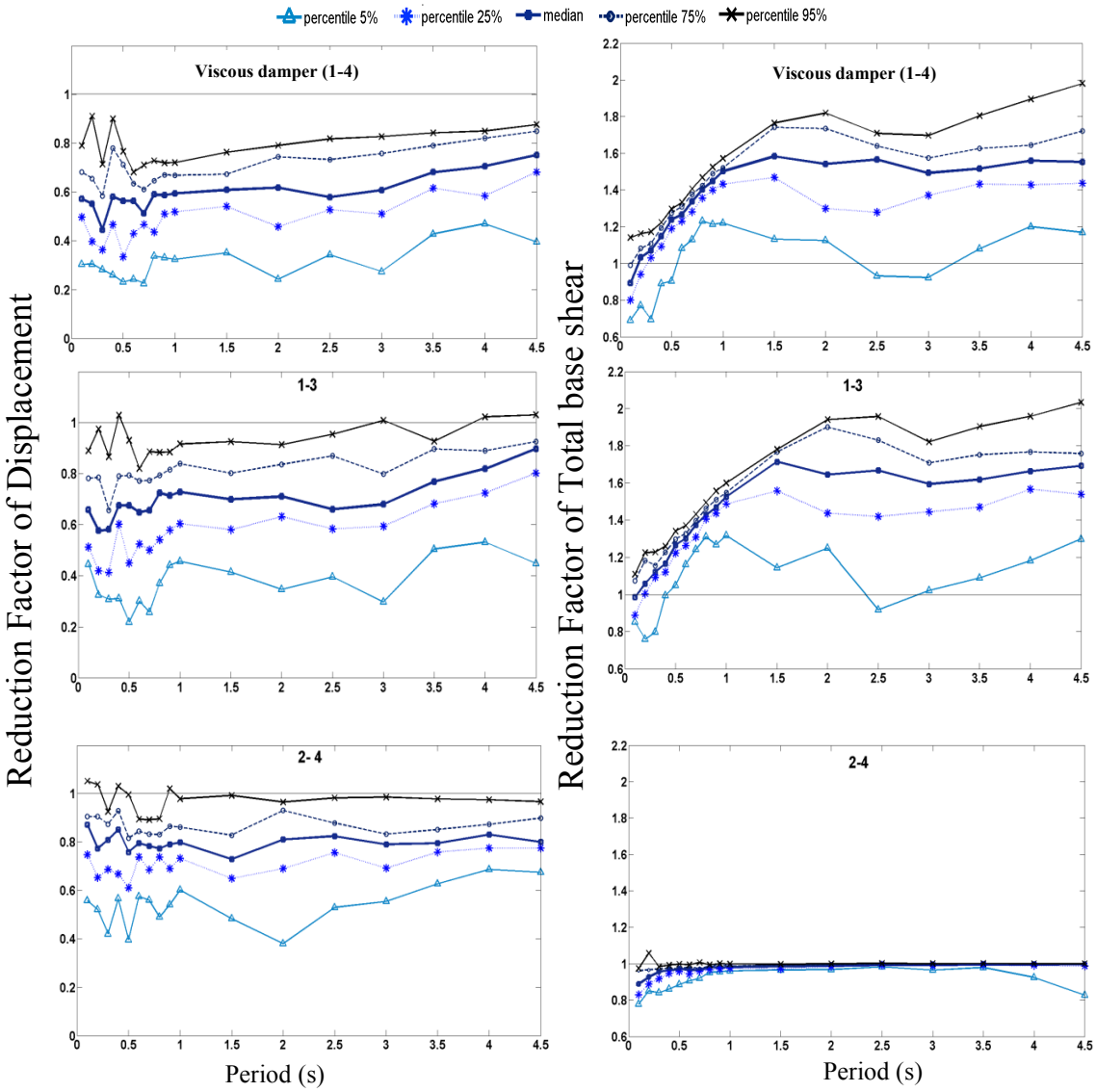

Figure 4-8. The difference percentiles and Median of displacement (S_d) and total base-shear (V_b) response reduction factor (RF) spectra for the typical (1-4), 1-3 and 2-4 viscous damper with 15% additional damping under 20 ground motion of the medium suite.

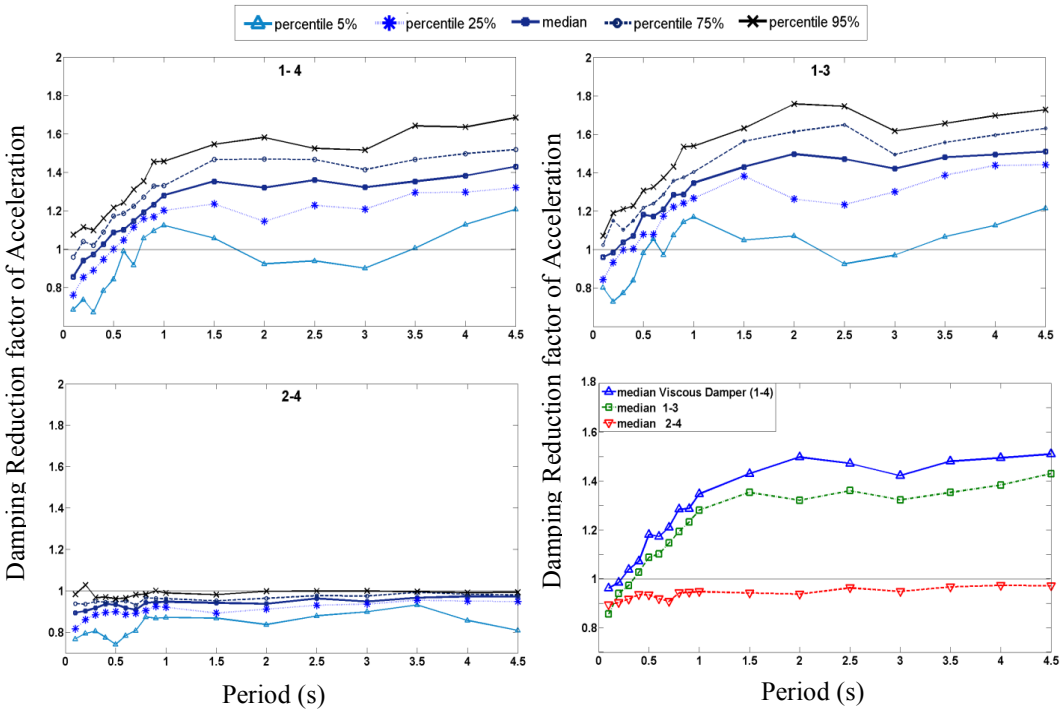

Figure 4-9.The difference percentiles and Median of acceleration (Sa) response reduction factor (RF) spectra for the typical (1-4), 1-3 and 2-4 viscous damper with 15% additional damping for medium suite ground motion.

To show more detail, the RF for S_d, V_b, and S_a (RF_{Sd}, RF_{Vb} and RF_{Sa}) for the SDOF system with period 0.7 s, with R= 2.0 and 4.0, are compared for all 3 devices and all 60 earthquakes in Figure 4-10. Figure 4-10 illustrates the trade-offs in 3D of the different reduction factors. The box of $RF_{Sd} = RF_{Vb} = RF_{Sa} = 1.0$ indicates the boundary between increased and decreased responses and results inside the box are thus desirable. Table 4-2 shows the number of cases within the box for each device summarizing all results for periods T=0.7, 1.0 and 1.5 seconds, by ground motion input suite.

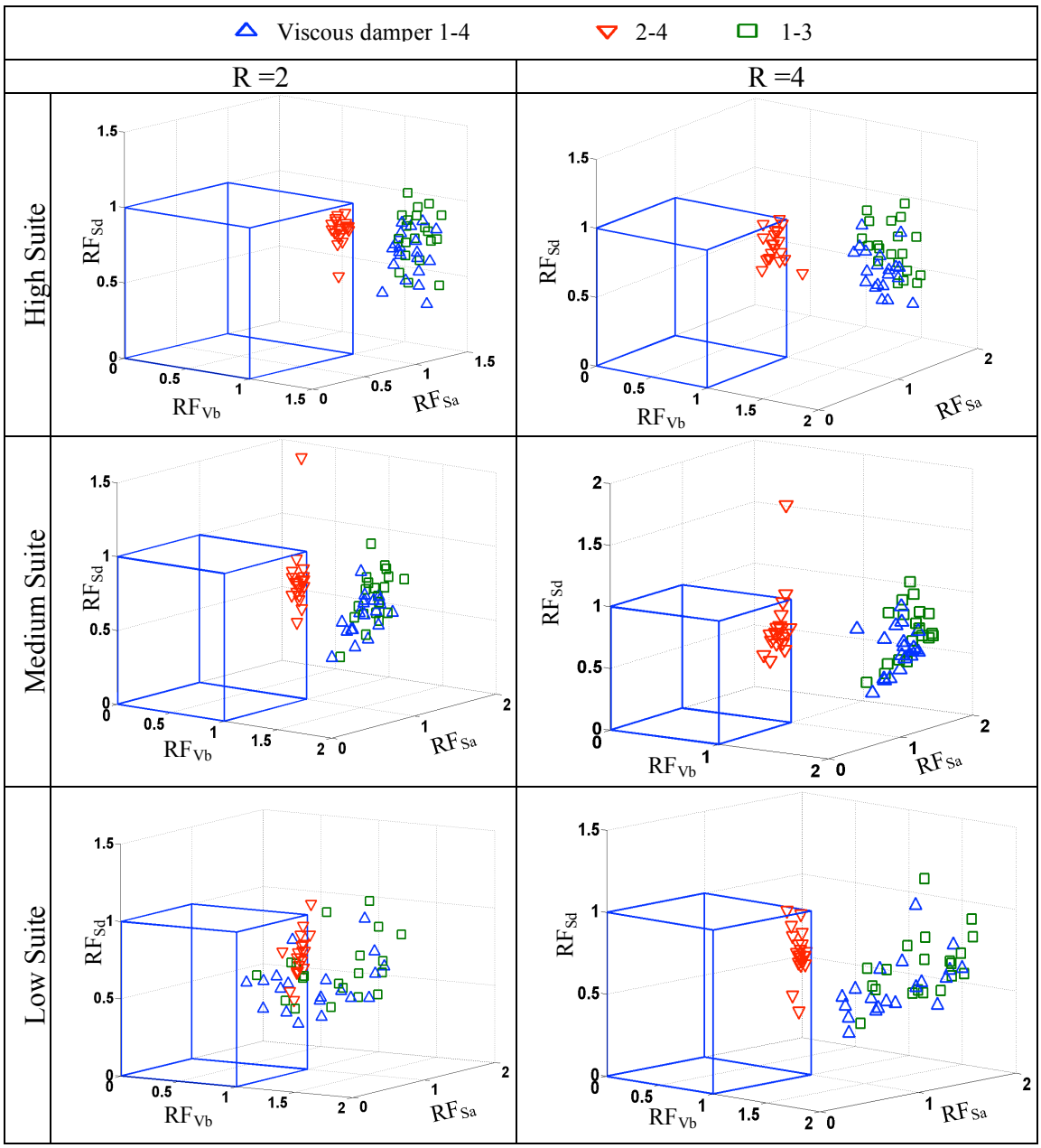

Figure 4-10. 3d Medium high low R=2 and 4 at period T=0.7 s.

The results in Table 4-2 indicate that only 7, 6, 7 and 9, 3, 5 cases of 120 are inside the box for the typical viscous and 1-3 devices, respectively, for T=0.7, 1.0 and 1.5 seconds. All of them are structures with R=2 under the low suite ground

motion. In contrast, 111, 81, 86 of 120 cases for T=0.7, 1.0 and 1.5 seconds are inside the box for the 2-4 viscous damper and remaining cases outside the box are from the much less likely to occur high suite events. These results further support and quantify the outcomes presented.

Table 4-2. No of cases in the box of Figure 4-10 that shows cases that RF of all of S_d, V_b and S_a are less than 1.0

Period (s)	Device type	R=2 60 Cases	R=4 60 Cases	Total result 120 cases
0.7	Viscous (1-4)	7	0	7
	1-3	9	0	9
	2-4	57	54	111
1	Viscous (1-4)	6	0	6
	1-3	3	0	3
	2-4	57	29	86
1.5	Viscous (1-4)	7	0	7
	1-3	5	0	5
	2-4	56	25	81

4.3. Design and analysis procedure

In this section, a design and analysis procedure for rocking systems utilizing supplemental 2-4 viscous damping devices is described. Hazaveh et al. 2016a; 2016b), as discussed in Chapter 3, suggested calculating the damping reduction factor of a structure with a 2-4 viscous damper using:

$$\begin{cases} RF = (0.048\,(\xi_0 + \xi)^{-0.5} - 0.15) * T + 0.9 & T \leq 2.7s \\ RF = \left(\frac{0.07}{0.02+(\xi_{el}+\xi)}\right)^{0.22} & 2.7 < T\ s \end{cases} \quad (4\text{-}7)$$

where ξ_{el} represents the inherent elastic damping and ξ is damping ratio provided by the 2-4 viscous device. Thus, for a targeted damping reduction factor *RF*, the required damping ratio for the device can be obtained by solving Equation 4-7, yielding (Hazaveh et al. 2016b):

$$\begin{cases} \xi = \left(\frac{0.048T}{RF-0.9+0.15\,T}\right)^2 - 0.05 & T \leq 2.7\,s \\ \xi = \left(0.07 - 0.02\,\sqrt[0.22]{RF}\right) RF^{-4.54} & 2.7 < T\,s \end{cases} \quad (4\text{-}8)$$

To use the Equation 4-7 and Equation 4-8, and reduce the number of variables of the rocking system, the system was simplified by representing the non-linear elastic post tensioned (PT) spring as an effective elastic spring with secant stiffness to the target displacement, Δ_d (Marriott et al. 2008; Priestley et al. 2007; Priestley 1991; Priestley and Tao 1993). This approach is illustrated in Figure 4-11, where K_{eff} is the effective elastic stiffness of the post tensioned spring, and defined in Equation 4-9. The non-linear elastic post tensioned spring has been replaced with an equivalent elastic spring of stiffness K_{eff}, where the response of the viscous damper is not affected by the linearization of the PT spring. K_{eff} is defined:

$$K_{eff} = \frac{K(1+r\mu-r)}{\mu} \quad (4\text{-}9)$$

where K, r and μ are the initial stiffness, the ratio of post-rocking stiffness, and the ductility, respectively. The period of system using K_{eff} is thus defined:

$$T_{K_{eff}} = 2\pi\sqrt{\frac{m}{K_{eff}}} \tag{4-10}$$

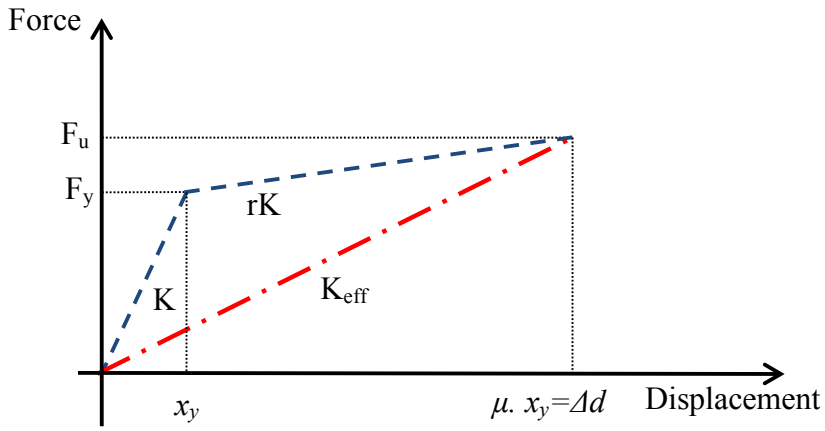

Figure 4-11. a) the effective elastic stiffness (K_{eff}) of the post tensioned spring

The period T_{keff} can be used in Equation 4-7 and 4-8 to find the damping reduction factor of the rocking system with the 2-4 viscous damper. Therefore, the damping reduction factor and required damping to obtain the desired RF for the rocking system can be computed:

$$\begin{cases} RF = (0.048\,(\xi_{el}+\xi)^{-0.5} - 0.15) * T_{K_{eff}} + 0.9 & T_{K_{eff}} \leq 2.7\,s \\ RF = \left(\frac{0.07}{0.02+(\xi_{el}+\xi)}\right)^{0.22} & 2.7s < T_{K_{eff}} \end{cases} \tag{4-11}$$

$$\begin{cases} \xi = \left(\frac{0.048\, T_{K_{eff}}}{RF-0.9+0.15\, T_{K_{eff}}}\right)^2 - 0.05 & T_{K_{eff}} \leq 2.7\, s \\ \xi = \left(0.07 - 0.02\, \sqrt[0.22]{RF}\right) RF^{-4.54} & 2.7s < T_{K_{eff}} \end{cases} \quad (4\text{-}12)$$

Figure 4-12 provides a flowchart for calculating the RF of the bi-linear rocking system when a number, N, of 2-4 viscous dampers are added to the system. For example, three 2-4 viscous dampers, each with 5% added damping, are installed to a structure with period of 1.0 s, 125.66 kN/m stiffness, 1% the post-rocking stiffness and ductility 2.0. The effective stiffness and period is 63.46 kN/m (Equation 4-9) and 2.49 s (Equation 4-10), respectively. These values give a reduction factor of 0.79 (Equation 4-11). The actual damping reduction factor from simulation, directly calculated, is ~ 0.80, which is well estimated by the proposed method (Figure 4-5, 4-10).

Figure 4-13 shows the flowchart for calculating the required size and number of 2-4 viscous dampers to achieve a desired, pre-specified damping reduction factor (RF). For instance, assuming that a 0.70 displacement damping reduction factor (RF_{sd}) is desired for a structure with T=2.0 s, r=1%, K= 31.4 kN/m and μ=R=2 is desirable, then 33% (Equation 4-11) added damping is needed to have a RF_{sd}= 0.7. Therefore, a device or devices with ξ=35% additional damping is conservatively needed, which could be two devices with 17.5% added damping or a single device with 35% added damping.

Damping reduction factor determination for 2-4 viscous damper

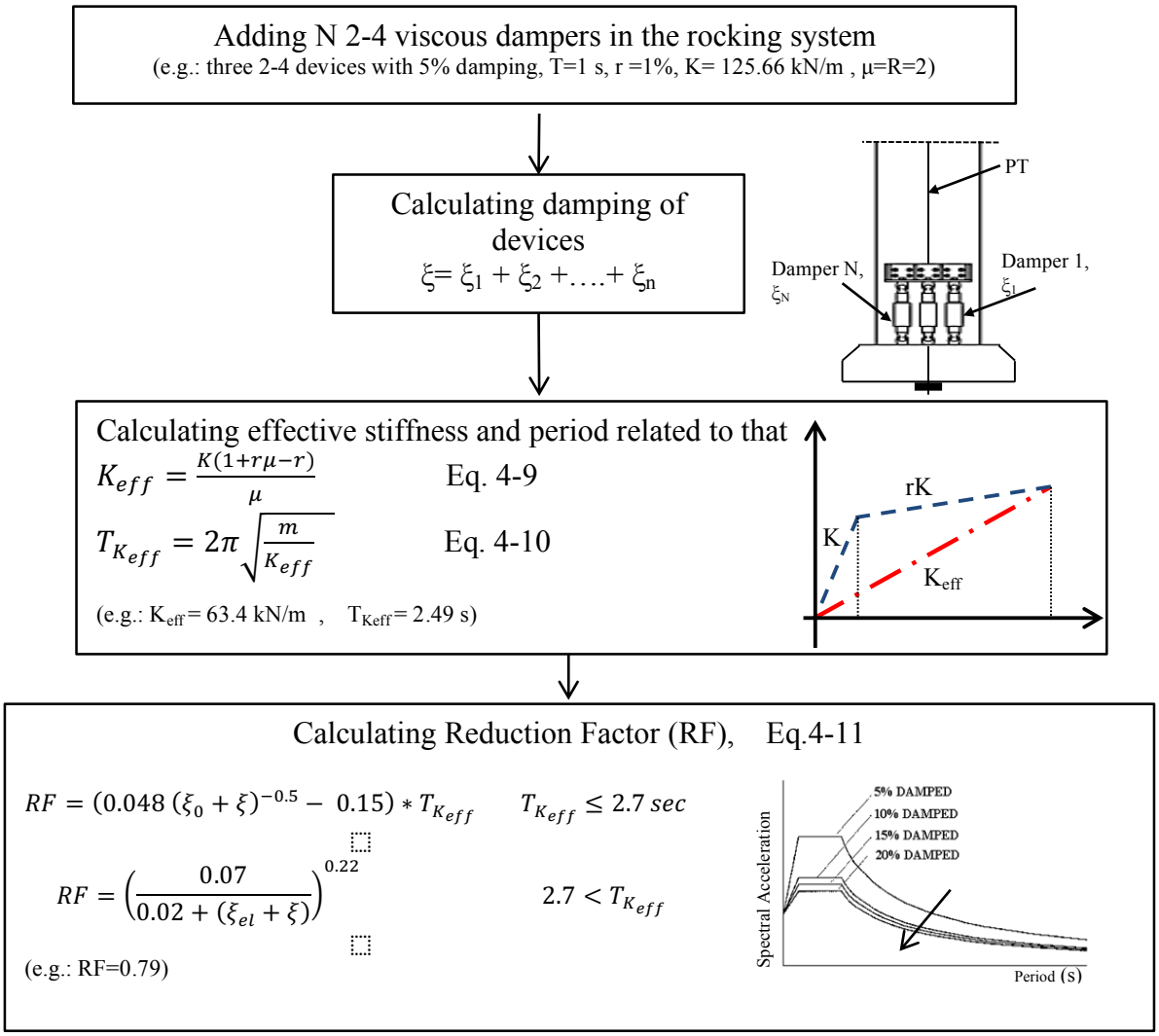

Figure 4-12. The flowchart for calculating the RF when the N 2-4 viscous dampers are added to the rocking system.

Required 2-4 viscous devices to achieve a desirable RF

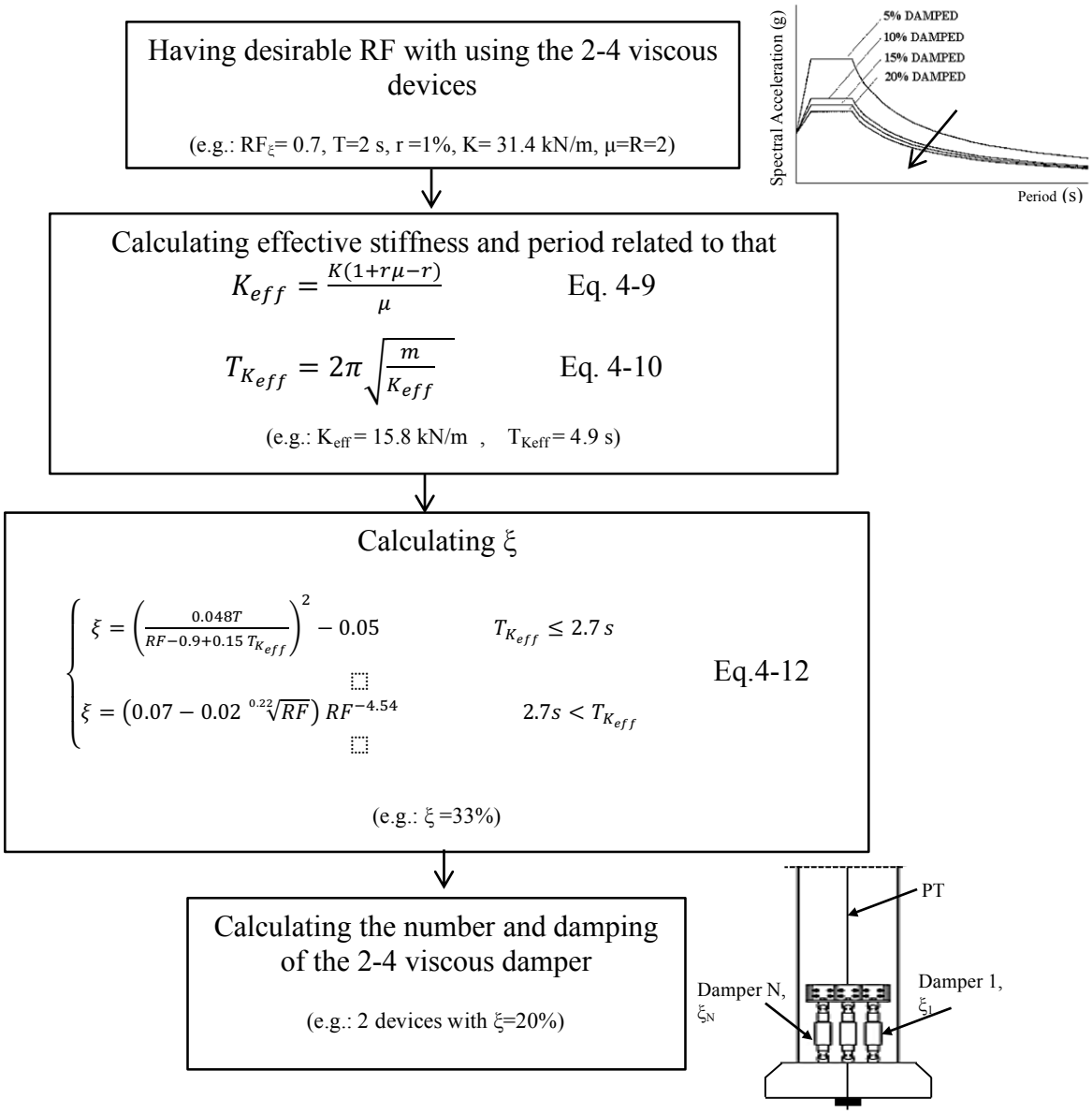

Figure 4-13 . Flowchart to find out the required dampers to have a desirable damping Reduction Factor.

4.4. Summary

This chapter presents an analysis using a 2-4 viscous damping device to re-shape structural hysteretic behavior to improve the seismic behavior of rocking structures using supplemental damping. Maximum displacement (S_d), total base-shear (V_b) and acceleration (S_a) are calculated to determine the impact and efficiency of typical, 1-3 and 2-4 viscous damper on the seismic structural performance of bi-linear elastic rocking structures over a range of periods and ductility factors R=2 and 4. The main findings include:

1. The base shear increases for almost all periods in rocking system with the typical viscous damper by up to 3.5 times for high periods while in linear elastic structures adding viscous damper increases base shear only for longer periods, typically greater than 2.7s, as shown in Chapters 2 and 3. Hence, greater supplemental damping can be added to linear structures than bi-linear cases without penalty of increased base shear, making the analysis presented here more conservative and likely more realistic.
2. A 2-4 viscous damper can simultaneously reduce the values of displacement (S_d), base shear (V_b) and acceleration (S_a) in all period ranges for bi-linear elastic systems under low and medium suite ground motions. For few cases with the high-velocity excitations in the high suite ground motion, applying a 2-4 viscous damper increases the base shear slightly, but the values were not as significant as the base shear of the

structures with typical and 1-3 viscous damper. Hence, 2-4 damping devices provide a robust alternative with minimal to no penalty in other performance metrics.

3. Displacement reduction factors, are similar for different design ductilities (R=2 and 4). However, base shear, RF_{vb}, differs significantly in all cases for different ductility. In general, the total base shear and acceleration of the structures designed with higher ductility is greater than designed with lower ductility by approximately 50% for the 1-3 and typical viscous devices. However, RF_{vb} for the 2-4 devices is less dependent on ductility and provides more stable and constant behavior over different periods.
4. A simple method to determine the effect of the 2-4 device when added to new or existing bi-linear rocking systems and an overall design approach has been provided to enable more direct use of the results.

These results indicate the robustness of simple 2-4 viscous dampers that can effectively mitigate seismic response of the self-centering system, and reduce the demand on the foundation and risk to contents and non-structural components.

4.5. References

Filiatrault A, Tremblay R, Wanitkorkul A (2001) Performance evaluation of passive damping systems for the seismic retrofit of steel moment-resisting frames subjected to near-field ground motions Earthquake Spectra 17:427-456

Hazaveh NK, Chase JG, Rodgers GW, Pampanin S (2015) Control of Structural Response with a New Semi-Active Viscous Damping Device. Paper presented at the 8th International Conference on Behavior of Steel Structures in Seismic Areas

Hazaveh NK, Rodgers GW, Chase JG, Pampanin S (2016a) Reshaping Structural Hysteresis Response with Semi-active Viscous Damping Bulletin of Earthquake Engineering 15:1789-1806 doi: 10.1007/s10518-016-0036-z

Hazaveh NK, Rodgers GW, Pampanin S, Chase JG (2016b) Damping reduction factors and code-based design equation for structures using semi-active viscous dampers Earthquake Engineering & Structural Dynamics 45:2533-2550 doi:10.1002/eqe.2782
Kam W, Pampanin S, Palermo A, Carr A (2008) Implementation of advanced flag-shaped (AFS) systems for moment-resisting frame structures
Kam WY, Pampanin S, Palermo A, Carr AJ (2010) Self-centering structural systems with combination of hysteretic and viscous energy dissipations Earthquake Engineering & Structural Dynamics 39:1083-1108
Lin WH, Chopra AK (2002) Earthquake response of elastic SDF systems with non-linear fluid viscous dampers Earthquake engineering & structural dynamics 31:1623-1642
Mander TJ, Rodgers GW, Chase JG, Mander JB, MacRae GA, Dhakal RP (2009) Damage avoidance design steel beam-column moment connection using high-force-to-volume dissipators Journal of structural engineering 135:1390-1397
Marriott D, Pampanin S, Bull D, Palermo A (2008) Dynamic testing of precast, post-tensioned rocking wall systems with alternative dissipating solutions
Marriott D, Pampanin S, Palermo A (2009) Quasi-static and pseudo-dynamic testing of unbonded post-tensioned rocking bridge piers with external replaceable dissipaters Earthquake Engineering & Structural Dynamics 38:331-354
Miyamoto HK, Singh J (2002) Performance of structures with passive energy dissipators Earthquake spectra 18:105-119
Mulligan K, Chase J, Mander J, Rodgers G, Elliott R, Franco-Anaya R, Carr A (2009) Experimental validation of semi-active resetable actuators in a ⅕th scale test structure Earthquake Engineering & Structural Dynamics 38:517-536
NZS1170 (2004) NZS1170. 5: 2004 Structural Design Actions-Part 5
Priestley M, Calvi G, Kowalsky M Direct displacement-based seismic design of structures. In: 2007 NZSEE Conference, 2007.
Priestley MN (1991) Overview of PRESSS research program PCI journal 36:50-57
Priestley MN, Tao JR (1993) Seismic response of precast prestressed concrete frames with partially debonded tendons PCI Journal 38:58-69
Rodgers GW, Mander JB, Geoffrey Chase J, Mulligan KJ, Deam BL, Carr A (2007) Re-shaping hysteretic behaviour—spectral analysis and design equations for semi-active structures Earthquake engineering & structural dynamics 36:77-100
Rodgers GW, Solberg KM, Mander JB, Chase JG, Bradley BA, Dhakal RP (2010) High-force-to-volume seismic dissipators embedded in a jointed precast concrete frame Journal of Structural Engineering 138:375-386
Sarti F, Palermo A, Pampanin S (2015) Development and Testing of an Alternative Dissipative Posttensioned Rocking Timber Wall with Boundary Columns Journal of Structural Engineering 142:E4015011
Somerville PG (1997) Development of ground motion time histories for phase 2 of the FEMA/SAC steel project. SAC Joint Venture,
Somerville PG, Venture SJ (1997) Development of ground motion time histories for phase 2 of the FEMA/SAC steel project. SAC Joint Venture,
Vargas R, Bruneau M (2007) Effect of supplemental viscous damping on the seismic response of structural systems with metallic dampers Journal of Structural Engineering 133:1434-1444

Chapter 5: Experimental Test and Validation of a Direction and Displacement Dependent (D3) Viscous Damper [1] [2]

Semi-active devices offer the opportunity to customize the device response, and thus overall structural hysteretic response. However, they are actively controlled and thus entail a significant addition of complexity and potentially cost for the added performance. This chapter introduces the concept, design and experimental validation of a Direction and Displacement Dependent (D3) device using viscous damping. D3 devices provide viscous damping in any individual or multiple quadrants of the force-displacement response. Previously only achievable using semi-active devices, this chapter presents an entirely passive and thus more robust and lower cost device.

The fluid viscous damper is a well-known damping device with numerous experimental and analytical investigations (Lin and Chopra 2002; Symans and Constantinou 1995; Tsopelas and Constantinou 1994). Several studies have tried to improve the behaviour of the viscous damper including a pressurized fluid restoring viscous damping device (Tsopelas and Constantinou 1994) and variable

[1] Based on: Hazaveh, N. K., G. W. Rodgers, J. G. Chase, and S. Pampanin. (2017). Experimental Test and Validation of a Direction and Displacement Dependent (D3) Viscous Damper. Journal of Engineering Mechanics (ASCE), DOI: 10.1061/(ASCE)EM.1943-7889.0001354.

[2] Based on: Hazaveh, N. K., G. W. Rodgers, J. G. Chase, and S. Pampanin. (2017). Passive Direction Displacement Dependent Damping (D3) Device. Bulletin of the New Zealand Society for Earthquake Engineering, BNZSEE1710.

damping viscous devices (Symans and Constantinou 1995). However, while viscous dampers can reduce displacement demand, they can increase the overall base shear demand as they provide resistive forces in all four quadrants (Filiatrault et al. 2001; Lin and Chopra 2002; Miyamoto and Singh 2002; Symans and Constantinou 1995; Vargas and Bruneau 2007), as seen in Chapter 2-4. This outcome can lead to more difficult design in retrofit applications and increase foundation cost in new structures.

To address this problem, Hazaveh et al. (2015; 2014; 2016a; 2016b) examined the concept of a semi-active Direction and Displacement Dependent (D3) viscous damper, and examined three types of device control laws (a 1-2-3-4, 1-3 and 2-4) to sculpt hysteretic behavior similar to semi-active resettable device, as discussed in chapters 2 to 4. In the proposed semi-active device, the orifices of the devices are actively controlled to open or close depending on velocity and displacement to produce damping in a specified quadrant or quadrants. When the orifices are closed there is a minimal total opening and significant damping force. When they are open the total orifice area is large enough to allow essentially free motion and thus minimum dissipation. To control this semi-active device requires sensors across the device for displacement and velocity, added significant complexity (Mulligan et al. 2009; Rodgers et al. 2007) .

Thus, semi-active devices are far more complex and costly than passive devices, require an external power source and competition, and, as a result, are potentially much less robust. Hence, this chapter first focuses on evaluating the

characteristics of a classic, very simple oil based viscous damper. This classic viscous damper is then modified in distinct steps to obtain a prototype viscous device with customized hysteretic response. In particular, it is modified to provide direction dependent and displacement dependent damping. The goal is to obtain a passive device design that can produce damping in any one quadrant of the hysteresis loop. In combination, two such devices could then create a passive version of the 1-3 or 2-4 semi-active devices, a major step forward in enabling these devices in practical application give the results of chapter 2-4. Experimental validation and characterization of a prototype D3 device with 30-60kN force capacity is undertaken using an MTS-810 hydraulic test machine.

5. 1. Modelling and evaluation approach of a standard viscous damper

A viscous damping device was produced with grips for testing a 100 kN capacity MTS hydraulic test. General purpose Castrol Axle EPX 80W-90 oil was chosen as the fluid to be used. This fluid was selected as a very low-cost and easily accessible option, while expected the fluid has a kinematic viscosity of approximately 140 mm^2/s (140 cSt) at 40°C to provide reasonable force at the expected flow rate. A more expensive fluid option, such as silicone fluid could be

used, but this study is intended to provide proof of concept validation of the device design, particularly at low cost, rather than a final, fluid-specific result.

The prototype piston was constructed with 30 independent orifices of different sizes. These orifices have a range of sizes and can be individually blocked to experimentally test different configurations and damping levels. Figure 5-1 shows the dimensions and layout of orifices on the piston. Tests were done with three different orifice combinations (Figure 5-1):

- Case 1: 12× Ø4.5mm + 6× Ø3.5mm orifice open, total open orifice area= 994.3 mm^2
- Case 2: 6× Ø3.5mm orifice open, total open orifice area= 230.9 mm^2
- Case 3: 3× Ø3.5mm orifice open, total open orifice area=115.4 mm^2

The main aim of having different orifice areas open is to characterize the viscous damping force obtained. As the piston moves at a given velocity, it dictates a flow rate that must pass through the open orifice area. This flow rate is equal to piston area multiplied by the velocity (mm/s). A much higher fluid velocity through the orifices is required, as their area is significantly smaller than the piston force area, creating velocity dependent dissipation.

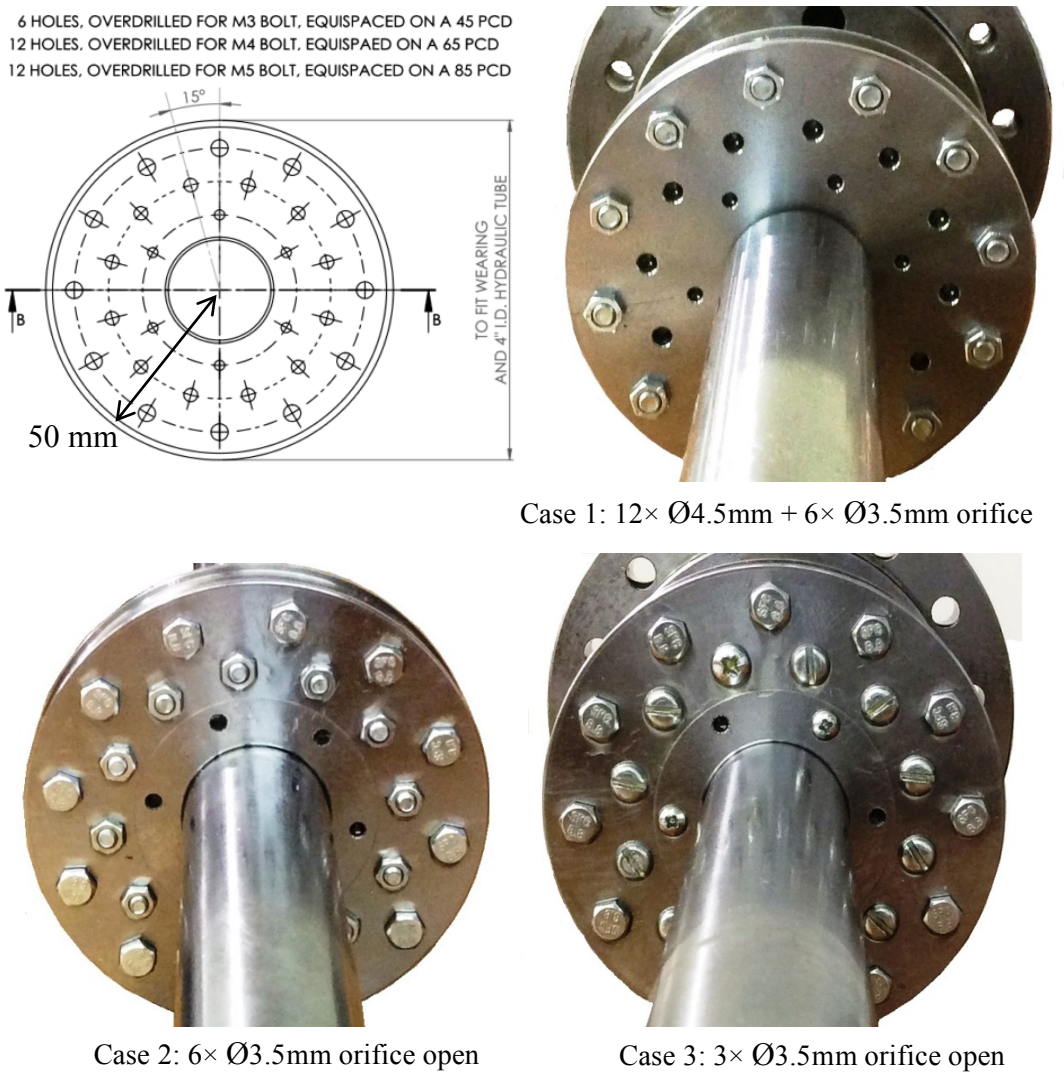

Figure 5-1. : Geometry of piston showing the orifice orientation and Case1 of orifice combinations. 18 orifices open (12× Ø4.5mm and 6× Ø3.5mm), 6 orifices open (6× Ø3.5mm) and 3 orifices open (3× Ø3.5mm)

The end caps were fastened using 12×M8 hex socket bolts, sealed with an O-ring and back-up. Each end cap contained a threaded hole for a pressure sensor and a grub screw, which could be easily removed to add or remove oil. Both holes were

sealed with thread tape and the use of copper washers. Figure 5-2 shows a schematic model of the damping prototype.

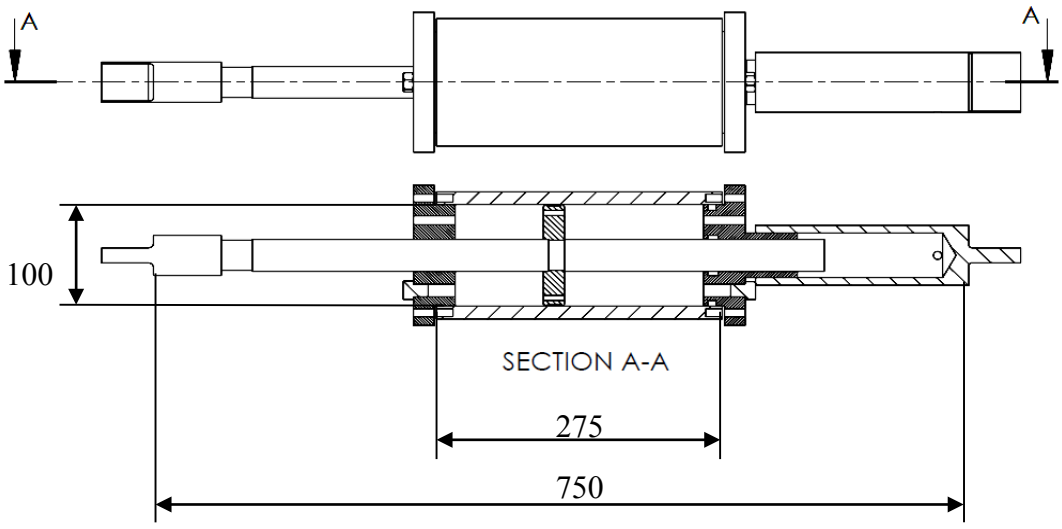

Figure 5-2. Model of damping device (dimensions is mm).

Linear viscous dampers are typically characterized using sinusoidal test inputs and constitutive law where the force (F) is a function of velocity (v):

$$F = Cv \tag{5-1}$$

$$v_{\max} = 2\pi f A \tag{5-2}$$

where, C is a constant expressed in units of a force divided by a velocity (kN.s/m), v_{max} is maximum velocity, and f and A are frequency and amplitude of a sinusoidal excitation, respectively.

Figure 5-3 shows the hysteresis loop when 18 orifices are open (Case 1) under sinusoidal inputs with frequencies of 0.3 Hz to 0.9 Hz and amplitude of 60 mm. As expected increasing velocity with increasing frequency leads to larger forces. Table 5-1 shows good agreement between the maximum experimental velocities with values from Equation 5-1. Figure 5-3 also shows the relationship between analytical and experimental velocity, including saturation of velocity of the MTS machine at 340 mm/s. Beyond this limit, the MTS hydraulic test machine did not have the flow rate required to accurately track the command displacement profile, leading to this velocity saturation. The saturation is thus a limitation in this specific test machine, no issue or effect due to the viscous damper.

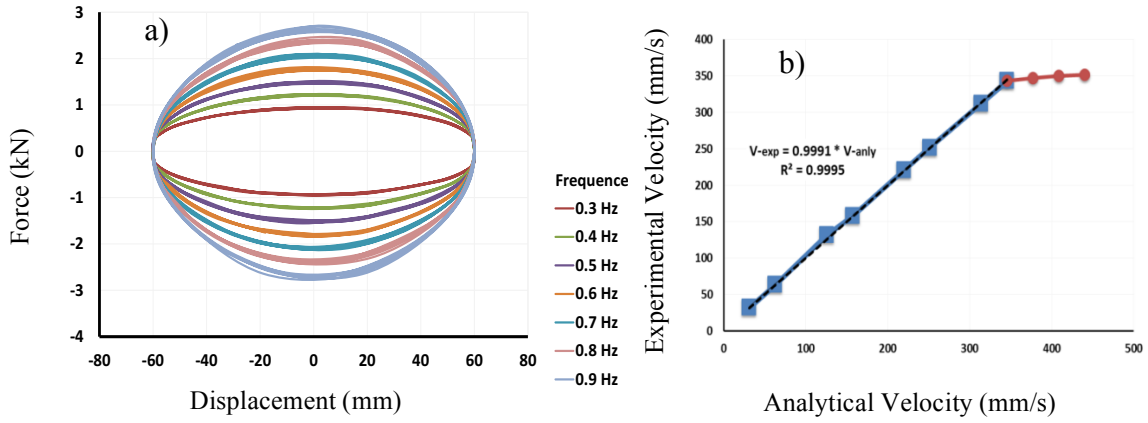

Figure 5-3 . a) Force-displacement of the viscous damper with 18 orifices open under sinusoidal loading with different frequencies, b) Relationship between analytical and experimental velocity of the viscous damper with 18 orifices open.

Table 5-1. Compression between the maximum experimental velocities with analytical ones that calculated from Equation 1 of viscous damper with 18 orifices open.

Frequency (Hz)	Amplitude (mm)	Analytical Velocity (mm/s)	Experimental Velocity (mm/s)
0.25	20.00	31.42	31.73
0.50	20.00	62.83	63.28
1.00	20.00	125.66	131.36
1.25	20.00	157.08	157.67
1.75	20.00	219.91	220.74
2.00	20.00	251.33	251.44
2.50	20.00	314.16	312.22
2.75	20.00	345.58	343.26
3.00	20.00	376.99	347.00
3.25	20.00	408.41	350.50

In particular, as the test machine reached maximum speed, it produces non-sinusoidal 'triangle waves' at a saturated constant velocity that also saturates device force, as shown in Figure 5-4. The structure thus yields a content derivation at the maximum MTS input velocity. Equally, a relatively flat device force is obtained.

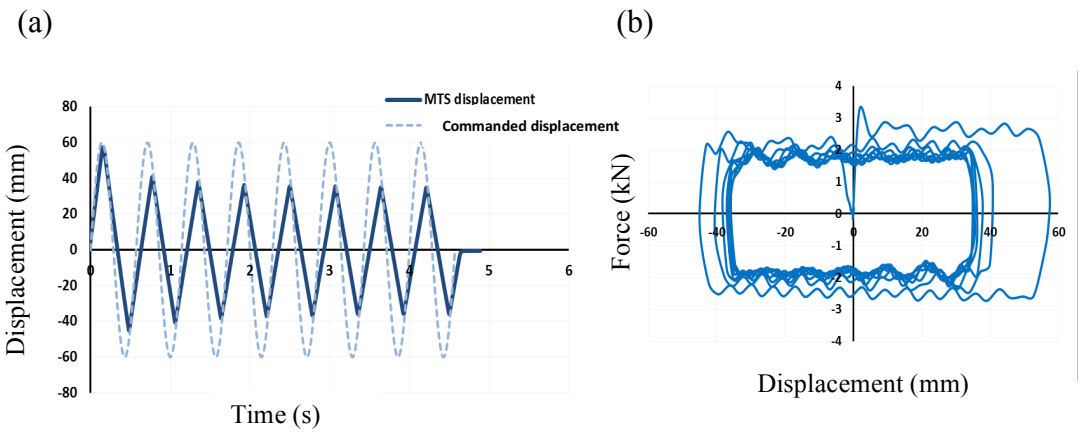

Figure 5-4. Results of the device under sinusoidal loading with frequency of 1.75 Hz and amplitude of 60 mm, (a) command input displacement and actual measured displacement (b) force-displacement of the device.

Figure 5-5 shows maximum force and velocity for all three cases. As expected, the maximum force increases with decreased open orifice area. The calculated damping, *C,* is approximately 152125, 52159 and 8951 N.s/m for Cases 1, 2 and 3, respectively.

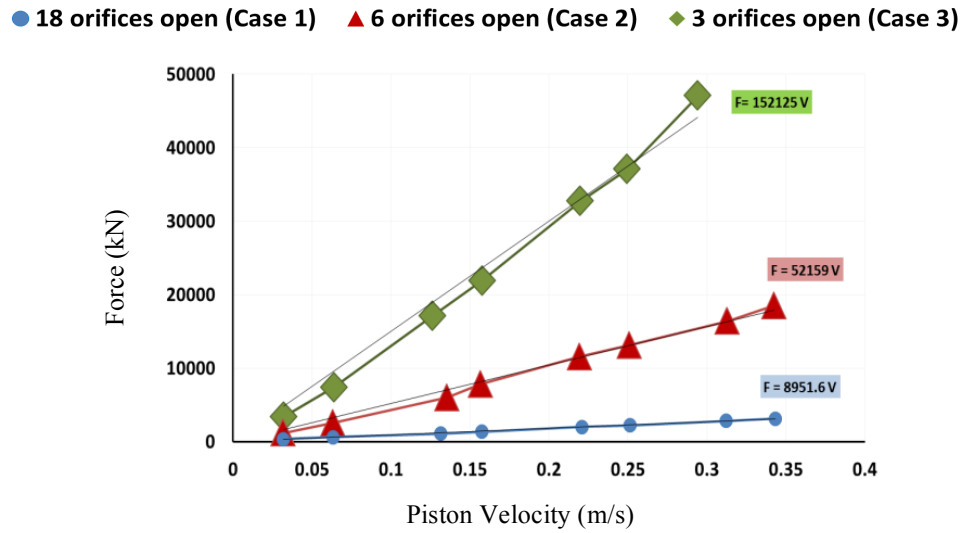

Figure 5-5. Maximum force and velocity of the viscous damper for all three cases.

The velocity of flow through the orifices (v_o) is a function of piston velocity (v_p) and the ratio of the area of the piston (A_p) to the open orifice area (A_0):

$$v_o = v_p \frac{A_p}{A_o} \tag{5-3}$$

$$A_p = \frac{\pi}{4}\left({d_{cyl}}^2 - {d_{shaft}}^2\right)$$

$$A_0 = n \times \frac{\pi}{4}\left({d_0}^2\right)$$

where d_{cyl} is the internal cylinder diameter, d_{shaft} is the shaft diameter, n is the number of open orifices, d_0 is the diameter of the open orifices.

Figure 5-6 shows the maximum force versus orifice flow velocity for all three cases. The results indicate that the relationship between maximum force and orifice flow velocity has the same value for all of three cases, as expected since the assumption is a function of v_0 explicitly. Hence, the prototype behaves as expected.

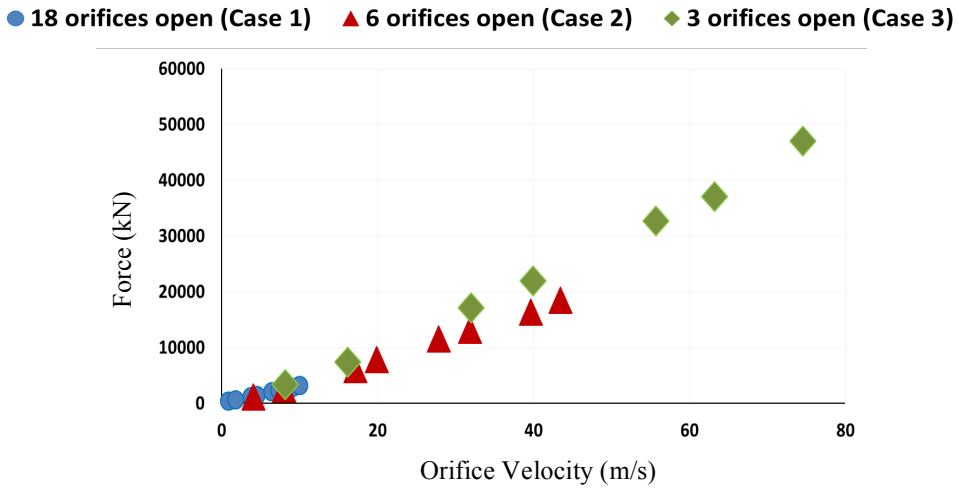

Figure 5-6. Maximum force and orifice velocity for all three cases.

In a typical earthquake there are not many large, repeated cycles. The viscous damper does lose some portion of force due to heating when many input cycles are undertaken. Figure 5-7 presents the results for sinusoidal input amplitude of 60 mm and a loading rate of 0.7 Hz producing a peak input velocity of 264 mm/s. Two sets of results are presented for the same input, one undertaken at the start of a sequence of testing, and the other at the end of a sequence of testing that

comprised a total of 136 cycles across a time period of 12 minute, which is significantly more than in a major earthquake. The comparative results show a reduction in resistive force of approximately 17%. This loss of force is attributed to dynamic heating effects and the corresponding reduction in fluid viscosity, and would not be an issue in an earthquake where many fewer such large response cycles could be expected.

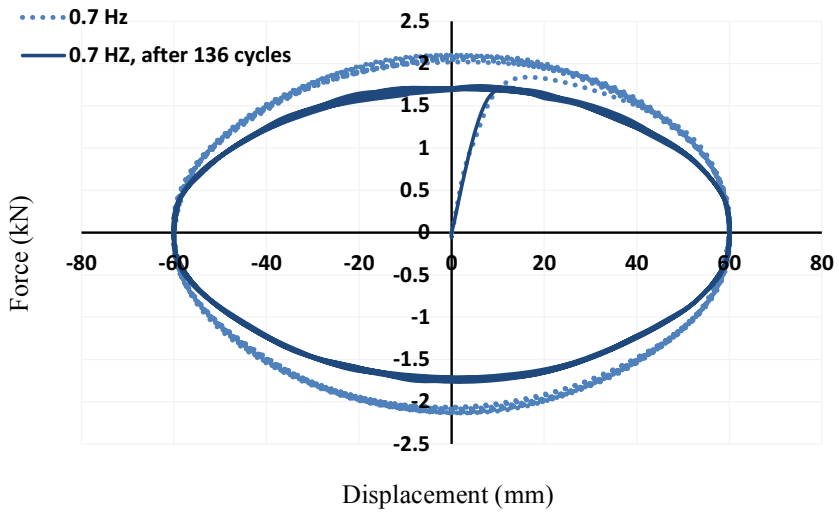

Figure 5-7. Force-displacement the viscous damper with 18 orifices opened under 0.7 Hz sinusoidal load before and after a sequence of testing the included 136 cycles.

5. 2. Creating Direction Dependent Damping

Direction dependent damping implies that there is significant damping when the piston moves in only one direction for the entire length of the cylinder, and essentially no damping in the other direction. One way to achieve this outcome is to provide one way valves on several of the holes that allow flow in only one

direction. Thus, when the piston moves in one direction the valves allow flow and all holes are open, providing minimal damping. In the other direction, only a select number of holes are open to allow flow, thus raising the resistive forces and damping considerably, as the same mass flow rate of fluid must go through a much smaller area and number of holes in the piston.

In the proof of concept prototype presented, one way valves are simply achieved by using an annular plate that slides on a central hub and is retained by screws set into the piston face to cover the larger outer ring of 12 × 6mm orifices in one direction of motion. When the plate faces the flow, it is pushed to cover the larger holes, and is pushed open away from the holes when moving in the other direction. The piston and plate design that enables this behaviour is shown in Figure 5-8, but the same effect could be achieved using a wide array of passive one-way valves.

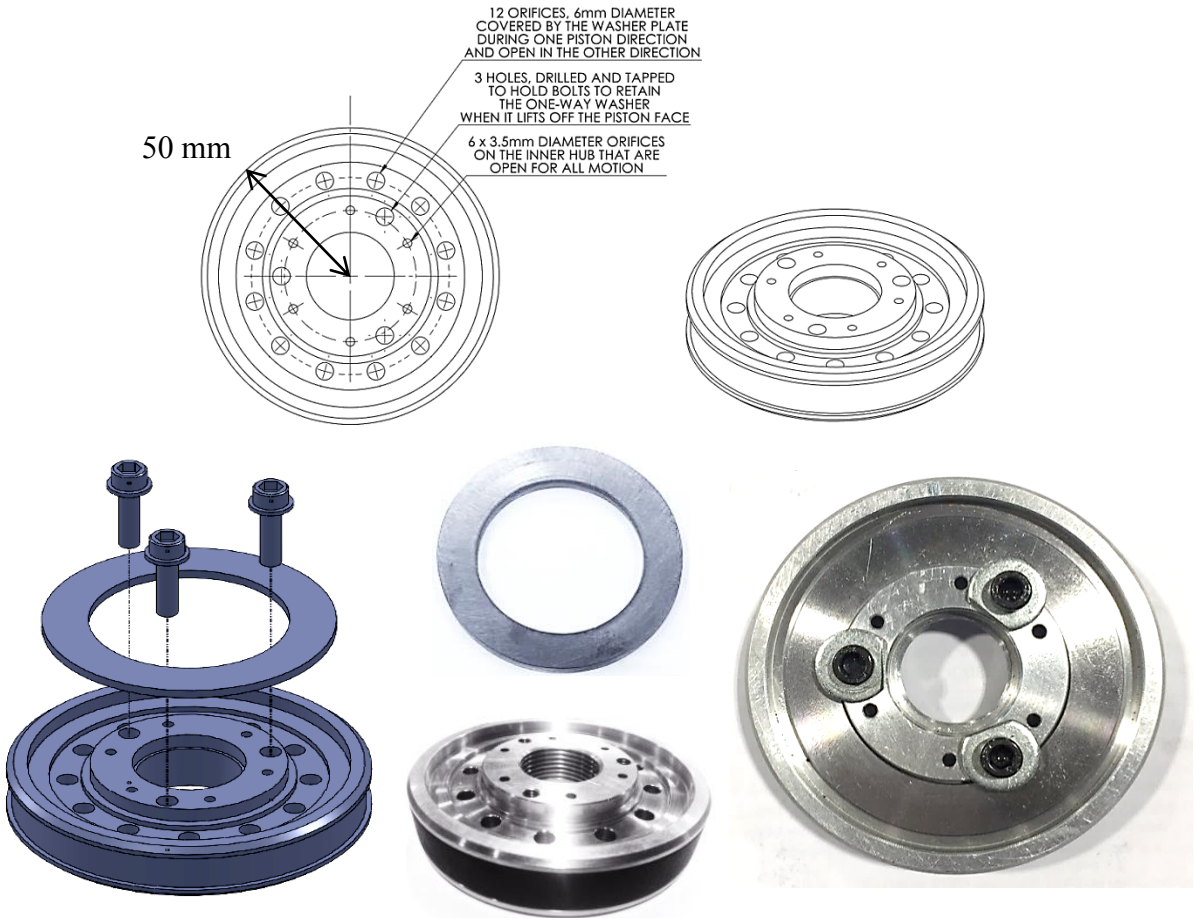

Figure 5-8. Scheme and photo of the modified piston.

More specially, by adding the flat ring to the piston, there are two set of resisting forces dependent on the direction of the piston:

1. Large resisting forces: In one direction, with flow pressure against the ring, the fluid forces the ring plate to cover the longer outer ring of 12× Ø6mm orifices. Therefore, the fluid is forced to flow through only the 6× Ø3.5mm orifices.

2. Low resisting forces: In the reverse direction when the flow moves through the 12× Ø6 mm orifices, the plate lifts off the piston face allowing fluid flow through the longer orifices. Therefore, the orifices flow rate, V_0, drops substantially, as does the resulting damping force.

The modified piston alone produces a half hysteresis loop viscous damper. Figure 5-9 shows force-displacement of the device with the modified piston under sinusoidal loading with 2.5 Hz frequency and 20 mm amplitude. The damping forces are otherwise in line with those of Figure 5-5. Reversing the side of the piston with the one way valves, thus reversing the direction dependence, would flip the hysteresis loop shown.

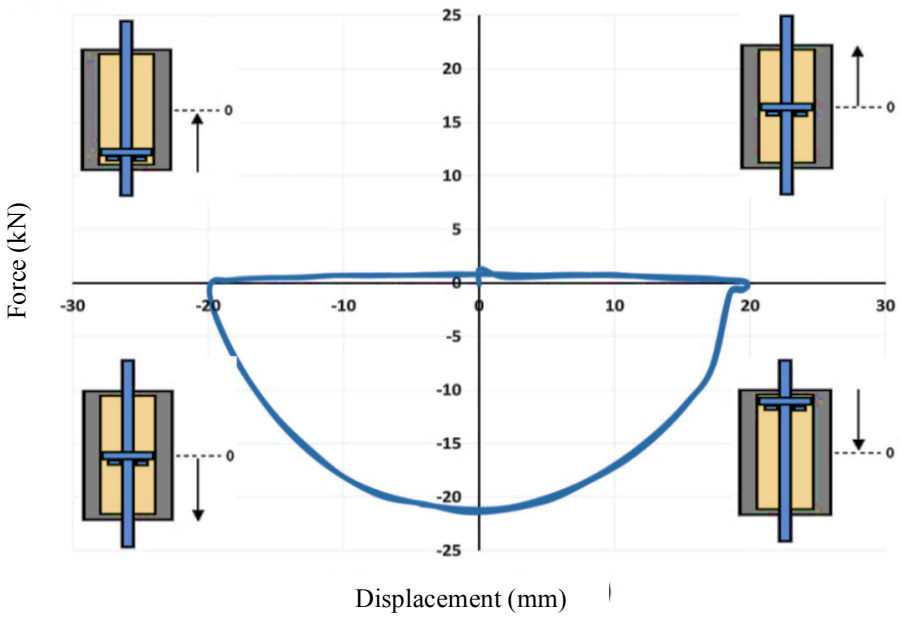

Figure 5-9. Force-displacement of the device showing half the hysteresis loop (2-3 quadrants only) of a viscous damper when 6 orifices are open under sinusoidal loading with frequency 2.5 Hz and amplitude 20 mm.

Figure 5-10 shows time delay of covering orifices by the flat ring plate. The device has a delay about 0.03s (from 0.81s to 0.84s in Figure 5-10c) until the flat ring covers the orifices. This delay should not have a significant effect for most structures with typical fundamental frequencies in the 0.2-5.0 Hz range. The timing delay represents the time taken for a differential pressure to be established across the faces of the circular plate, causing it to be pushed against the piston face.

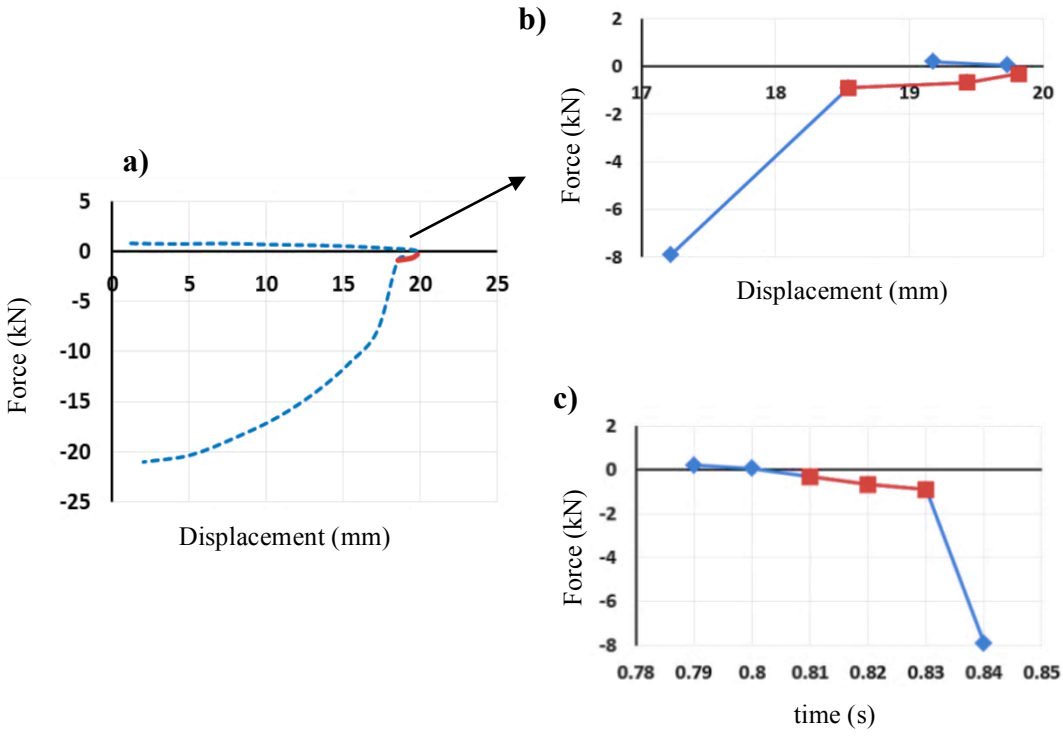

Figure 5-10. Time delay of covering orifices by the flat ring plate.

Figure 5-11 shows the hysteresis loops for 0.5 Hz to 2.5 Hz and an amplitude 20 mm. Using the modified piston with one way valves provides direction dependent damping over a half hysteresis loop of viscous damper. As in Figure 5-3, the maximum force increases with increasing velocity, as expected, just for half a cycle only.

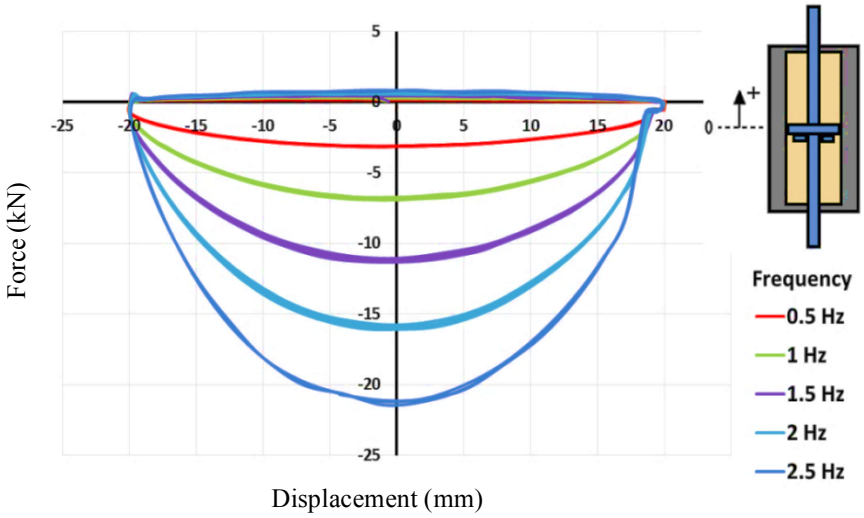

Figure 5-11. Force-displacement of the device that could have a half hysteresis loop of the viscous damper under sinusoidal loading with different frequencies and amplitude of 20 mm.

5. 3. Creating Displacement Dependent Dissipation

Displacement dependent damping implies that there is significant damping only when the piston is located in one part of the cylinder, regardless of the direction of motion. In this case, to achieve damping in a single quadrant of the hysteresis loop, the cylinder can be split into halves. In one half, the piston and cylinder walls are very near to flush with a wear ring or seal, and little to no fluid passes between the piston and cylinder, ensuring there is significant damping if the one-

way valves are closed in the piston. In the other half, the cylinder can be machined to a wider diameter, allowing fluid to pass freely through an annular gap around the piston, regardless of the position of one-way valves, thus ensuring the device provides very little damping in this half of the cylinder. The design illustration is shown in Figure 5-12.

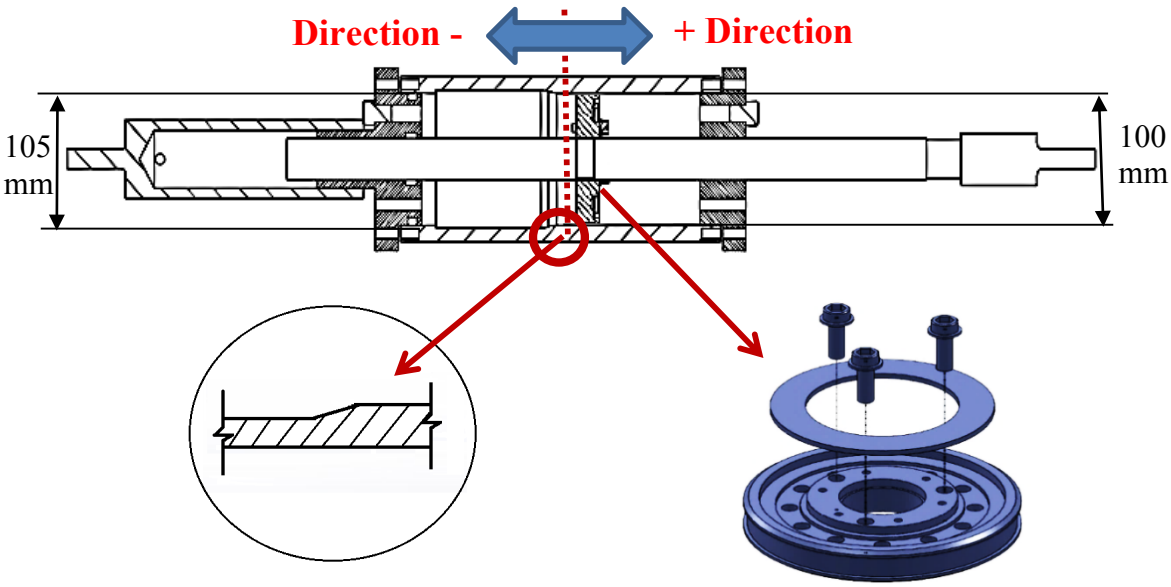

Figure 5-12. Single quadrant viscous damping device prototype showing variable cylinder bore and one way valves in the piston face. It provides a 1st quadrant viscous damping device.

Step-by-step representation of piston position under a sinusoidal input for a single quadrant hysteresis loop is shown in Figure 5-13. Only in quadrant 2 when the piston goes downward, does the circular ring cover the 12× Ø4.5mm orifices and the piston is within the narrower bare section of the cylinder are larger damping forces produced. At all after times, there is minimal damping as fluid can flow

through all the open orifices and/or through the annular gap around the piston circumstance. The result is an expected single quadrant damping device. Reversing the piston head and/ or cylinder can provide damping in any given quadrant.

More specifically, by changing the direction of the piston within the cylinder and the device, four shapes of single quadrant hysteresis loop can be achieved. Figure 5-14 shows four ways of assembling the device to capture only one quadrant of the hysteresis loop as an active viscous damper. Combining these four options provides the full hysteresis loop of the viscous damper. Figure 5-14 shows a few experimental hysteresis loops for each case with sinusoidal input.

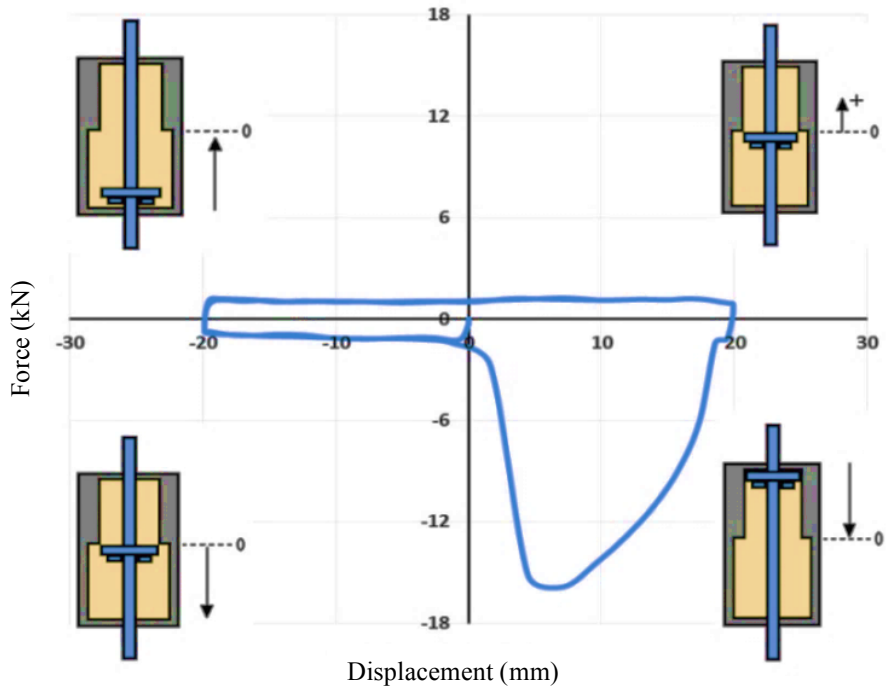

Figure 5-13. Step-by-step representation of position of the modified piston in the modified cylinder under a sinusoidal loading.

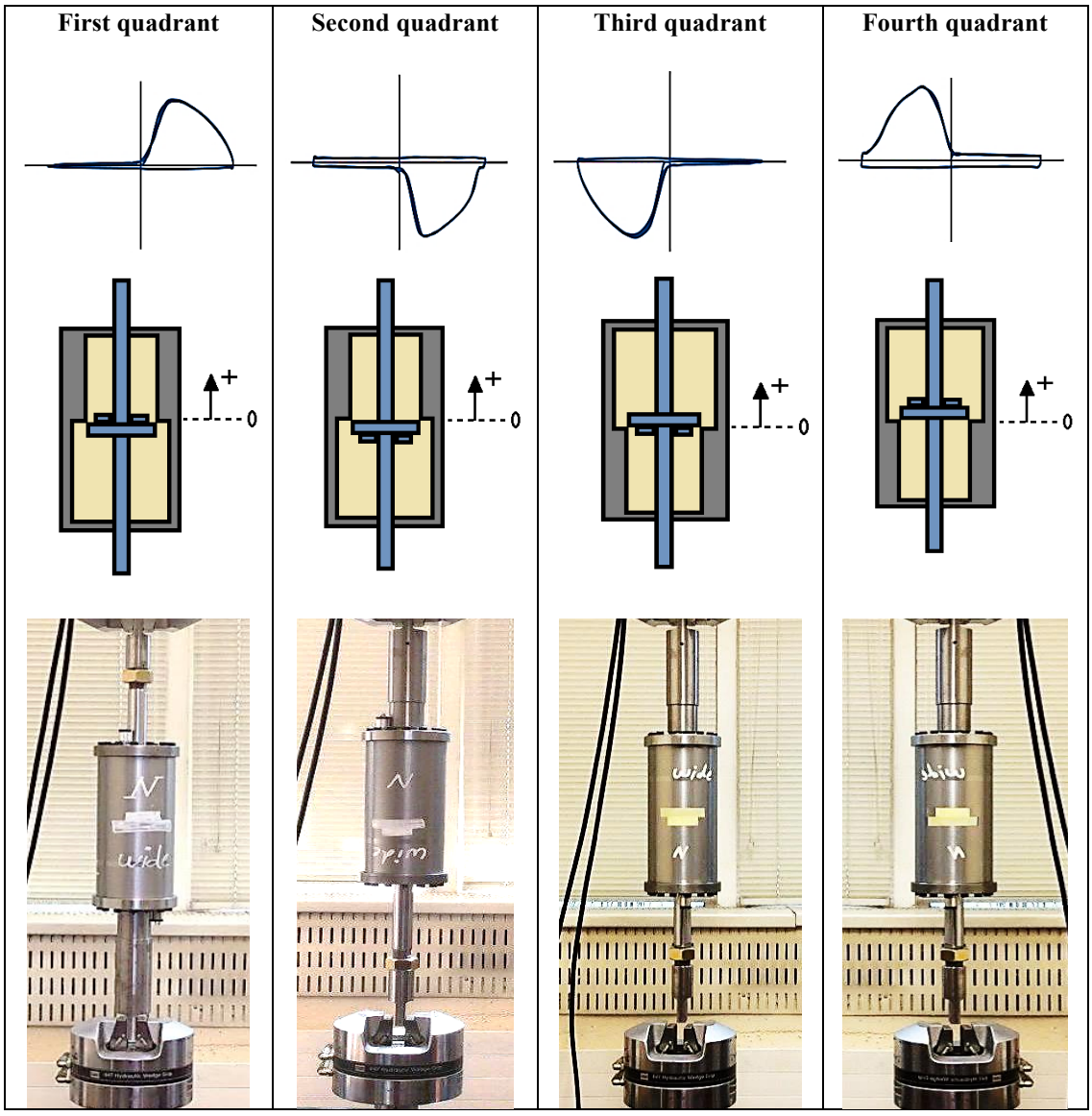

Figure 5-14. Four ways of assembling of the device to produce hysteresis loop in each of the four quadrants.

Figure 5-15 shows force-displacement loops for all four single quadrant D3 device configurations, for frequencies from 0.25 Hz to 2.5 Hz and amplitude 20 mm. As expected, the device force increases with increasing input velocity in Table 5-2.

The close match of analytical and experimentally obtained velocities helps ensure the test machine inputs were correct.

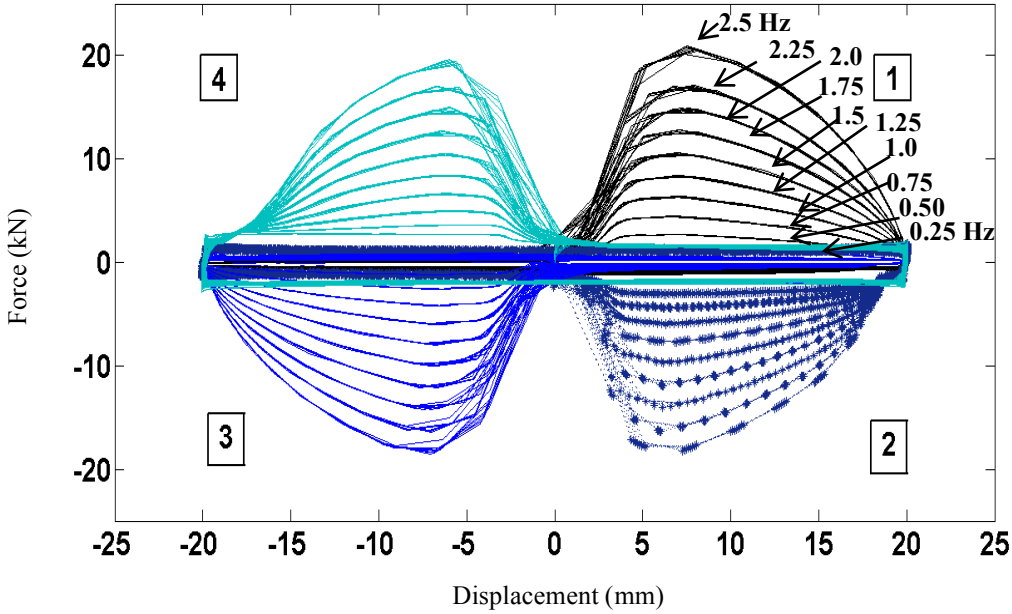

Figure 5-15. Force-displacement of four ways of assembling of the device under sinusoidal loading with range of frequency from 0.25 Hz to 2.5 Hz and amplitude of 20 mm.

Table 5-2. Comparison between the maximum experimental velocities of four ways of assembling of the device with analytical ones.

Frequency (Hz)	Amplitude (mm)	Analytical Velocity (m/s)	Experimental Velocity			
			Quadrant 1 (m/s)	Quadrant 2 (m/s)	Quadrant 3 (m/s)	Quadrant 4 (m/s)
0.25	20	0.03	0.03	0.03	0.03	0.03
0.50	20	0.06	0.06	0.06	0.06	0.06
0.75	20	0.09	0.09	0.09	0.09	0.09
1.00	20	0.13	0.12	0.12	0.12	0.12
1.25	20	0.16	0.15	0.15	0.15	0.15
1.50	20	0.19	0.18	0.19	0.18	0.19
1.75	20	0.22	0.22	0.22	0.22	0.22
2.00	20	0.25	0.25	0.25	0.25	0.25
2.25	20	0.28	0.28	0.28	0.28	0.28
2.50	20	0.31	0.31	0.32	0.31	0.32

5. 4. Overall D3 Device Design

Figure 5-12 shows the resulting overall single quadrant viscous damping device prototype using both a one-way valves and variable cylinder bore. In this configuration, motion in the positive direction provides damping but only in the positive (right) side of the device, where the piston and cylinder are near flush, providing damping in only the first quadrant. Figure 5-14 provides a schematic of all possible configurations of the some piston and cylinder, and the resulting single quadrant hysteresis loop.

The overall device concept and this design are entirely generalizable to a range of valve types and other mechanisms for direction and displacement dependent dissipation. To obtain 1-3 or 2-4 behaviour in an entirely passive, not semi-active, manner is thus just a matter of either:

1. Combining multiple single-quadrant devices in series configuration with shared shaft or in a parallel configuration with a shared connection
2. Creating a combined device design with two pistons and a shared shaft in a single cylinder with 2 stepped portions of the cylinder bore.

Hence, there is no specific limitation to the type of damping hysteresis loop that might be obtained in terms of which quadrants or parts of quadrants experience viscous damping and which do not.

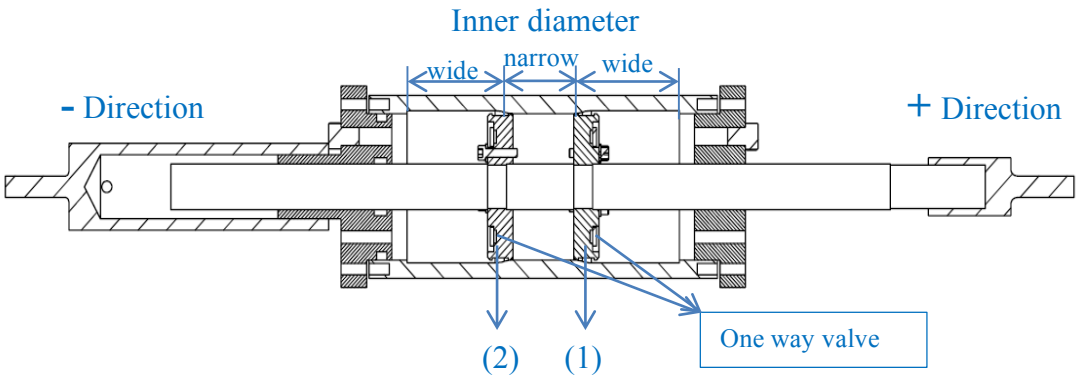

Figure 5-16 . 2-4 configuration of D3 viscous device prototype

A double-tapered cylinder and double piston with one-way valves enables a passive 2-4 D3 viscous damping device, previously only achievable semi-actively. The 2-4 configuration of the displacement direction dependent viscous damper is shown in Figure 5-16. When moving in the positive direction, the valves of piston 1 close and the valves of piston 2 open. In the negative direction, the opening and closing of the piston is the opposite. Large resisting forces are provided by the piston when the valves are closed in a narrow part of cylinder. Figure 5-17 shows the resulting experimental force-displacement under sinusoidal loading with input amplitude 35 mm and a range of input frequencies. It is clear a 2-4 device behaviour is obtained.

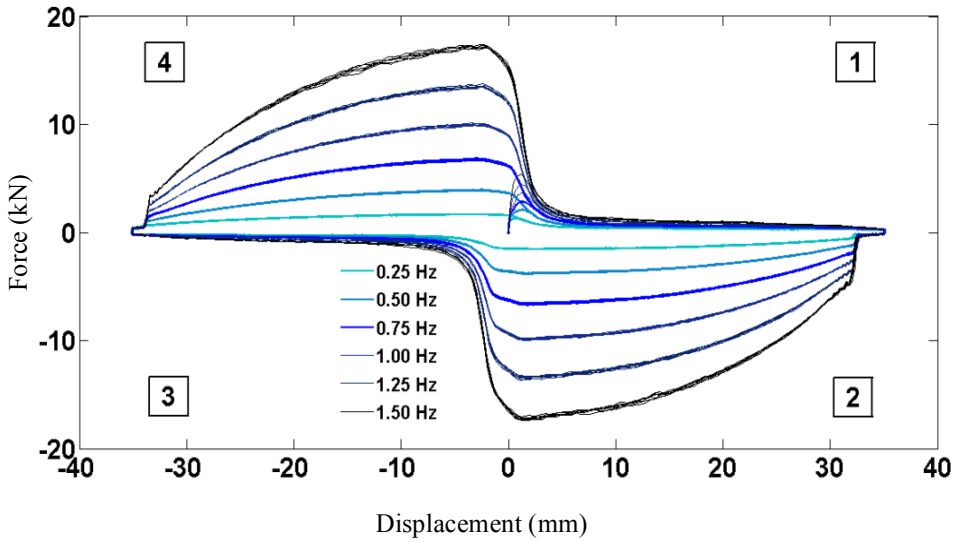

Figure 5-17 Force-displacement of the 2-4 D3 device with 6 orifices open when providing damping force under sinusoidal loading with different frequencies and an input amplitude 35 mm.

In addition, Figure 5-18 shows experimental displacement, velocity and force for the 2-4 D3 device with 6 orifices open when providing damping force under sinusoidal loading with input frequency and amplitude of 1.5 Hz and 35 mm. Figure 5-18.d shows significant resisting force when the sign of the displacement is different from the sign of the velocity, as desired for a 2-4 device resisting motion only towards equilibrium. Equally, the force-velocity plot in Figure 5-18.f shows essentially zero force at non-zero velocities, as these are locations where the D3 device is inactive because displacement and velocity have the same sign and it is not yet in the active quadrant.

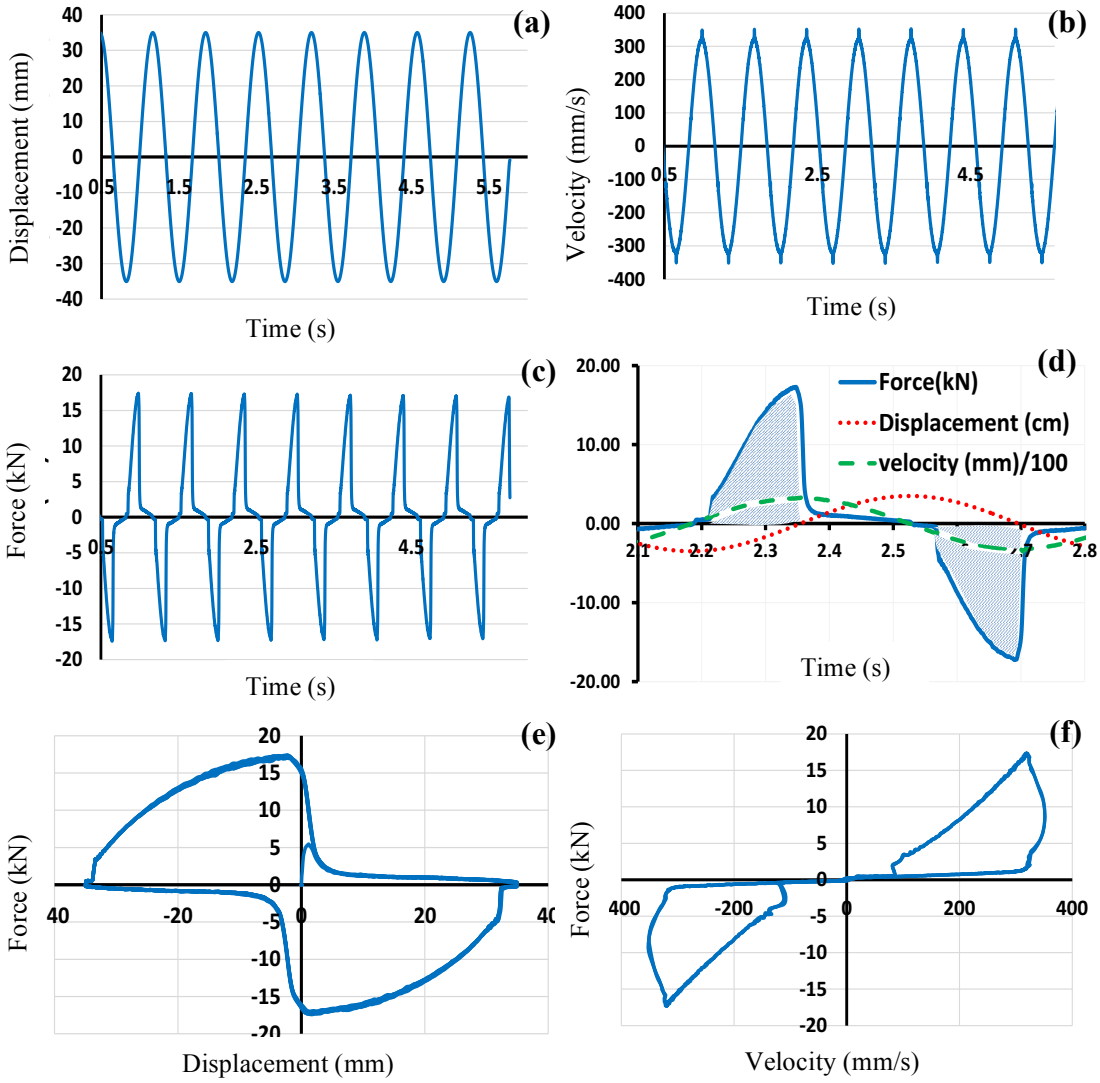

Figure 5-18. a)displacement, b) velocity and c) device force time history and e) force-displacement, f) force- velocity of the 2-4 D3 device with 6 orifices open when providing damping force under sinusoidal loading with 1.5 Hz frequency and an input amplitude 35 mm

All results in Figure 5-15 to Figure 5-18 had 6 orifices open when providing damping. Closing 3 more orifices yields larger damping as in Figure 5-8 for the viscous device. Figure 5-19 shows the results with 3 and 6 orifices open have a linear correlation between velocity and force, and different force levels. The

damping coefficient from the linear regression of the data through the origin, C, is 131 and 46 kN.s/m for 3 and 6 orifices open, respectively. The small asymmetry in the extreme displacements are due to the device being tested vertically in the hydraulic test machine, where gravity slightly aids the washer covering the piston one-way valves in one direction, but hinders this action in covering the orifices in the other, resulting in a small added delay before force is generated.

Figure 5-19 also shows the maximum force normalized to orifice velocity using (v_o) Equation 5-3, where the expected linear damping behaviour is confirmed over the velocity range tested. Finally, it should be noted that the oil used is a Newtonian fluid and thus higher velocities should follow the same overall linear behaviour. More specifically, the devices were not tested past 350 mm/s due to hydraulic test machine limitations that limit the peak velocity input. However, this velocity input is a representative limit for most structural applications.

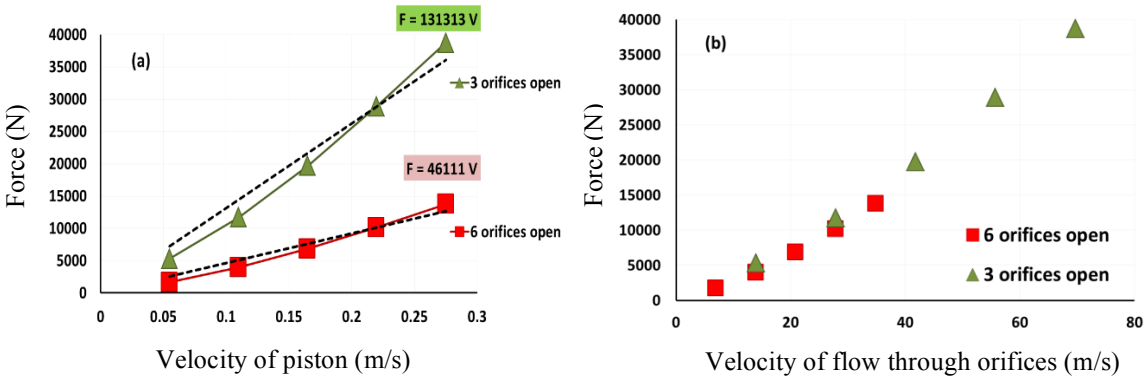

Figure 5-19. a) Maximum force and velocity of the piston. b) Maximum force and orifice velocity for both cases.

5. 5. Summary

This chapter presents the concept, design and experimental validation of a Displacement Direction Dependent (D3) dissipation device that provides viscous damping in any single quadrant, and a second prototype providing a 2-4 D3 device which provides damping in two quadrants. These devices achieve these results entirely passively and can be designed for a wide range of forces and configuration. Experimental validation of a proof of concept device validates the direction dependent and displacement dependent damping has been obtained, and confirms the capability of providing this viscous damping entirely passively in relatively low device cost design. Through a combination of the design principles applied, any configuration of damping in any one or more quadrants could be obtained.

5. 6. References

Filiatrault A, Tremblay R, Wanitkorkul A (2001) Performance evaluation of passive damping systems for the seismic retrofit of steel moment-resisting frames subjected to near-field ground motions Earthquake Spectra 17:427-456

Hazaveh NK, Chase JG, Rodgers GW, Pampanin S (2015) Control of Structural Response with a New Semi-Active Viscous Damping Device. Paper presented at the 8th International Conference on Behavior of Steel Structures in Seismic Areas

Hazaveh NK, Pampanin S, Rodgers G, Chase J Novel Semi-active Viscous Damping Device for Reshaping Structural Response. In: Conference: 6WCSCM (Sixth World Conference of the International Association for Structural Control and Monitoring), 2014.

Hazaveh NK, Rodgers GW, Chase JG, Pampanin S (2016a) Reshaping Structural Hysteresis Response with Semi-active Viscous Damping Bulletin of Earthquake Engineering 15:1789-1806 doi: 10.1007/s10518-016-0036-z

Hazaveh NK, Rodgers GW, Pampanin S, Chase JG (2016b) Damping reduction factors and code-based design equation for structures using semi-active viscous dampers Earthquake Engineering & Structural Dynamics 45:2533-2550 doi:10.1002/eqe.2782

Lin WH, Chopra AK (2002) Earthquake response of elastic SDF systems with non-linear fluid viscous dampers Earthquake engineering & structural dynamics 31:1623-1642

Miyamoto HK, Singh J (2002) Performance of structures with passive energy dissipators Earthquake spectra 18:105-119

Mulligan K, Chase J, Mander J, Rodgers G, Elliott R, Franco-Anaya R, Carr A (2009) Experimental validation of semi-active resetable actuators in a ⅕th scale test structure Earthquake Engineering & Structural Dynamics 38:517-536

Rodgers GW, Mander JB, Geoffrey Chase J, Mulligan KJ, Deam BL, Carr A (2007) Re-shaping hysteretic behaviour—spectral analysis and design equations for semi-active structures Earthquake engineering & structural dynamics 36:77-100

Symans MD, Constantinou MC (1995) Development and experimental study of semi-active fluid damping devices for seismic protection of structures vol NCEER-05-0011. National Center for Earthquake Engineering Research, State University of New York at Buffalo, Department of Civil Engineering, Buffalo, New York 14260

Tsopelas P, Constantinou M (1994) NCEER-Taisei Research Program on Sliding Seismic Isolation Systems for Bridges: Experimental and Analytical Study of a System Consisting of Lubricated PTFE Sliding Bearings and Mild Steel Dampers. National Center for Earthquake Engineering Research, State University of New York at Buffalo, Department of Civil Engineering,Buffalo, New York 14260

Vargas R, Bruneau M (2007) Effect of supplemental viscous damping on the seismic response of structural systems with metallic dampers Journal of Structural Engineering 133:1434-1444

Chapter 6: Shake table test a structure retrofitted using 2-4 Direction Displacement Dependent (D3) viscous dampers [1]

This chapter studies the seismic performance of a 1/2 scale, two storey steel frame building with passive 2-4 D3 dampers and subjected to uni-directional shake table testing. Two 2-4 D3 devices are used and attached via diagonal braces from the base to the first floor. Performance in mitigating structural response and foundation demand are assessed by evaluating maximum drift, acceleration and base shear.

6.1. Introduction

When not designed to remain elastic under a severe seismic event, many existing structures, as well as new structures, would rely on large inelastic deformations and structural hysteretic behaviour to dissipate the energy of ground motions. Instead of damaging the main structural elements to absorb energy, supplemental energy dissipation devices can be incorporated to protect structures, leading to lower damage and repairable structures.

Fluid viscous damping adds energy dissipation to a structural system in the lateral direction without involving major building modifications. However, the addition

[1] Based on: Hazaveh, N. K., G. W. Rodgers, J. G. Chase, and S. Pampanin, Q.T. Ma.(2107) Shake table test a structure retrofitted using 2-4 Direction Displacement Dependent (D3) viscous dampers., New Zealand Society for Earthquake Engineering (NZSEE), Wellington, New Zealand.

of the dampers into the building frame can lead to a substantial increase in the maximum base shear and column axial forces, which, in practice, would likely require strengthening of columns and foundations (Filiatrault et al. 2001; Martinez-Rodrigo and Romero 2003; Miyamoto and Singh 2002; Uriz and Whittaker 2001). Hence, any device that can robustly dissipate energy without increasing column and base shear demands would offer significant potential advantages.

A nonlinear structure with a standard viscous device subject to sinusoidal loading has hysteresis loop definitions like those schematically shown in a Figure 6-1a, where the elliptic force-deflection response due to the viscous damper is added (in parallel) to the nonlinear force deflection response of the structure. A standard viscous damper provides a robust, well-understood method to dissipate significant energy. However, the resulting base-shear force is increased, as shown in the schematic diagram (Figure 6-1).

Considering Chapters 2 to 5, to address this problem, Hazaveh et al. (2015; 2014; 2016ba; 2016cb) introduced the concept of a Direction Dependent Dissipation (D3) device and examined two types of device control laws (a 1-3 and 2-4) to sculpt hysteretic behaviour. The 2-4 device can reduce the base-shear demand by providing damping forces only in the second and forth quadrants of the force deformation plot, resisting motion only toward a zero-displacement configuration (Figure 6-1b). Therefore, the 2-4 D3 device appeared to be an appealing solution

for reducing seismic response in displacement (structural demand) and base shear (foundation demand).

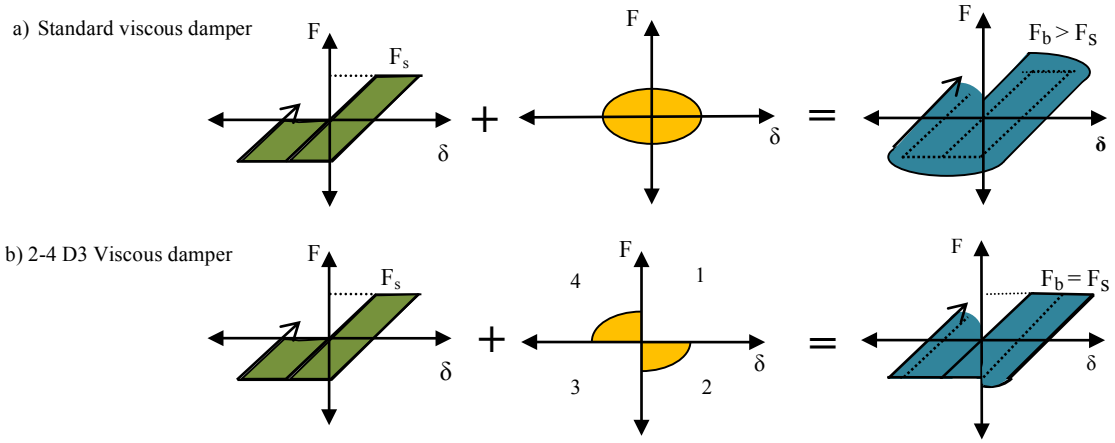

Figure 6-1. Schematic hysteresis for a standard viscous damper and a 2-4 D3 device, F_b = total base shear, F_S = base shear for undamped structure. $F_b > F_S$ indicates an increase due to the additional damping.

Recent research efforts have focused on developing new superior structural design solutions that seek to minimize the possibility of structural damage during an earthquake. Such low-damage structures may be achieved by developing a behaviour that is elastic and/or by incorporating the use of energy dissipaters such as friction connections. Friction connections can be categorized as the Symmetric Friction Connection (SFC) and Asymmetric Friction Connection (AFC) (Clifton 1996; Clifton 2005; MacRae et al. 2010). In these connections, energy is dissipated by permitting sliding of two surfaces that are in contact with each other. Oftentimes, the sliding force is increased by a clamping force from pre-tensioned high strength bolts. A notable case study is that by Yang and Popov Yang and Popov (1995) where the researchers utilized SFCs in the top and bottom flanges of

beams in rotational beam-column connections for steel MRFs. The experimental test results showed a non-linear frictional behaviour with limited degradation. However, the performance of this particular SFC, where sliding occurs in the top flange, is affected by an overlaying floor slab (Khoo et al. 2015). Connections which do not slide at the top flange have also been developed and tested. These rotate about the top flange plate and sliding only occurs in the bottom flange plate thus minimizing interactions with the overlaying floor slab and the effects of beam elongation. This occurs in asymmetric friction connections (AFCs) (Clifton 1996; Clifton 2005; MacRae et al. 2010) and symmetric friction connections with sliding on the bottom flange only.

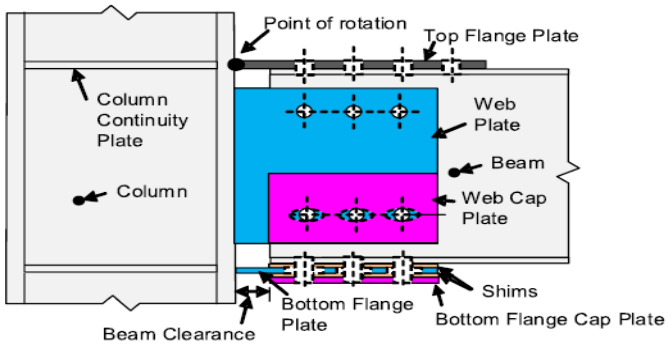

Figure 6-2: Asymmetric friction connection (AFC) in beam column joint (MacRae et al. 2010).

As shown in Figure 6-2, the top flange of the beam is fixed to a plate extending from the column. As mentioned above, there are two sliding surfaces. A shim is placed in the first sliding surface, between the bottom-flange plate and beam.

Another shim is placed in the second sliding interface, between the column-flange plate and a cap plate. When beam ends starts to rotate about the top flange plate, initial sliding occurs at the first sliding surface, then, it occurs at the second one. Since sliding does not occur at the same time, it is referred to as an asymmetric friction connection.

AFCs also have been used at the base of the steel columns (Borzouie et al. 2015a; Borzouie et al. 2015b) as shown in Figure 6-3. Sliding surfaces were placed in two states; i) parallel and ii) perpendicular to the column-strong axis. It was shown that these base–friction connections can tolerate high levels of drift without significant strength degradation. Also based on this study, a simplified procedure to estimate the strength of the base connection was developed.

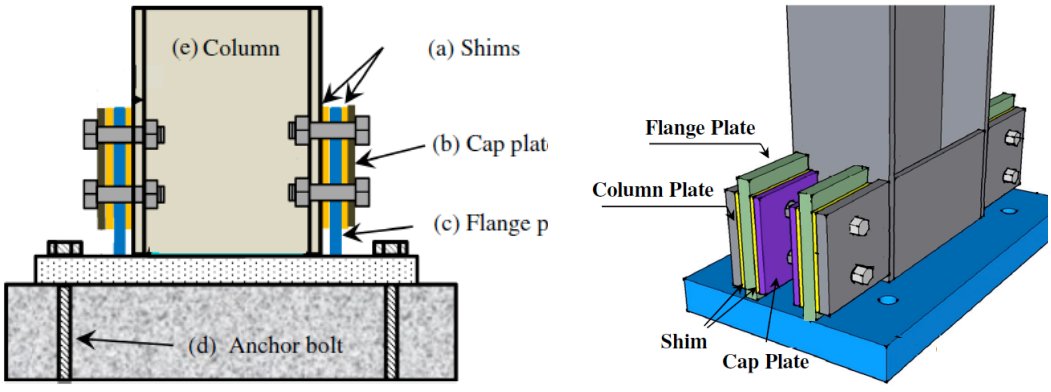

(a) Parallel to the column-strong axis

(b) Perpendicular to the column-strong axis

Figure 6-3: Asymmetric friction connection (AFC) in base column joint (Borzouie et al. 2015a; Borzouie et al. 2015b).

Past studies of AFC were mostly experimental studies with AFC applied to beam-to-column moment resisting joints (Clifton 2005; MacRae 2010), braces (Chanchí et al. 2012; Chanchí et al. 2014) and base-columns connections (Borzouie et al. 2015a; Borzouie et al. 2015b). All of these configurations can possess good seismic performance. However, the dynamic performance of AFCs in entire steel moment resisting frames (SMRFs) has not been validated.

In this chapter, the structural performance of a 1/2 scale, 13 tonne, two-storey steel frame building with asymmetric friction connections and the 2-4 D3 viscous damper is investigated with shake table testing, as shown in Figure 6-4. Successful outcomes would indicate the benefit of developing and characterizing a specific, low-cost device for practical implementation, incorporating the specialised response characteristics of semi-active devices into a fully passive damping device to improve the structural response without increasing the total base shear and column axial forces.

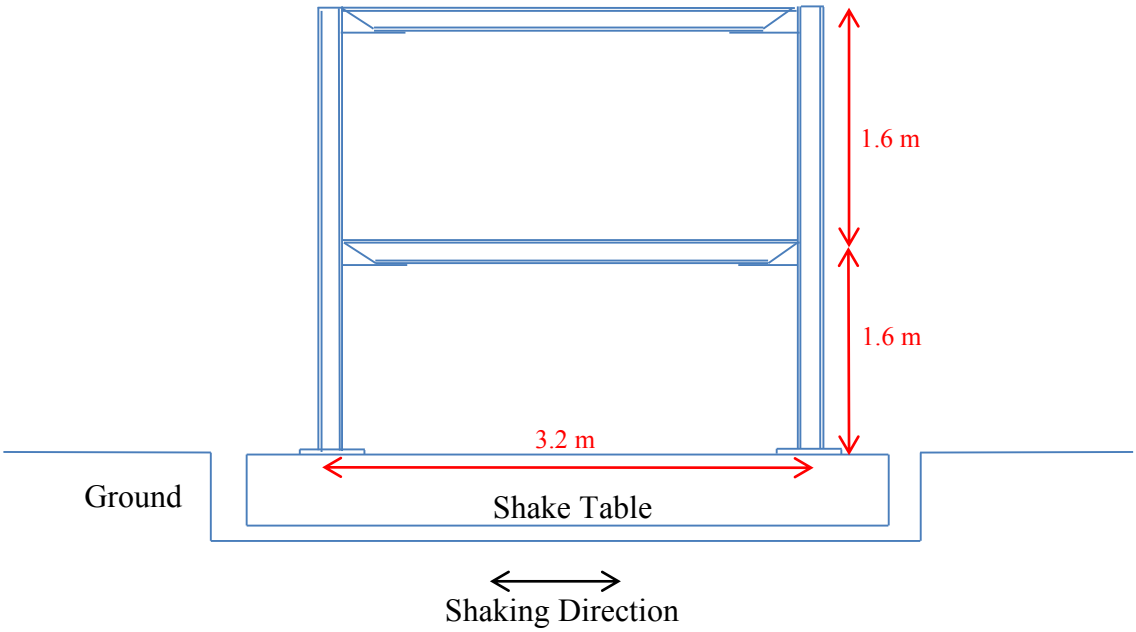

Figure 6-4. Test building constructed frame

6.2. Modeling and evaluation approach

The test specimen is a half scale two story frame (13 tonne mass, 3.2m height, 3.2m length) low-damage steel building with asymmetric friction connections (AFC) in the column base and beam-to-column connection, as shown in Figure 6-5. The AFC, in this study is designed to rotate about the top flange plate and slide only in the bottom flange plate, which minimises the interaction with the overlaying floor slab and the effects of beam elongation. In the transverse direction of the test specimen, the two frames are joined by short transverse beams. The length of the beams, columns and the amount of the mass at each floor are provided in Table 6-1.

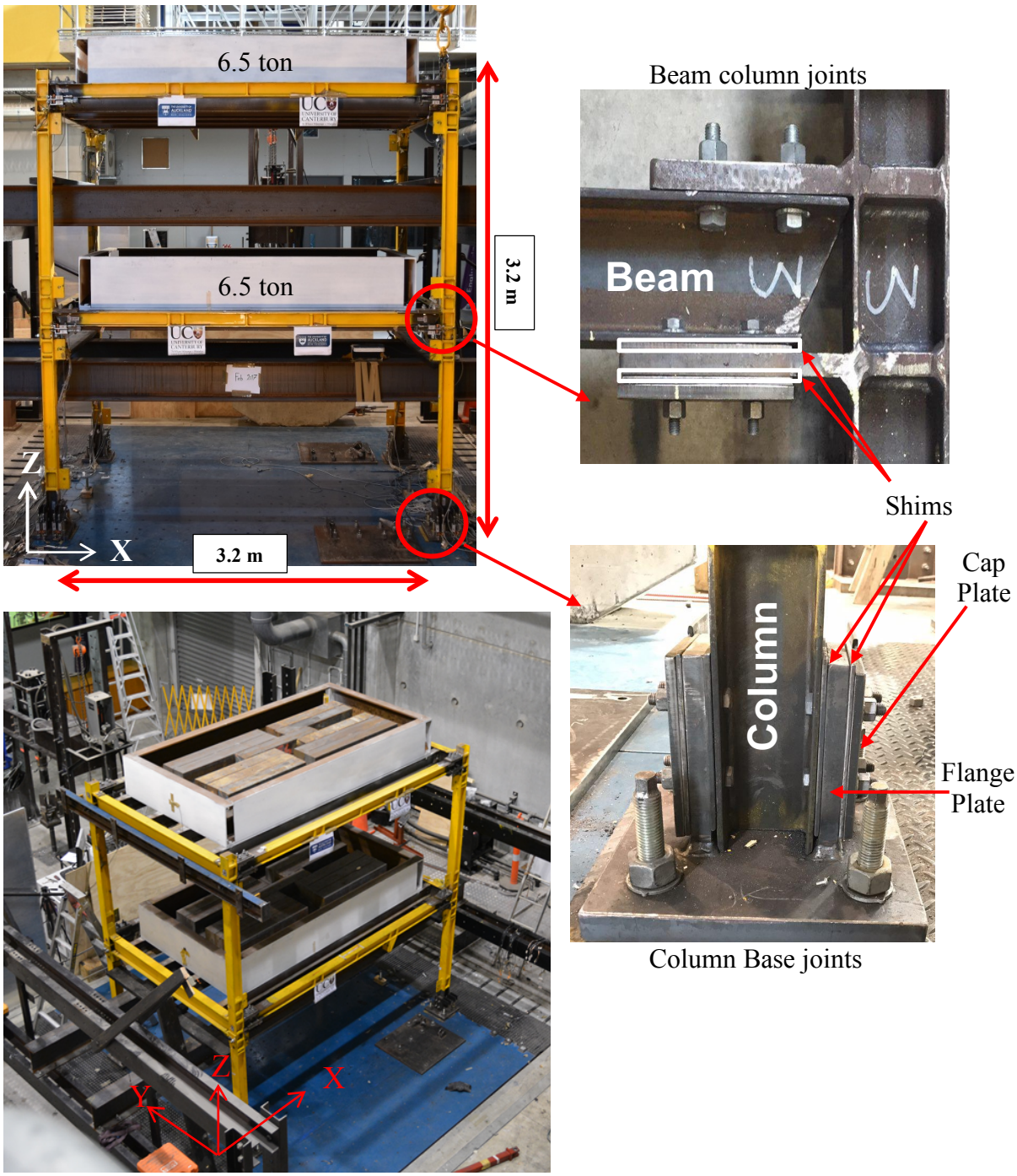

Figure 6-5. Test building constructed frame. Two steel frames with asymmetric friction connections (AFC) in the column base and beam-to-column joints.

Table 6-1. Properties of the two-story test buildings

Items	Properties
Inter-storey height [m]	1.6
Bay length [m]	3.2
Building width [m]	2
Mass per floor [tonne]	6.5
Column Section	100 UC 14.8
Beam Section	100 UC 14.8

The test input was a set of 4 earthquake ground motions selected from both NZ local earthquake events and the NGA database (Campbell and Bozorgnia 2006; Chiou et al. 2008), and are listed in Table 6-2. The prototype was scaled to meet the requirements of the shake table by:

$$\alpha_t = \sqrt{\frac{\alpha_m}{\alpha_s \alpha_l}} \tag{6-1}$$

where α_l , α_m and α_s for length, mass and stress fundamental Scaling Factors (SF), respectively. Based on the limitations of the shake table the as $\alpha_l = 0.5$, $\alpha_m = 0.25$ and $\alpha_s = 1.0$ were set. Therefore, the time-step of each ground motion was reduced by a factor of $\alpha_t = 0.7$ to fulfil similitude requirements and to ensure similar peak acceleration. The input motions were scaled to represent a range of earthquake levels (acceleration magnitude as a 50%, 75% and 100% of the as-recorded ground motion) from low-intensity frequent earthquakes to large intensity very rare earthquakes. Figure 6-6 shows the displacement time history of the records and compares the NZ code (NZ1170.5) spectra with spectral acceleration of ground motions with different scales.

Table 6-2. Ground motions specifications

No	Earthquake name	Station Name	Orientation	Date	M_w	PGA (g)	PGV (mm/s)	PGD (mm)
1	Christchurch, NZ	CCCC	N-S	22nd Feb. 2011	6.2	0.49	480	100.83
2	Christchurch, NZ	REHS	N-S	22nd Feb. 2011	6.2	0.71	587	143.84
3	Northridge, US	Sylmar	N-S	1994	6.7	1.02	467.6	110.94
4	Kobe, Japan	KJM	N-S	1995	6.9	0.82	569.1	86.73

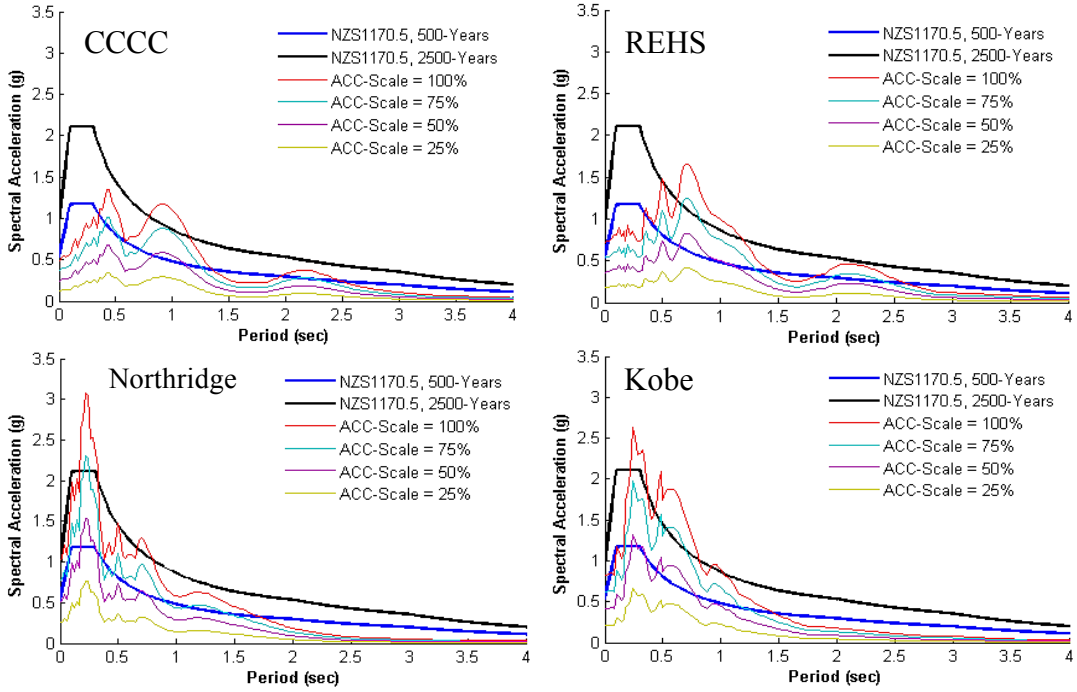

Figure 6-6. Spectral Acceleration of ground motions compared with NZ Code Spectra (NZ1170.5), (5% damping, Z=0.4, Soil C, Sp=1.0), Time scale=0.7.

To improve the structural performance and reduce the drift, without increasing base shear and acceleration responses, the 2-4 D3 viscous devices are added to the structure using a diagonal bracing system, as shown in Figure 6-7. Experimental component validation and characterization of a prototype D3 device was undertaken using an MTS-810 hydraulic test machine (Hazaveh et al. 2016a;

Hazaveh et al. 2017). Figure 6-8 shows the force-displacement hysteresis loop of the 2-4 D3 device with 3 orifices open that installed in the prototype structure when subjected to sinusoidal displacement inputs of frequencies from 0.25 Hz to 1.5 Hz and amplitude 35 mm along with the prototype test setup.

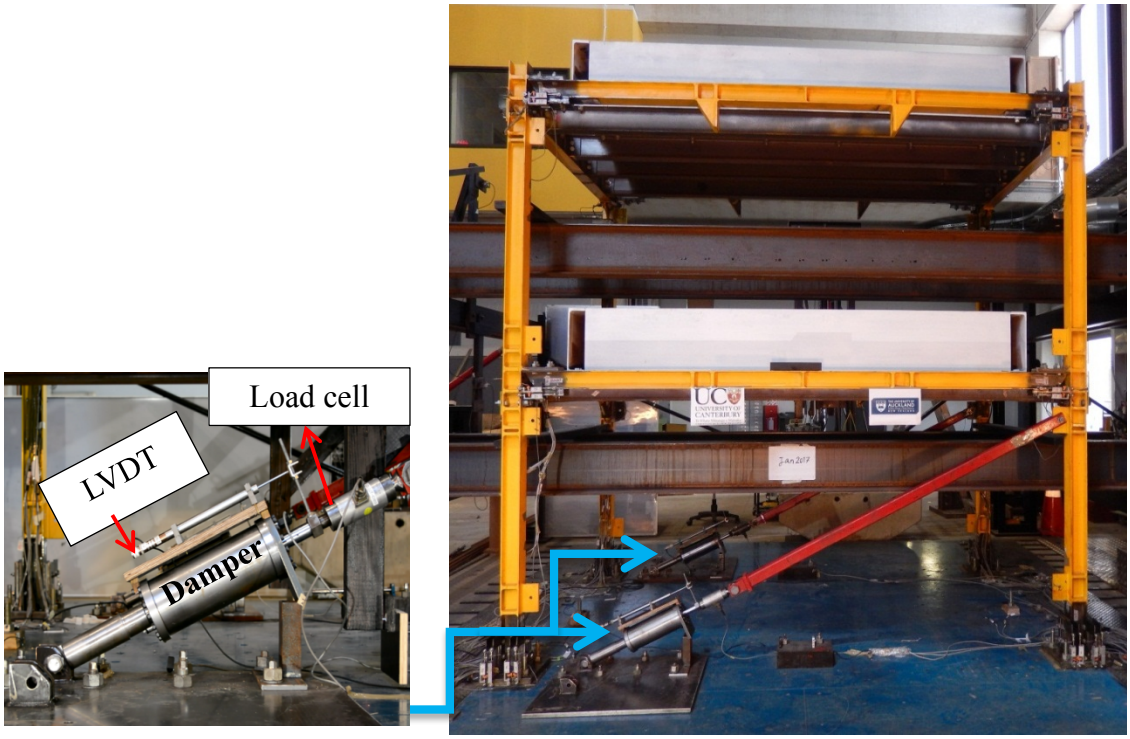

Figure 6-7. Constructed test building frame was retrofitted with two 2-4 D3 viscous damper prototypes.

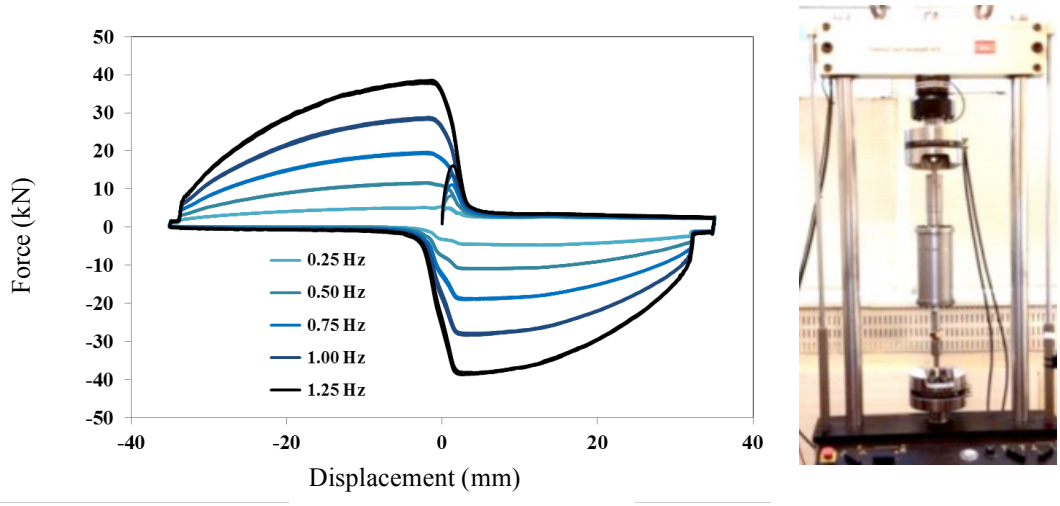

Figure 6-8. Force-displacement of the 2-4 D3 device with 3 orifices open when providing damping force under sinusoidal input loading with different frequencies and an input amplitude 35 mm. The experimental test setup in the MTS-810 machine.

6.3. Instrumentation

For this study, the instrumentation of the test frame consisted of a combination of string potentiometers, accelerometers, strain gauges, potentiometers and load cells, as shown in Figure 6-9. The relative displacement of each storey, along with the location of each string potentiometer allowed determination of the inter-storey drifts. These string potentiometers were attached between the columns and a fixed reference frame as shown in Figure 6-10. The string pots had a maximum displacement of 1000 mm in each direction from the resting position.

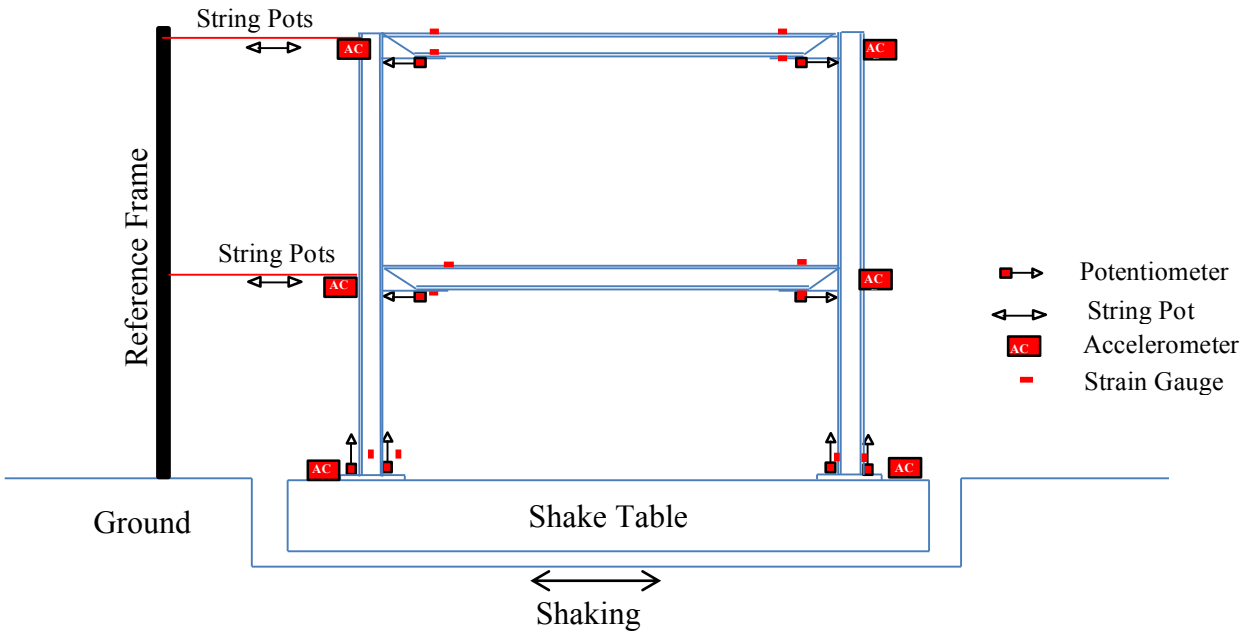

Figure 6-9. Instrumentation arrangement

To measure acceleration and enable estimation of the base shear, two accelerometers are installed in each floor to measure the acceleration. The force and displacement of the devices was recorded by a load cell and LVDT, as shown in Figure 6-7, in-line device motion.

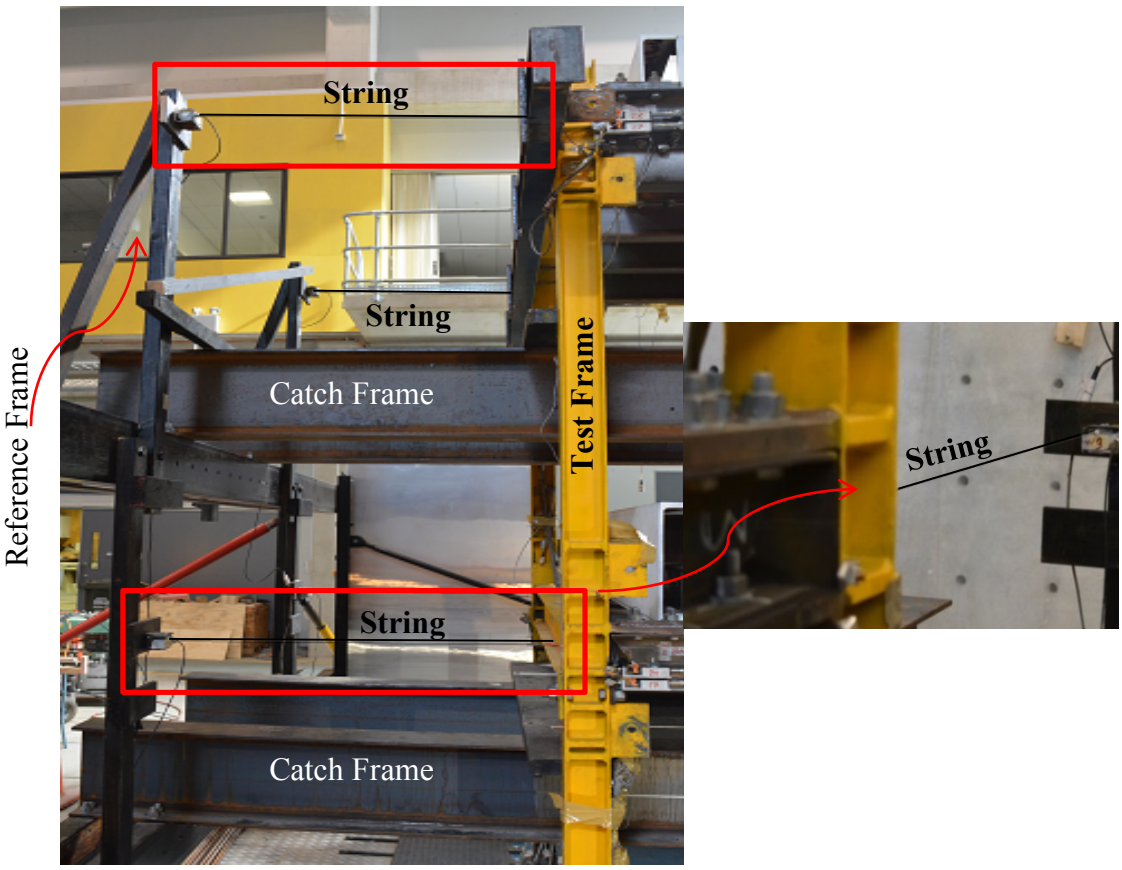

Figure 6-10. Typical string pot connection to a reference frame, along with instrumentation of each floor.

6.4. Results and Discussion

Figure 6-11 shows the maximum drift of the first and second floor, maximum total base shear and maximum acceleration of 2nd floor of the structure with and without (bare frame) the 2-4 D3 viscous devices for all 4 earthquake ground motions with 3 scales considered. Base shear calculated from floor acceleration time to the floor mass. The results show that simultaneous reductions in displacement, base-shear and acceleration demand are available with the 2–4 D3 viscous device. Table 6-3 shows the percentage of reduction in maximum drift for

the first and second floor, total base shear, and acceleration of the 2nd floor after applying the 2-4 D3 devices. On average, the maximum drift of the 1st and 2nd floor was reduced ~25%, as shown in Table 6-3. Given the unique hysteresis loop provided by the 2-4 D3 devices, the total base shear and acceleration are also reduced ~21% and ~25%, respectively across all the input events.

Table 6-3. Reduction of Structural response under 12 earthquakes, maximum drift 1st and 2nd floor, maximum total base shear and maximum acceleration 2nd floor when using the 2-4 D3 Viscous damper. Note: an increase in a metric is shown as a negative reduction.

EQ Scale	EQ	Peak Drift 1st Floor	Peak Drift 2nd Floor	Max Base Shear (kN)	Max Acceleration 2nd floor (g)
50%	CCCC	27.1%	24.57%	36.5%	27.1%
	REHS	25.0%	26.18%	33.7%	59.3%
	Northridge	30.1%	38.13%	28.6%	40.7%
	Kobe	23.8%	25.75%	14.9%	1.8%
75%	CCCC	25.8%	16.83%	31.6%	21.6%
	REHS	22.4%	19.31%	30.9%	40.0%
	Northridge	22.0%	18.30%	15.7%	12.5%
	Kobe	23.9%	27.82%	2.4%	25.0%
100%	CCCC	36.9%	30.09%	32.2%	9.9%
	REHS	30.1%	20.66%	16.2%	63.4%
	Northridge	22. 5%	26.54%	15.3%	-20.9%
	Kobe	18.6%	27.65%	33.3%	49.4%
Average		**25.7%**	**25.2%**	**21.9%**	**27.5%**

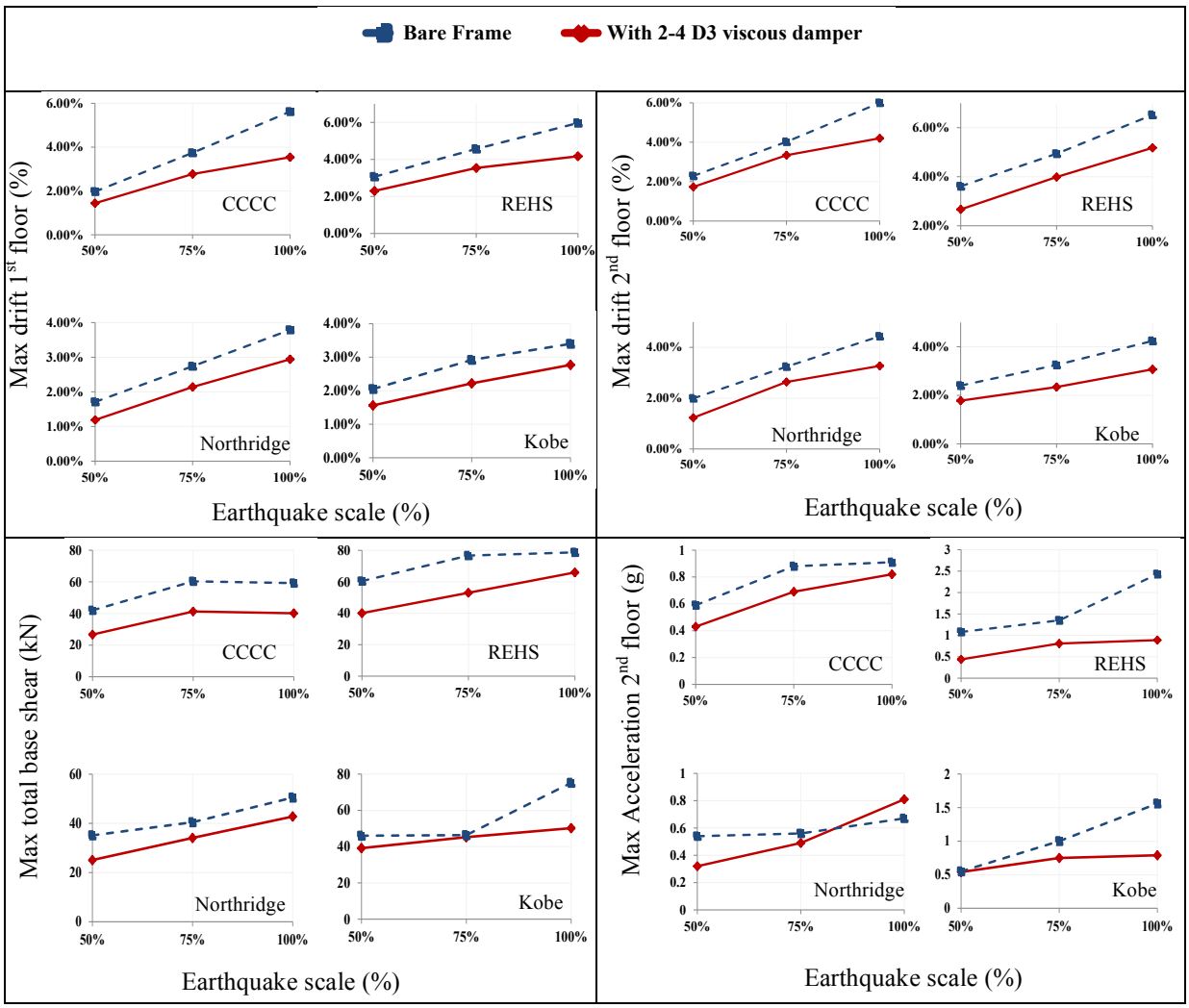

Figure 6-11. Maximum drift first and second floor, maximum base shear and acceleration 2nd floor without and with 2-4 D3 devices under 4 earthquakes with scale of 50%-75%and 100%.

Using the 2-4 viscous damper decreased the structural drift, while decreasing the total base shear, as seen in Table 6-3 and Figure 6-11. In particular, Figure 6-12 shows the base shear versus displacement of 2nd floor of the structure before and after applying the 2-4 D3 devices. These results show that applying damping in only quadrants 2 and 4 not only reduces structural displacements, but, as so expected and desired it also reduces the base shear. Hence, there is no additional

foundation demand or structural displacement demand on the structure using the 2-4 D3 devices.

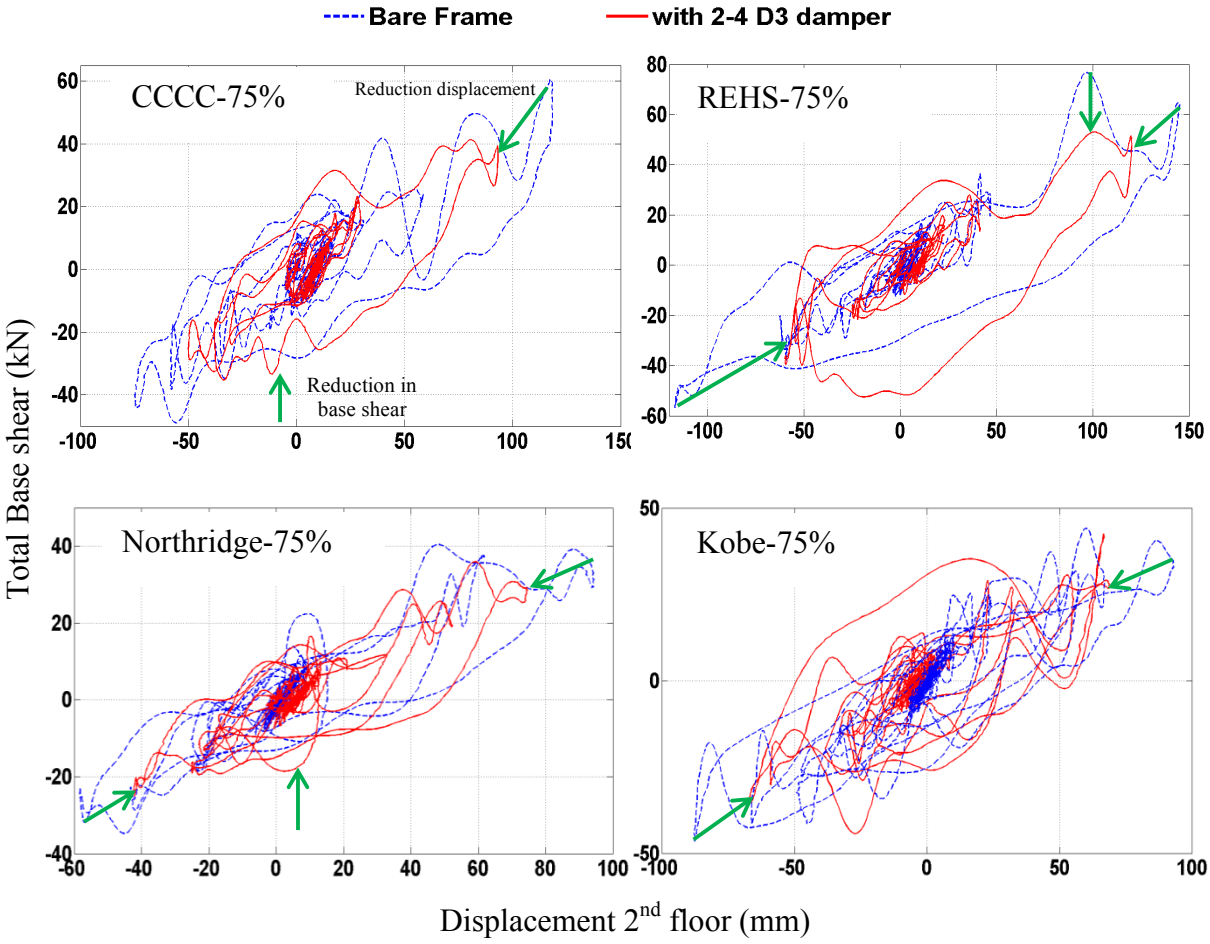

Figure 6-12. Structural hysteresis loop with and without the 2-4 D3 viscous damper under CCCC, REHS, Northridge, Kobe with scale 75%.

Table 6-4 shows residual drift of the bare frame and the structure with 2-4 D3 devices for all four earthquakes and all three acceleration levels. Residual drifts less than 0.1% have been considered as 0.0. The results show that for smaller earthquakes at 50% scale the 2-4 D3 devices do not affect the residual drift.

However, for the larger 75% and 100% scales, the residual displacements increase because the 2-4 devices resist motion back toward zero. Thus, there is a limitation of the added single direction dissipation in this case. However, the magnitude of the increase in residual deformation is relatively small for these ground motions.

Table 6-4. Residual drift of 1st and 2nd floor with and without the 2-4 D3 viscous damper.

EQ Scale	EQ	Residual 1st Floor Drift (%)			Residual 2nd Floor Drift (%)		
		Bare frame	Frame with 2-4 D3	difference	Bare frame	Frame with 2-4 D3	difference
50%	CCCC	0.2%	0.1%	-0.1%	0.3%	0.2%	-0.1%
	REHS	0.0	0.0	0.0%	0.0%	0.0%	0.0%
	Northridge	0.1%	0.0	-0.1%	0.0%	0.0%	0.0%
	Kobe	0.2%	0.0	-0.2%	0.3%	0.0%	-0.3%
75%	CCCC	0.3%	0.3%	0.0%	0.3%	0.3%	0.0%
	REHS	0.1%	0.3%	0.2%	0.2%	0.3%	0.1%
	Northridge	0.0	0.1%	0.1%	0.0%	0.1%	0.1%
	Kobe	0.0	0.1%	0.1%	0.0%	0.1%	0.1%
100%	CCCC	0.5%	0.5%	0.0%	0.5%	0.4%	-0.1%
	REHS	0.0	0.1%	0.1%	0.0%	0.2%	0.2%
	Northridge	0.1%	0.2%	0.1%	0.1%	0.2%	0.1%
	Kobe	0.00%	0.1%	0.1%	0.0%	0.2%	0.2%

6.5. Numerical and Simulation

Torsional displacements of the frame were negligible. Thus, to describe and investigate the seismic behaviour of this structure, the two-dimensional model shown in Figure 6-13 was created using the software OpenSees (McKenna et al. 2000) to simulate the nonlinear response under earthquake excitation. As beams

and columns remained elastic during these tests, elastic elements were used. Nonlinear zero-length elements were used to capture the moment-rotation behaviour of the friction connections. Lateral and vertical displacements of the two nodes at the end of the connections were constrained to match that of the frame. A viscous material was used to model the 2-4 D3 device behaviour.

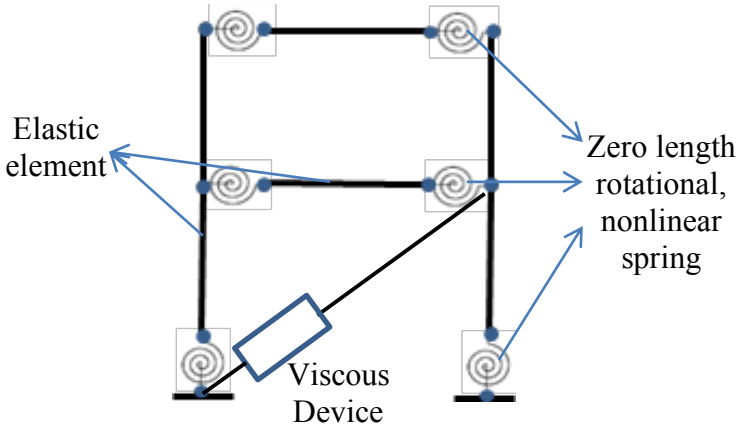

Figure 6-13. Numerical Model

The hysteretic behaviour of the AFC at beam ends is essentially trilinear. The first line refers to the initial elastic stiffness of the connection, the second line refers to the initial sliding at the interface between the bottom-flange plate and the beam/shim and the last line refer to the sliding occurs at the interface between the bottom-flange plate and the cap plate/shim. To model this behaviour *MultiLinear Material* from OpenSees is used as shown in Figure 6-14 and parameters were chosen based on the experimental results with following values; point (a): (M=3kN.m, θ=0.01%), point (b): (M=7kN.m, θ=1.0%), and point (c): (M=11kN.m, θ=4.0%).

The hysteretic behaviour of the AFC at the column base is essentially bilinear with high post elastic stiffness. To model this behaviour *Steel02 Material* (Giuffre-Menegotto-Pinto model) from OpenSees is used. Based on the experimental results the main parameters of the model were indicated and recommended values for parameters which control the transition from elastic to plastic branches were considered.

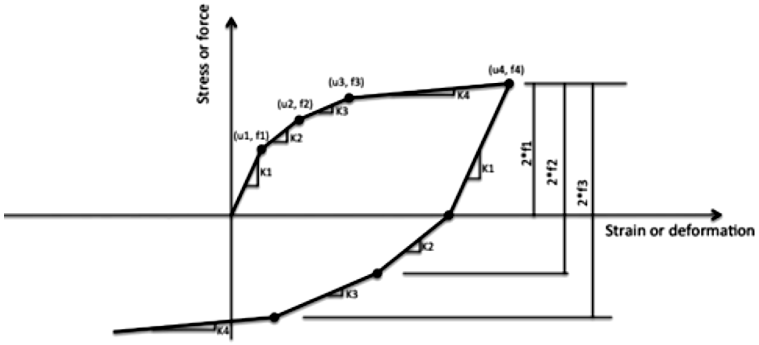

Figure 6-14. Multilinear Material

To verify the numerical methods of the experimental steel frame with 2-4 D3 devices, a series of nonlinear dynamic time history analyses were conducted. The actual table motions used in the experiments were applied to the numerical structural model. For validation, the experimental model simulated device hysteresis loops are compared along with peak drift, base shear, and 2nd floor displacement time history. These comparisons provide strong validation of the modelling approach. Rayleigh damping and an inherent structural damping ratio of 3.5% based on the test results were assigned to the first mode of the structure.

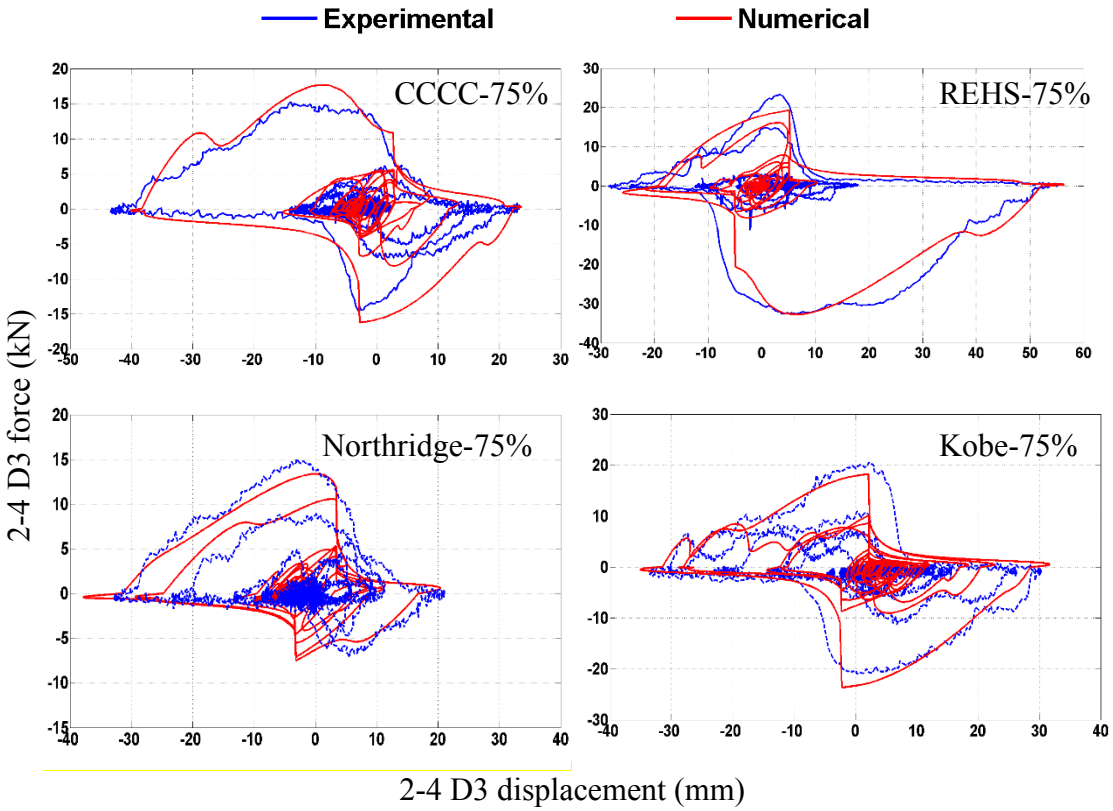

Figure 6-15. Numerical and experimental 2-4 D3 viscous device hysteresis loop under 4 earthquakes.

Figure 6-15 compares the numerical and experimental hysteresis loops of the 2-4 D3 devices. The device force of experimental results in Figure 6-15 is the average force of the two load cells representing both experimental devices and thus captures the average behaviour for model validation. Figure 6-15 shows good agreement to the test results. For the Northridge test the device was offset by ~ 3mm due to the movement of piston during installation of the device in the structure. Therefore, the hysteresis loop of the experimental model of the 2-4 device is offset ~3mm from experimental data. Figure 6-16 compares the numerical and experimental time histories of the 2nd floor displacement with the

2-4 D3 devices. The results indicate good agreement to the test results especially for maximum displacement.

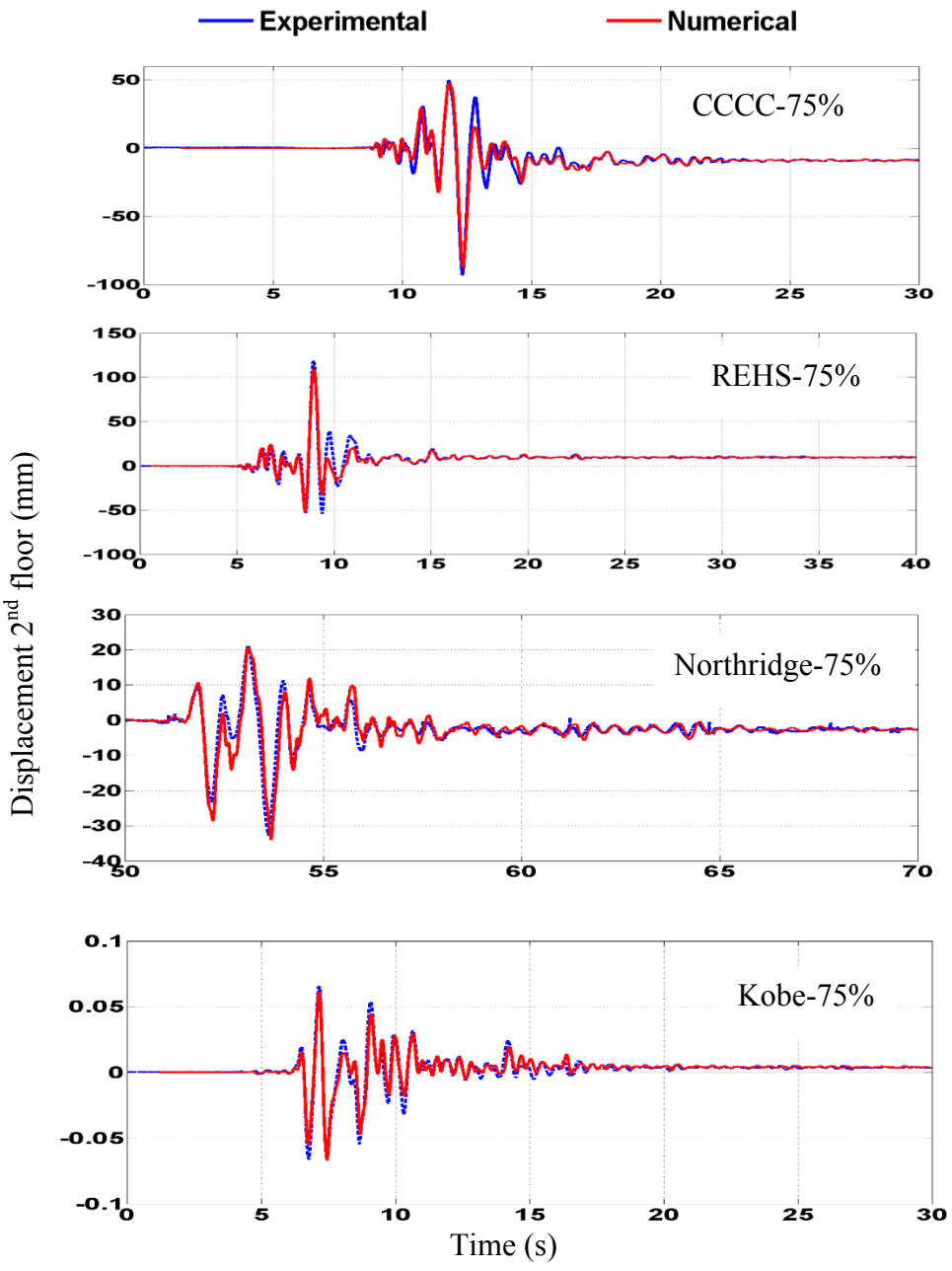

Figure 6-16. Numerical and experimental time history of Second floor Displacement under 4 earthquakes.

Table 6-5 compares the simulated and experimental peak drift and base shear for all records and acceleration scale factors. The results indicate most of the differences between simulation and test are within 5-10%, which is very good agreement. These comprehensive results indicate the model captures both linear and highly nonlinear responses well across range of seismic inputs.

Table 6-5. Comparing the peak drift of 1st and 2nd floor and maximum of base shear of simulated and experimental method.

EQ Scale	EQ	Peak Drift 1st Floor		Peak Drift 2nd Floor		Max Base Shear (kN)	
		Numerical	Experimental	Numerical	Experimental	Numerical	Experimental
50%	CCCC	1.3%	1.4%	1.7%	1.7%	24.7	26.7
	REHS	2.2%	2.3%	2.6%	2.7%	39.6	40.1
	Northridge	1.0%	1.2%	1.2%	1.2%	23.0	25.1
	Kobe	1.6%	1.6%	1. 8%	1.8%	36.3	39.2
75%	CCCC	2.5%	2.8%	3.2%	3.3%	37.7	41.3
	REHS	3.5%	3.5%	4.1%	4.0%	57.7	53.0
	Northridge	2.1%	2.1%	2.2%	2.6%	31.2	34.1
	Kobe	2.0%	2.2%	2.4%	2.3%	42.4	45.3
100%	CCCC	3.4%	3.5%	4.4%	4.2%	39.7	40.2
	REHS	4.4%	4.2%	5.1%	5.2%	64.1	65.9
	Northridge	2.9%	2.9%	3.1%	3.3%	42.0	42.8
	Kobe	2.6%	2.8%	3.2%	3.1%	50.8	50.2

Considering Chapter 5, the damping reduction factor for the nonlinear system can be computed from Equation 4-11 repeated here and defined:

$$\begin{cases} RF = (0.048\,(\xi_{el} + \xi)^{-0.5} - 0.15) * T_{K_{eff}} + 0.9 & T_{K_{eff}} \leq 2.7\,sec \\ RF = \left(\frac{0.07}{0.02+(\xi_l+\xi)}\right)^{0.22} & 2.7s < T_{K_{eff}} \end{cases} \quad (6\text{-}2)$$

where ξ_{el} represents the inherent elastic damping and ξ is damping ratio provided by the 2-4 D3 device. T_{Keff} can be defined :

$$T_{K_{eff}} = 2\pi\sqrt{\frac{m}{K_{eff}}} \tag{6-3}$$

where effective stiffness, K_{eff}, is defined:

$$K_{eff} = \frac{K(1+r\mu)}{\mu} \tag{6-4}$$

where K, r and μ are the initial stiffness, the ratio of post-rocking stiffness, and ductility, respectively.

The effective period of the specimen structure is 2.06 s calculated by Equation 6-3 and the damping ratio of the device is ζ= 0.36. Therefore, the RF can be calculated from Equation 6-2 is RF≈0.75. This value indicates the drift of the structure is reduced ~ 25% with the 2-4 D3 devices. This reduction is in line with the value of shown in Table 6-3, as an initial experimental validation of the reduction factor equations developed in Chapter 5.

6.6. Summary

This study uses 2-4 D3 devices to improve seismic structural response. Experimental validation using the proposed devices is undertaken via shake table tests of a half-scale, two story steel structure under different earthquake ground motions. Results show that the structure with the 2-4 D3 devices reduces displacement and inter-storey drift up to 38% without increasing base shear and

floor accelerations. Therefore, there is no additional demand to the foundation and potential reduction in damage to contents. A computational numerical model was developed and validated through the experimental data. It shows that there is a good agreement between test results and numerical model. The overall results show that simultaneous reductions in displacement, base-shear and displacement demand for nonlinear structural deformation is available with the 2–4 D3 viscous fluid damper.

6.7. References

Borzouie J, MacRae G, Chase J, Rodgers G, Clifton G (2015a) Experimental studies on cyclic performance of column base strong axis–aligned asymmetric friction connections Journal of Structural Engineering 142:04015078

Borzouie J, MacRae G, Chase J, Rodgers G, Clifton G (2015b) Experimental studies on cyclic performance of column base weak axis aligned asymmetric friction connection Journal of Constructional Steel Research 112:252-262

Campbell KW, Bozorgnia Y Next generation attenuation (NGA) empirical ground motion models: can they be used in Europe. In: Proceedings, First European Conference on Earthquake Engineering and Seismology, 2006.

Chanchí J, MacRae G, Chase J, Rodgers G, Clifton C Behaviour of asymmetrical friction connections using different shim materials. In: NZSEE Conference, 2012.

Chanchí J, Xie R, MacRae G, Chase G, Rodgers G, Clifton C Low-damage braces using asymmetrical friction connections (AFC). In: NZSEE Conf., The New Zealand Society for Earthquake Engineering, Wellington, New Zealand, 2014.

Chiou B, Darragh R, Gregor N, Silva W (2008) NGA project strong-motion database Earthquake Spectra 24:23-44

Clifton G Development of perimeter moment-resisting steel frames incorporating semi-rigid elastic joints. In: Proc. New Zealand National Society for Earthquake Engineering Conference, 1996. pp 177-184

Clifton GC (2005) Semi-rigid joints for moment-resisting steel framed seismic-resisting systems. ResearchSpace@ Auckland

Filiatrault A, Tremblay R, Wanitkorkul A (2001) Performance evaluation of passive damping systems for the seismic retrofit of steel moment-resisting frames subjected to near-field ground motions Earthquake Spectra 17:427-456

Hazaveh NK, Chase JG, Rodgers GW, Pampanin S (2015) Control of Structural Response with a New Semi-Active Viscous Damping Device. Paper presented at the 8th International Conference on Behavior of Steel Structures in Seismic Areas

Hazaveh NK, Pampanin S, Rodgers G, Chase J Novel Semi-active Viscous Damping Device for Reshaping Structural Response. In: Conference: 6WCSCM (Sixth World Conference of the International Association for Structural Control and Monitoring), 2014.

Hazaveh NK, Pampanin S, Rodgers G, Chase J Design and experimental test of a Direction Dependent Dissipation (D3) device with off-diagonal (2-4) damping behaviour. In: NZSEE, Christchutch, New Zealand, 2016a.

Hazaveh NK, Rodgers GW, Chase JG, Pampanin S (2016b) Reshaping Structural Hysteresis Response with Semi-active Viscous Damping Bulletin of Earthquake Engineering in press doi: 10.1007/s10518-016-0036-z

Hazaveh NK, Rodgers GW, Chase JG, Pampanin S (2017) Experimental Test and Validation of a Direction and Displacement Dependent (D3) Viscous Damper Journal of Engineering Mechanics Accepted

Hazaveh NK, Rodgers GW, Pampanin S, Chase JG (2016c) Damping reduction factors and code-based design equation for structures using semi-active viscous dampers Earthquake Engineering & Structural Dynamics 45:2533-2550 doi:10.1002/eqe.2782

Khoo HH, Clifton C, MacRae G, Zhou H, Ramhormozian S (2015) Proposed design models for the asymmetric friction connection Earthquake Engineering & Structural Dynamics 44:1309-1324

MacRae GA, Clifton GC, Mackinven H, Mago N, Butterworth J, Pampanin S (2010) The sliding hinge joint moment connection Bulletin of the New Zealand Society for Earthquake Engineering 43:202

MacRae GA, Clifton, G. C., Mackinven, H., Mago, N., Butterworth, J., and Pampanin, S. (2010) The sliding hinge joint moment connection NZSEE Bull 43: 202–212

Martinez-Rodrigo M, Romero M (2003) An optimum retrofit strategy for moment resisting frames with nonlinear viscous dampers for seismic applications Engineering Structures 25:913-925

McKenna F, Fenves G, Scott M (2000) Open system for earthquake engineering simulation University of California, Berkeley, CA

Miyamoto HK, Singh J (2002) Performance of structures with passive energy dissipators Earthquake spectra 18:105-119

Uriz P, Whittaker A (2001) Retrofit of pre-Northridge steel moment-resisting frames using fluid viscous dampers The Structural Design of Tall and Special Buildings 10:371-390

Yang T-S, Popov EP (1995) Experimental and analytical studies of steel connections and energy dissipators. University of California, Berkeley

Chapter 7: Conclusions

Supplemental damping devices are critical elements of emerging low damage structures. Most reduce displacement at the cost of increasing total base shear and acceleration, and thus increased risk of damage to foundations and/or contents. This thesis presents the analytical and experimental development of novel direction and displacement dependent (D3) viscous dampers and their impact on structural performance. They reduce displacement without increasing total base shear and acceleration response, which has not been considered previously possible without active or semi-active devices.

Time history analysis of linear structures shows 2-4 D3 viscous devices controlling motion only toward equilibrium can simultaneously reduce displacement, total base shear and acceleration for all period ranges. However, the typical viscous damper, and the 1-3 viscous damper controlling motion only away from equilibrium, decrease displacement with increasing base shear for structures with longer periods. Hence, these passive D3 devices offer unique capabilities similar to those seen for less robust and more complex semi-active stiffness based devices.

Nonlinear time history analysis of rocking systems indicates typical viscous dampers and 1-3 viscous dampers increase base shear and acceleration for most structural periods. However, the viscous 2-4 D3 device gives the opportunity to

simultaneously reduce all these response metrics. Hence, the 2-4 D3 viscous damper provides a unique and appealing solution for reducing seismic response, with minimal risk of structural or foundation damage. These outcome make it suitable for more economic new designs, as well as retrofit.

Damping reduction factors are developed to provide guidelines for adding a 2-4 D3 viscous devices into standard structural design procedures. A simple method is proposed to incorporate the design or retrofit of structures with these devices using standard design approach. These outcomes directly link these devices to industry-based structural design approaches.

Given the potential, the concept, design and analysis of a Displacement Direction Dependent (D3) dissipation device that provides viscous damping in any single quadrant, a prototype providing a 2-4 D3 device providing damping in only two quadrants is presented. These devices achieve these results entirely passively and can be designed for a wide range of forces and configuration. Experimental validation of a proof of concept device validates the direction dependent and displacement dependent damping has been obtained, and confirms the capability of providing this viscous damping entirely passively in relatively low device cost design. Through a combination of the design principles applied, any configuration of damping in any one or more quadrants can be obtained.

Shake table testing of a ½ scale, two story steel frame building with the passive 2-4 D3 damper shows reduction in displacement and inter-story drift, without

increasing base shear and floor accelerations. Most of the differences between nonlinear model simulation and test are within 5-10%, which is very good agreement and provides further links to design and industry uptake. These comprehensive results validate the overall concept experimentally and practice a modelling frame work that captures both linear and highly nonlinear responses well across a range of seismic inputs.

In summary, the unique contributions this research and thesis make to the field of improving seismic structural performance include:

- Introducing and evaluating a novel semi-active viscous damping device control method to re-shape structural hysteretic behavior with three semi-active control laws, 1-4, 1-3 and 2-4. This evaluation shows the 2-4 control law is an appealing solution for reducing seismic response, with minimal risk of structural or foundation demand, implying it is suitable for more economic new design, as well as retrofit.
- Illustrating the relationship between damping of the 2-4 semi-active viscous device (ξ) and structural damping reduction factor, RF_{ξ} and describing a simple method to determine the effect of the 2-4 device when added to new or existing structural systems has been provided to enable easy uptake in existing design procedures.
- Evaluating the seismic behavior of rocking structures with re-shaped structural hysteretic behavior through the addition of a 2-4 viscous

damping device. This evaluation gives a better understanding of using the 2-4 viscous device in the nonlinear systems with different range of ductility and periods.

- Designing and manufacturing of a Displacement Direction Dependent (D3) dissipation device that provides the 2-4 viscous damper entirely passively. Experimental results show that the D3 viscous damper can be designed for a wide range of forces and configuration that engineers need in typical structures.
- Conducting half-scale shake table tests which validate the devices developed, the analytical studies as well as proving the efficacy of the 2-4 D3 viscous device in the control of real structures.

Chapter 8: Future Work

The research within this thesis provided significant insight into the enhancing seismic performance of structure with the proposed dissipation devices. Several areas that have potential for further studies have been identified as a result of this work, and these are detailed within this chapter.

8.1. Device characteristic

In the proposed devices General purpose Castrol Axle EPX 80W-90 oil was chosen as the fluid to be used. This fluid was selected as a very low-cost and easily accessible option. A more expensive fluid option, such as silicone fluid could be used, but this study is intended to provide proof of concept validation of the device design, particularly at low cost, rather than a final, fluid-specific result. Hence, future experimental test should include testing the device with silicone fluid that offers nonlinear force-velocity behaviour and improves seismic performance as it is less dependent on velocity.

8.2. Structure residual deformation

The presented experimental shake table tests in this thesis showed that the 2-4 D3 viscous devices are promising dissipation devices. However, there is the

possibility of increasing residual deformation because the 2-4 devices resist motion back toward zero. Hence, there is a need to undertake additional analysis of structures with bi-linear hysteresis behaviour to investigate the effect of the 2-4 D3 device on the structural seismic performance and residual deformation.

8.3. Seismic response of a 2-4 D3 viscous damper in Multi degree of freedom system

Determining the optimal configuration and location of dissipation devices in multi-degree freedom (MDOF) structures plays an important role in seismic structural performance. Moreover, higher mode effect should consider for the MDOF system. Hence, there is a need to do more study on the seismic performance of MDOF system with the 2-4 D3 viscous damper.

8.4. Evaluating other configuration of the D3 device in improving seismic structural performance

This thesis evaluates the seismic performance of the 2-4 D3 devices. However, D3 devices give a unique opportunity to have a resisting force in any quadrants. Future study could include evaluating other configurations of the direction displacement dependent viscous devices in seismic structural performance. For example, the 1-3 D3 devices could be an appealing solution for retrofitting and re-

centering the tilted structures and may also be favourable in base-isolation systems.

8.5. Experimentally evaluating the seismic behavior of the rocking system with the 2-4 viscous damper

The numerical results indicate that the 2-4 D3 viscous damper improves the seismic performance of rocking system. Hence a future work should include in a large-scale rocking wall shake table tests utilizing the 2-4 D3 devices to enhance the overall dissipation of these systems and compare with analytical results of this thesis.

8.6. Implementation in the Field

The final step for any useful research is implementing by practitioners. A few consultant engineers have used dissipation devices in their projects in New Zealand, and their interest has been expressed in different stages of this research. The presented research in this thesis, in addition to the published papers from this study, provided all the basic tools needed for these devices to be implemented into a design. Future research topics may result from discussions with practitioners, fabricators and contractors. Ongoing work will hopefully result in implementation of the dissipation devices in both new building designs and retrofit applications.